Farnesylation-dependent regulation of transcripts by PARP13

by

Lilen Uchima

B.S. Industrial Biotechnology
University of Puerto Rico at Mayagüez, 2009

SUBMITTED TO THE DEPARTMENT OF BIOLOGY IN PARTIAL FULFILLMENT OF THE REQUIREMENTS FOR THE DEGREE OF

DOCTOR IN PHILOSOPHY

at the

MASSACHUSETTS INSTITUTE OF TECHNOLOGY

AUGUST 2015 [september 2015]

Signature of author: Signature redacted
Department of Biology
August 31st, 2015

Certified by: Signature redacted
Co-Supervisor: Paul Chang
Research Scientist

Certified by: Signature redacted
Supervisor: Stephen P. Bell
Professor of Biology

Accepted by: Signature redacted
Michael Hemann
Associate Professor of Biology
Co-Chair, Biology Graduate Committee

Farnesylation-dependent regulation of transcripts by PARP13

By

Lilen Uchima

Submitted to the Department of Biology on August 31st, 2015 in partial fulfillment of the requirements for the degree of Doctor in Philosophy

Abstract

PARP13 is a RNA-binding and catalytically inactive member of the poly(ADP-ribose) (PARP) family. PARP13 was first identified as a host antiviral factor that selectively binds to viral mRNAs and targets them for degradation by mRNA decay factors. Recently, functions of PARP13 in post-transcriptional regulation of cellular mRNAs were identified. In this context, PARP13 indirectly regulates the miRNA silencing pathway, restricts human retrotransposition by regulating LINE-1 mRNA and downregulates the mRNA levels of TRAIL-R4 –a pro-survival TRAIL ligand receptor.

Farnesylation is a post-translational lipid modification that causes proteins to associate to membranes and is required for the activity of some proteins such as Ras. Farnesyl modification adds a 15-carbon prenyl group to the C-terminus of proteins, including PARP13, that contain a CaaX motif. Because PARP13 has two splice isoforms, the full-length PARP13.1 and the C-terminal truncated isoform PARP13.2, only the full-length isoform PARP13.1 is farnesylated.

Here we show that PARP13.1 localizes to the cytoplasm and the endoplasmic reticulum and binds RNA at both compartments. Localization to the ER is mediated by farnesylation of cysteine 899 and to a lesser extent to RNA interactions through its CCCH zinc fingers. We also identify a set of putative PARP13.1 cellular mRNA targets by differential expression analysis of $PARP13^{-/-}$ cells expressing either full length PARP13.1, a RNA binding mutant ($PARP13.1^{VYFHR}$) or a farnesylation mutant ($PARP13.1^{C899S}$). Most of the transcripts that are regulated in a PARP13.1-dependent manner are membrane-associated and require the farnesylation of PARP13.1 for their regulation. These results possibly suggest that localization of PARP13.1 to the ER by farnesylation is important for the regulation of mRNAs that localize there. We furthermore, validate the regulation of *CERK* and *DNER*, two cellular mRNAs targets by PARP13.1. In addition we determine that the PARP13-dependent regulation of the transcript *DNER* affects neurite outgrowth in the human cell line U87-MG, possibly implicating PARP13.1 in yet another important cellular process such as neuritogenesis.

Thesis Supervisor: Stephen P. Bell
Thesis Co-Supervisor: Paul Chang

Table of contents

CHAPTER 1

INTRODUCTION

Poly(ADP-ribose) polymerases: activity and cellular functions

Post-translational modifications are modifications that occur on a protein after translation by the ribosome. These types of modification include the modification of amino acid residues, addition of covalent and non-covalent chemical groups, and the proteolytic cleavage of targeted proteins. Some post-translational modifications occur due to cellular and extracellular conditions and affect the protein's activity, localization, stability and interactions with other proteins or molecules. Examples of post-translational modifications include phosphorylation, ubiquitination, farnesylation and ADP-ribosylation.

ADP-ribose modification are reversible post-translational modification synthesized by a family of proteins called poly(ADP-ribose) polymerases (PARPs). PARPs utilize NAD^+ as a substrate to covalently attach ADP-ribose units to specific residues on acceptor proteins, which include the PARPs themselves (Amé et al., 2004; Gibson and Kraus, 2012; Vyas et al., 2013). The family of human PARPs is composed of 17 proteins that have been identified via bioinformatics based on sequence homology to the PARP-1 catalytic domain (Amé et al., 2004).

PARPs modify proteins with either polymers of ADP-ribose called poly(ADP-ribose) (pADPr) or monomers called mono(ADP-ribose) (mADPr). The type of modification generated has important implications on the mechanism of target protein regulation. Poly(ADP-ribose) modifications regulate protein function through covalent mechanisms, and also by recruiting the binding of pADPr binding proteins, whereas mono(ADP-ribose) modifications function like a traditional covalent protein

modification such as phosphorylation (Figure 1). The primary predictor of the type of modification generated by each PARP depends on the presence or absence of specific amino acid residues in the catalytic triad H-Y-E, three amino acids crucial for its enzymatic activity. Depending on the identity of these three amino acid residues, PARPs exhibit three exclusive types of activity: poly(ADP-ribosyl)ation, mono(ADP-ribosyl)ation or no enzymatic activity. Both the histidine and tyrosine are important for NAD^+ binding, while the glutamate is thought to be required for poly(ADP-ribose) synthesis (Hottiger et al., 2010; Kleine et al., 2008). Therefore, PARPs containing the H-Y-E catalytic triad synthesize poly(ADP-ribose) whereas PARPs containing H-Y-X triad synthesize mono(ADP-ribose) onto acceptor proteins. PARPs lacking the histidine residue in their catalytic triad have no ADP-ribosylation activity (Kleine et al., 2008, Vyas et al., 2014). Specific structural features in each PARP, such as the donor and acceptor loops, can also affect the enzymatic activity of the protein. The donor loop shapes the substrate binding pocket and interacts with the substrate NAD^+, whereas the acceptor loop is important in the binding of the acceptor either it be a protein substrate or a ADP-ribose molecule in the case of pADPr modifications (Kleine et al., 2008; Walhberg et al., 2012).

The ADP-ribosylation modifications catalyzed by PARPs are reversible. Mono(ADP-ribose) (mADPr) can be cleaved from the site of attachment by the enzymatic activity of MacroD1, MacroD2 and terminal(ADP-ribose) glycohydrolase (TARG) (Rosenthal et al., 2013; Jankevicius et al., 2013; Vyas et al., 2014). Poly(ADP-ribose) glycohydrolase (PARG) or the less efficient ADP-ribosylhydrolase 3

FIGURE 1

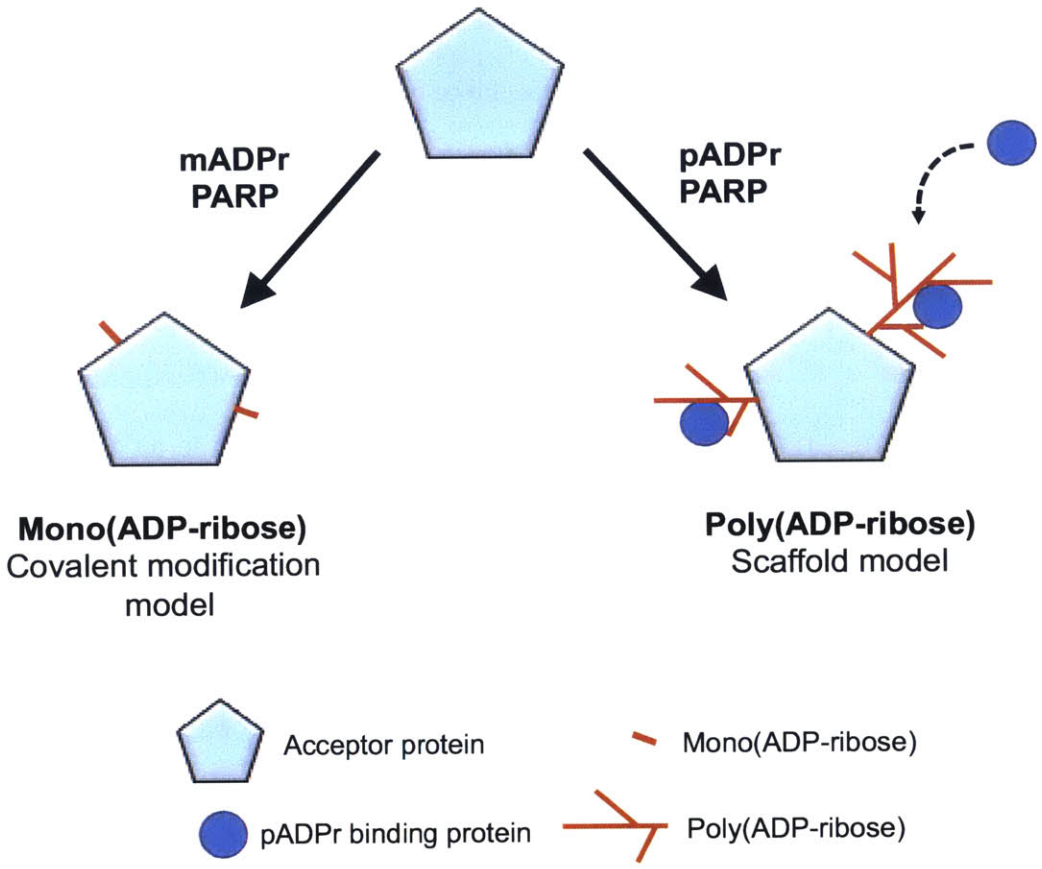

Figure 1. Mechanism of ADP-ribose modification by PARPs. Depending on their enzymatic activity, PARPs can synthesize mono or poly(ADP-ribose) onto acceptor proteins. Mono(ADP)ribose modifications are covalent modifications and like other posttranslational modifications can alter protein function, localization, structure etc. Poly(ADP-ribose) modifications, in addition, can act as a scaffold to bind and recruit poly(ADP-ribose) binding proteins.

(ARH3) are responsible for the hydrolysis of poly(ADP-ribose) (pADPr) chains into ADPr units (Lin et al., 1997; Oka et al., 2006; Slade et at., 2011; Vyas et al., 2014).

In addition to the conserved PARP domain, individual PARP family members contain a variety of domains specify their roles in different cellular processes (Amé et al., 2004; Otto et al., 2005; Vyas et al., 2013). Based on the identity of these domains, PARPs have been classified in five subfamilies: DNA-dependent, Tankyrase, Macro, CCCH-zinc finger and unclassified PARPs (Figure 2) (Amé et al., 2004). The DNA-dependent PARPs 1, 2 and 3 contain a proposed nucleic acid binding domain Tryptophan-Glycine-Arginine (WGR) and function in DNA repair pathways (reviewed in De Vos et al., 2012). The tankyrases subfamily is composed of PARP5a (Tankyrase 1) and PARP5b (Tankyrase 2). Tankyrases are characterized by the presence of 24 ankyrin repeats that mediate protein-protein interactions and are involved in telomere homeostasis, Wnt/β-catenin signaling and cell cycle progression (Smith et al., 1998; Chang et al., 2005; Huang et al., 2009).

Macro PARPs 9, 14 and 15 contain macro domains that bind to ADP-ribose and other related molecules like NAD^+. PARP9 has been implicated in B-cell lymphoma migration and interferon signaling pathways (Aguiar et al., 2000; Juszczynski et al., 2006) whereas PARP14 has a role in the regulation of interleukin-4 signaling through Stat6, JNK pro-survival signaling and focal adhesion dynamics (Goenka et al., 2007; Barbarulo et al., 2013; Vyas et al., 2013). PARP15 function has not been thoroughly studied but it is enriched in stress granules upon cytoplasmic stress (Leung et al., 2011). In addition, recent evolutionary analyses of PARP9,

FIGURE 2

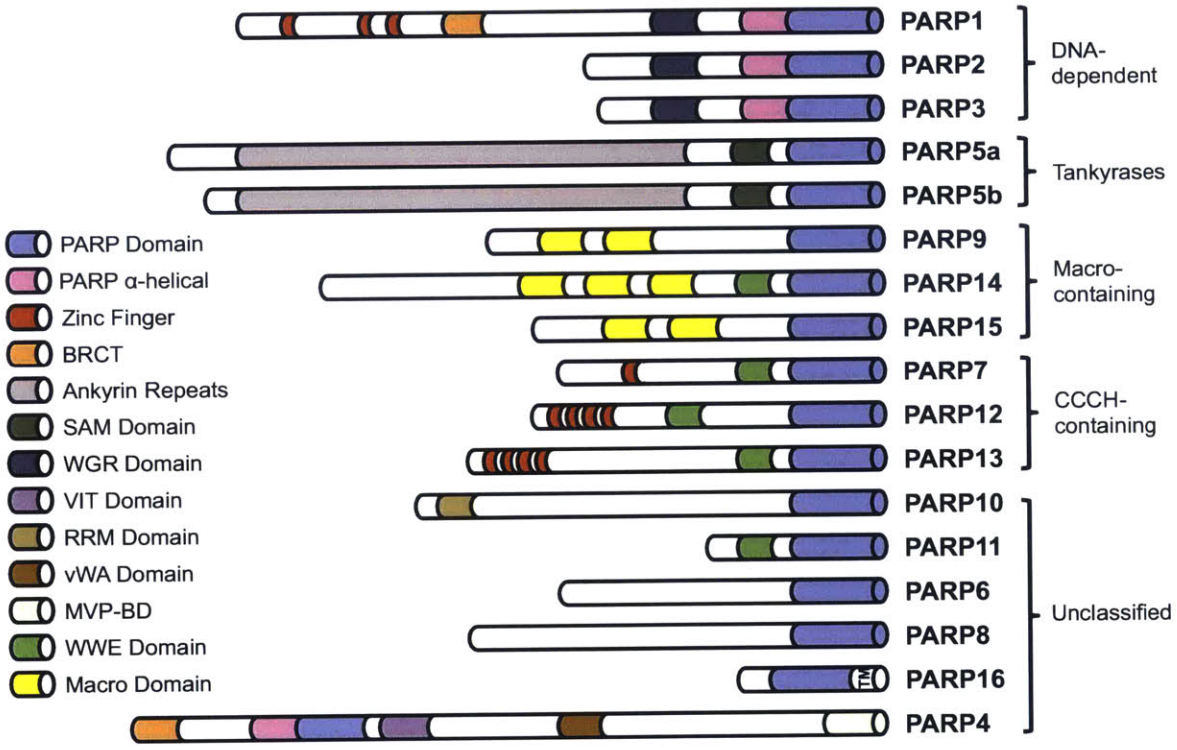

Figure 2. PARP family members. Human PARP family consists of 17 members classified by their domain homology outside of the PARP catalytic domain. Shown are the PARP family members divided into subfamilies: DNA-dependent, tankyrases, Macro domain containing, CCCH zinc-finger containing and unclassified. For simplification not all isoforms are shown. TM denotes a transmembrane domain in PARP16.

PARP14 and PARP15 suggest they could possess antiviral activity (Daugherty et al., 2014).

Zinc finger PARPs include PARP7, 12 and 13. Each zinc finger PARP contains at least one RNA-binding CCCH-zinc finger motif and a WWE pADPr binding domain. PARP7 has been shown to be a transcriptional repressor of the aryl hydrocarbon receptor (Diani-Moore et al., 2010, MacPherson et al., 2012; Ahmed et al., 2015) and PARP12 has been implicated in the antiviral response to alphaviruses. PARP12 is also found enriched in stress granules upon cytoplasmic stress along with PARP5a, PARP15 and PARP13 (Atasheva et al., 2012; Leung et al., 2011). The remaining member of the zinc finger PARPs, PARP13, is the focus of this thesis and will be discussed in detail in a subsequent section.

Finally, PARPs 4, 6, 8 10, 11 and 16, grouped as unclassified PARPs, contain no domain similarity to other subfamilies outside their PARP catalytic domain. PARP4 contains a BRCT domain, von Willebrand factor A (VWFA) domain and a vault inter alpha trypsin (VIT) domain and localizes to large cytoplasmic ribonucleoprotein particles known as vault particles, but its role in these particles is still unknown (Kickhoefer et al.,1999; Berger et al., 2009). PARP10 contains multiple domains, including a Myc-binding domain, ubiquitin interaction domain and a RNA recognition motif, regulates c-Myc and NF-κB signaling, and has a role in apoptosis and DNA damage (Yu et al., 2005; Verheugd et al., 2013; Herzog et al., 2013; Nicolae et al., 2014). PARP11 has an ADP-ribose binding WWE domain and was recently implicated in nuclear envelope stability and reorganization during spermiogenesis (Meyer-Ficca et al., 2015). Lastly, PARP6, 8, and 16 have no identified domains

outside of their conserved PARP domain, but functions have been identified for all except PARP8. PARP6 is thought to be a negative regulator of cell proliferation in colorectal cancer cells (Tuncel et al., 2012) whereas PARP16 is an ER transmembrane protein involved in the unfolded protein response (Di Paola et al., 2012; Jwa and Chang, 2012).

The PARP family of proteins is diverse in their domain composition and the cellular functions they regulate. Some of these functions require their mono or poly(ADP-ribosyl)ation activity, while others do not require catalytic activity. Because of this structural and enzymatic activity diversity, it is likely that not all possible functions of PARPs have been elucidated. Thus as a step towards a deeper understanding of PARP function, I have focused on the study of one of these PARPs, the catalytically inactive RNA-binding PARP13.

PARP13

Poly(ADP-ribose) polymerase 13 (PARP13), also known as Zinc Finger Antiviral protein (ZAP), is a catalytically inactive PARP family member capable of binding and regulating specific viral and cellular mRNAs through its N-terminal CCCH-zinc fingers (Gao et al., 2002; Kleine et al.,2008; Guo et al., 2004; Vyas et al., 2014; Todorova et al., 2014). Two experimentally verified PARP13 isoforms exist in human cells, the full length PARP13.1 and the truncated PARP13.2, which lacks a PARP domain (Figure 3) (Kerns et al., 2008; Vyas et al., 2013). In addition to the regulation of mRNAs, PARP13 has been shown have roles in other cellular processes such as miRNA silencing, translational repression and retrotransposition

inhibition (Leung et al., 2011; Zhu et al., 2012; Moldovan and Moran, 2015; Goodier et al., 2015). In the next sections, I will focus on PARP13's structure and functions.

PARP13 functional domains and structure

PARP domain

The human PARP13 gene encodes two protein isoforms that result from alternative splicing of the carboxy-terminal PARP domain. Full-length PARP13 (PARP13.1) and the shorter isoform PARP13.2 have identical N-terminal sequences that contains four CCCH-zinc fingers, a WWE domain and nuclear export and localization sequences. However, the isoforms differ at the C-terminus, where the shorter isoform lacks the PARP domain (Figure 3) (Kerns et al., 2008). Analyses of molecular evolution suggest that PARP13 is most closely related to PARP11, PARP12 and PARP7 and that the PARP domain-containing isoform PARP13.1 dates back to the origin of vertebrates. Evolutionary analyses also reveal evidence of positive selection of the PARP domain of PARP13 throughout primate evolution (Amé et al., 2004; Kerns et al., 2008). Despite the presence of a PARP domain, PARP13.1 is unable to synthesize mADPr or pADPr (Kleine et al., 2008; Leung et al., 2001; Vyas et al., 2014). As previously mentioned, catalytic activity in the PARP family is largely dictated by the catalytic triad HYE (Hottiger et al., 2010). In PARP13.1, this motif deviates from the conserved HYE to YYV. Structural analysis of PARP13's PARP domain revealed that the lack of ADP-ribosylation activity is due to

FIGURE 3

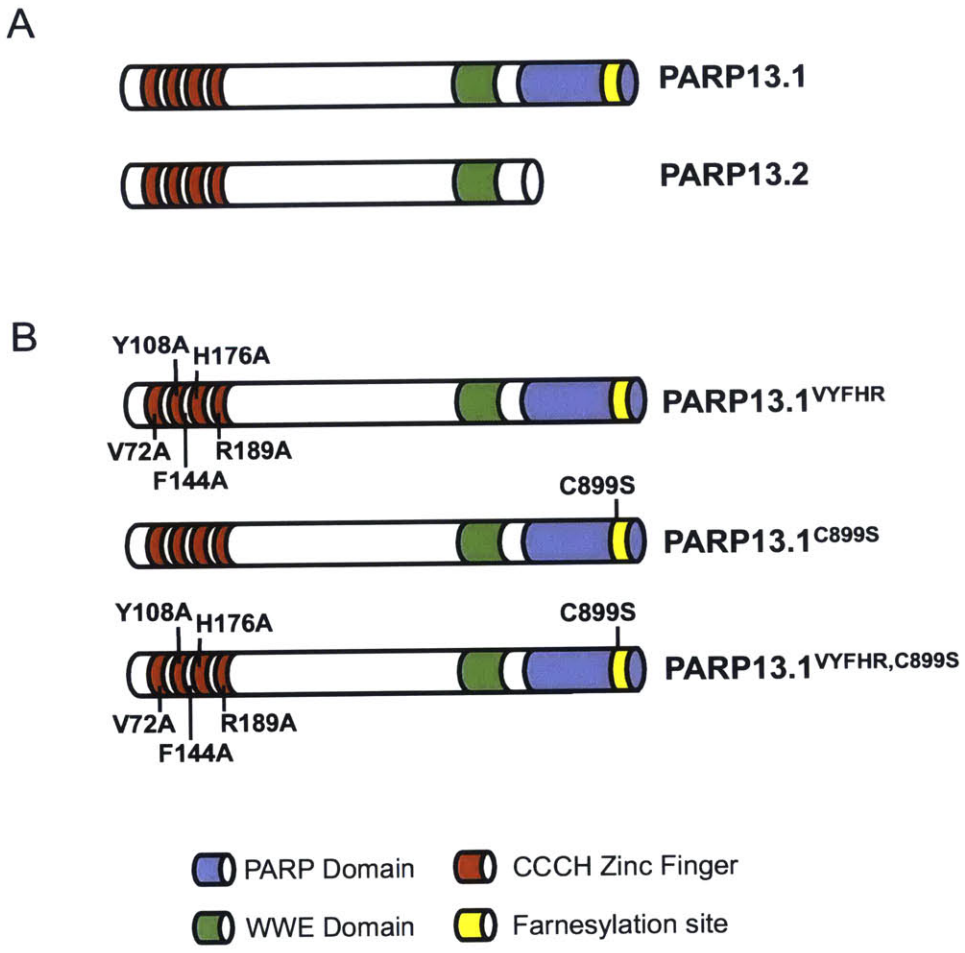
A
PARP13.1
PARP13.2
B
Y108A
H176A
V72A
F144A
R189A
PARP13.1VYFHR
C899S
PARP13.1C899S
PARP13.1VYFHR,C899S
PARP Domain
CCCH Zinc Finger
WWE Domain
Farnesylation site

Figure 3. PARP13 isoforms and mutants used in this study. (A) Schematic representation of PARP13 isoforms. Both isoforms have four RNA-binding CCCH zinc fingers and a WWE domain each, but only PARP13.1 contains a PARP catalytic domain and C-terminal farnesylation site. **(B)** Schematic representation of the mutants used in this study. RNA-binding mutant PARP13.1^{VYFHR} was described previously (Todorova et al., 2014). PARP13.1^{C899S} has a serine in place of the cysteine required for farnesylation modification, and the double mutant PARP13.1^{VYFHR,C899S} contains both RNA-binding and farnesylation mutations.

inhibited substrate binding ability. Karlberg and colleagues crystallized the PARP domain of PARP13 and demonstrated that the estimated volume of the NAD^+ binding pocket was three times smaller compared to the pockets in PARP12 and PARP15 (Karlberg et al., 2015). Furthermore, the structure revealed that the NAD^+ binding cleft of PARP13 has a closed conformation due to an interaction between Tyr^{826} and His^{810} that seals off the NAD^+ pocket, complemented by a stabilizing interaction from Tyr^{787} and Glu^{808} (Figure 4) (Karlberg et al., 2015). Despite the lack of PARP13 ADP-ribosylation activity, mutational analysis conducted by Gläsker and colleagues suggested that the integrity of the YYV catalytic triad motif of PARP13 is important for the protein's antiviral activity against Sindbis virus (Gläsker et al., 2014). This contrasts with other studies that show that the presence of the PARP domain, and thus the catalytic triad motif, is not required to inhibit the replication of viruses such as Hepatitis B or Xenotropic Murine Leukemia virus (Mao et al., 2013; Wang et al., 2012). The discrepancy between the two studies might be due to the different binding requirements of the different viral targets of PARP13.

CCCH-Zinc fingers

CCCH-zinc fingers (or Cys_3H zinc fingers) are an RNA-binding subclass of zinc finger motifs that coordinate one zinc ion with three cysteines and a histidine. Proteins typically contain one to five CCCH-zinc finger motifs, which are characterized by the $Cx_{5-8}Cx_{4-5}Cx_3H$ consensus sequence (Font and Mackay, 2010). Since the first description of this motif by Gomperts and colleagues in 1990, much progress has been made in studying its function in organisms ranging from yeast to

FIGURE 4

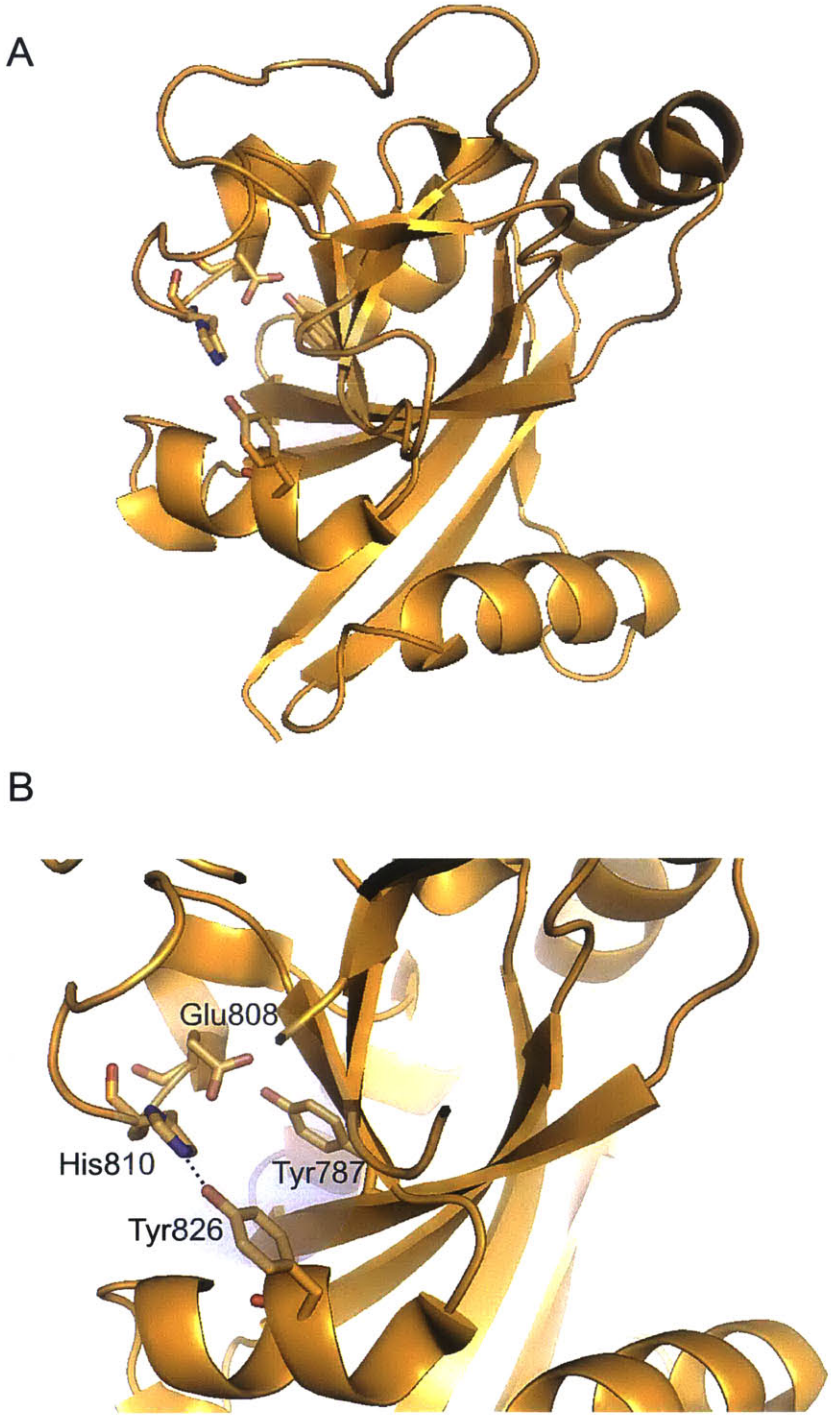

Figure 4. Structure of the PARP domain of PARP13. (A) Structure of the PARP domain of PARP13 (PDB: 2X5Y) rendered in MacPyMOL. Blue area represents the canonical NAD^+ binding site. **(B)** Zoomed-in view of the NAD^+ binding cleft in **(A)** depicting its closed conformation due to an interaction between Tyr826 and His810. Interaction between Tyr787 and Glu808 further stabilizes the closed conformation. Blue area represents the canonical NAD^+ binding site. Structure solved and published by Karlberg and colleagues (Karlberg et al., 2015).

mammals (Gomperts et al.,1990). Genome-wide surveys of CCCH-containing proteins in mice revealed that the majority (77%) of genes with known functions were involved in RNA metabolism processes like splicing, localization, stability and degradation, whereas a smaller subset (23%) were involved in transcription, ubiquitination and poly(ADP-ribosyl)ation (Liang et al., 2008). The best-characterized function of the CCCH-zinc finger motif comes from the study of tristetraprolin (TPP). TPP contains two tandem CCCH-zinc fingers that bind to AU-rich elements (ARE) in mRNA, leading to the removal of the poly(A) tail and increased rates of mRNA turnover (Lai et al., 2000; Carballo et al., 1998; Carrick et al., 2004). Unlike in TPP, PARP13's four CCCH-zinc fingers do not bind to consensus motifs but rather to a specific combination of nucleotide sequence and RNA conformation (Huang et al., 2010). X-ray crystallography studies have uncovered the basis of the interaction between PARP13's zinc fingers and its RNA substrate (Chen et al., 2012). Chen and colleagues determined that the zinc finger domain contains two cavities as well as a large RNA binding surface composed of positively-charged residues. The positive residues interact with the negatively-charged phosphate backbones of the substrate RNA, whereas the residues located in the cavities are involved in interactions with base groups of the RNA (Figure 5). Alanine substitution of residues along the cleft disrupt viral RNA-binding in *in vitro* experiments (Chen et al., 2012). Determining the structure of PARP13's CCCH zinc fingers has allowed the generation and analysis of the activity of PARP13 RNA-binding mutant. Our lab generated an RNA-binding mutant for human PARP13, PARP13.1^{VYFHR}, which harbors alanine mutations in residues present in the two RNA-binding cavities (Figure 3).

FIGURE 5

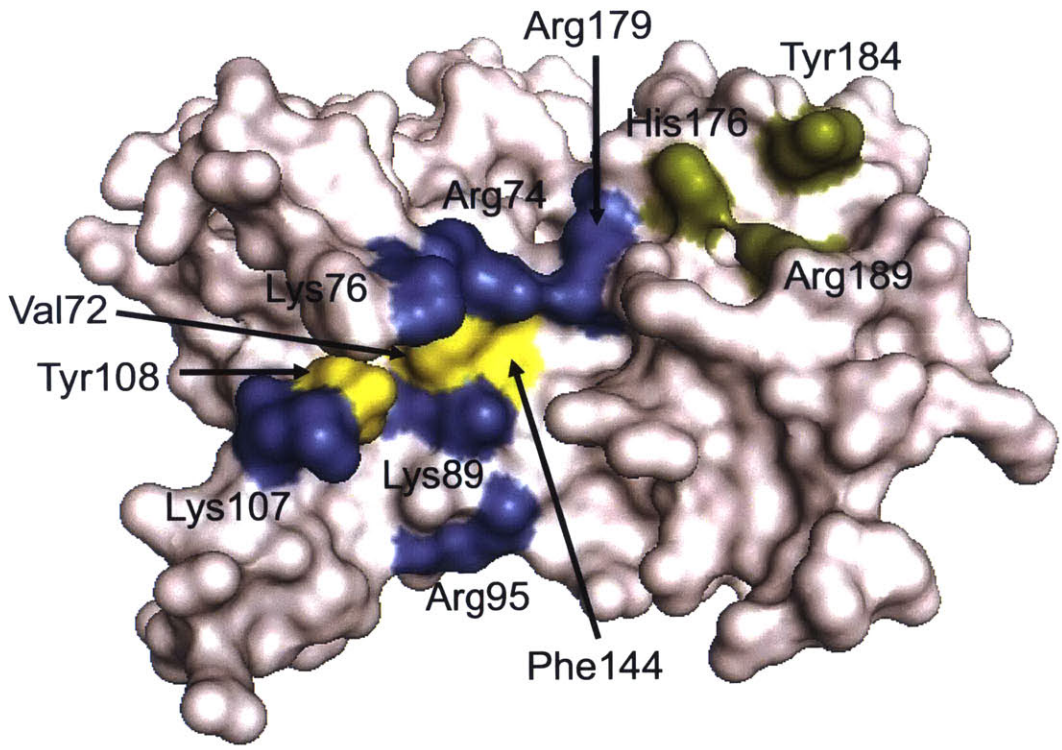

Figure 5. Structure of the CCCH zinc fingers of rat PARP13. Crystal structure of the N-terminus of rat PARP13 including the four CCCH zinc fingers (PBD: 3U9G) rendered in MacPyMOL. Depicted are the residues involved in RNA binding according to the study of Chen and colleagues (Chen et al., 2012). Positively charged residues important in interaction with phosphate groups of RNA are depicted in blue. Cavity residues important in base group interaction are depicted in yellow for cavity 1 and green for cavity 2. Figure adapted from (Chen et al., 2012).

WWE domain

The WWE domain, another feature of PARP13 structure, is a globular domain that contains two conserved tryptophan (W) residues and a glutamic acid (E) residue and occurs in a family of proteins associated with ubiquitination and poly(ADP-ribosyl)ation (Aravind, 2001). The mechanistic relationship between ubiquitination and poly(ADP-ribosyl)ation was not evident until Zhang and colleagues demonstrated that the E3 ubiquitin ligase RNF146 directly interacted with poly(ADP-ribose) through its WWE domain, promoting the ubiquitin-dependent degradation of the ADP-ribosylated protein (Zhang et al., 2011). This finding suggested that poly(ADP-ribosyl)ation of proteins might act as a mechanism for tagging proteins for ubiquitin-mediated degradation. Further analysis by Wang and colleagues showed that the WWE domain of RNF146 binds specifically to poly(ADP-ribose) but not to mono(ADP-ribose), suggesting that WWE domains recognize a select type of ADP-ribose modification (Wang et al., 2012). In this context, NMR perturbation experiments have revealed differences in ADP-ribose recognition modes of several WWE-containing proteins that correlate with their individual biological activities (He et al., 2012). Studies from our lab have shown that PARP13 is highly modified by poly(ADP-ribose) during cytoplasmic stress, and unpublished results suggest that the WWE domain in PARP13 binds poly(ADP-ribose) (Leung et al., 2011 and unpublished results). Although not thoroughly studied, the presence of a WWE domain in PARP13 suggests that binding to poly(ADP-ribose) could regulate PARP13 function.

Nuclear export and nuclear localization sequences

PARP13 also contains a nuclear export and localization sequence that allows it to shuttle between the cytoplasm and nucleus in a CRM1-dependent manner (Liu et al, 2004). Although all currently known PARP13 functions are in the cytoplasm, the presence of nuclear export and localization sequences suggests that PARP13 could have a yet unidentified nuclear function.

CaaX motif: site of farnesyl modification of PARP13

Another structural feature that influences PARP13's localization is the CaaX motif at the C-terminus of the protein (absent in the PARP13.2 isoform). The motif's name, CaaX, represents the four amino acid sequence at the C-terminus of proteins that harbor it (a is any aliphatic amino acid and X is M, S, Q, A, C, L or I, Zhang and Casey, 1996; Hougland et al., 2010). CaaX motifs are targeted by prenyltransferases that attach either a farnesyl (15-carbon) or a geranylgeranyl (20-carbon) isoprenoid to the cysteine residue of the motif (Zhang and Casey, 1996). The last residue in the CaaX motif (X) determines which lipid modification, farnesyl or geranylgeranyl, will be added. Farnesylation, the addition of a farnesyl group to the cysteine, occurs when the last residue is methionine, serine, alanine, cysteine or glutamine, while geranylgeranylation occurs when leucine or isoleucine occupy the position (Moores et al., 1991). The protein prenylation process includes 3 steps: polyisoprenylation, proteolysis, and carboxyl methylation. During polyisoprenylation, either farnesyltransferase (FTase) or geranylgeranyltransferase (GGTase), depending on

the identity of the last residue in CaaX, attaches the corresponding isoprenoid to the cysteine. Next, -aaX residues are proteolysed by prenyl protein peptidase Ras converting CaaX endopeptidase 1 (RCE1), and subsequently the enzyme isoprenyl-cysteine carboxyl methyltransferase (Icmt) methylates the exposed carboxy terminus (Figure 6) (Gao J. et al., 2009). These modifications are critical for their localization to the plasma membrane or other intracellular membranes (Gao J. et al., 2009; Gelb et al., 2006). In the case of PARP13, the CaaX motif is CVIS, and thus the protein is farnesylated (Charron et al., 2013).

Bioinformatics analysis predicts that hundreds of eukaryotic proteins are targets of farnesylation, but only a small subset has been experimentally validated (Maurer-Stroh and Eisenhaber, 2005). Known farnesylation targets are mostly G proteins (H-Ras, K-Ras, RhoA, etc.), nuclear membrane proteins (prelamin A, lamin B1/B2) and intracellular membrane proteins (HDJ2, CENP-E, etc.) (Philips et al., 2005; Roberts et al., 2008; Barrowman et al., 2008; Maske et al., 2003; Hussein and Taylor, 2002; Hata and Ohtsuka, 2000). These proteins are involved in important cellular functions such as differentiation and carcinogenesis. Given its oncogenic nature, Ras is one of the best-studied farnesylated proteins. Ras is a small G-protein involved in many signal transduction pathways that requires membrane association through farnesyl and/or geranylgeranyl modification for its signal transduction activity (Willumsen et al., 1984; Hancock et al., 1989; Jackson et al., 1990). Because lipid modifications are required for Ras to induce malignant transformation, invasion and metastasis, many FTase and GGTase inhibitors have been developed and studied as anticancer drugs (Jackson et al., 1990; Cox and Der, 1997; Downward, 2003;

FIGURE 6

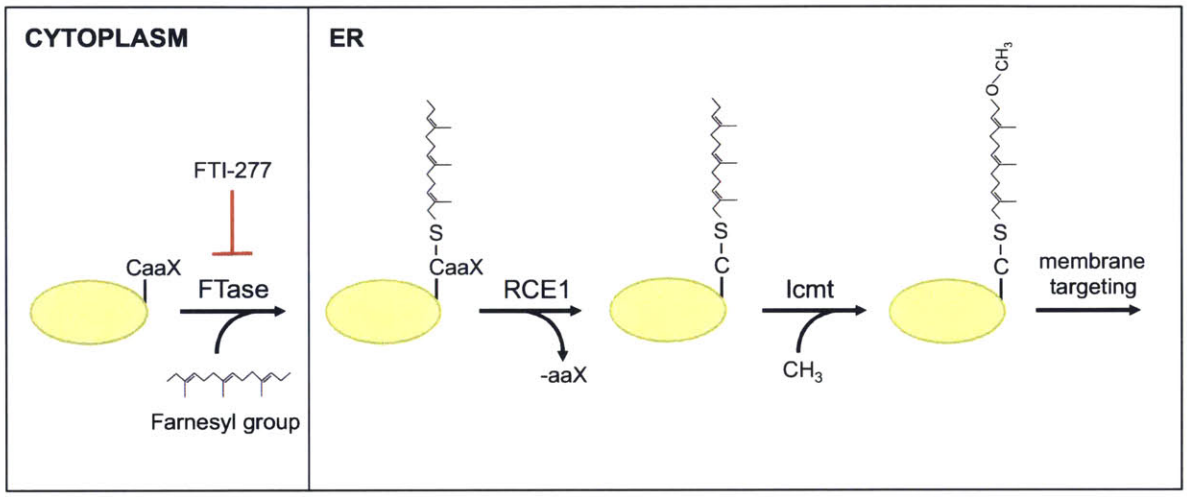

Figure 6. Mechanism of protein farnesylation. Schematic representing the farnesylation of a protein (represented in green) bearing a farnesylation CaaX motif. In the cytoplasm, farnesyltransferase (FTase) attaches a 15-carbon farnesyl group to the cysteine of the CaaX motif. The farnesylated protein is trafficked to the endoplasmic reticulum where the tripeptide aaX is cleaved by the Ras converting CaaX endopeptidase 1 (RCE1). Subsequently, the enzyme isoprenyl-cysteine carboxyl methyltransferase (Icmt) methylates the exposed carboxy terminus. The modified protein is finally targeted to membranes. Also shown is the inhibitor FTI-277 which inhibits FTase activity.

Gibbs and Oliff, 1997). One specific farnesylation inhibitor, FTI-277, acts as a structural analogue of the CaaX tetrapeptide (Lerner et al., 1995; Bernhard et al., 1998). FTI-277 is a potent inhibitor (IC_{50}= 0.5nM) and inhibits H-Ras and K-Ras farnesylation at IC_{50} values of 0.1 and 10μM, respectively, in whole cells (Lerner et al., 1995b; Sun et al., 1999).

The farnesyl modification of PARP13 was first described by Charron and colleagues. Farnesylated PARP13 was identified by prenylome profile analysis in mouse macrophages using the isoprenoid chemical reporter alkynyl-farnesol (alk-FOH) (Charron et al., 2013). The group mapped the farnesyl modification to cysteine 993 of mouse PARP13 and demonstrated that the modification targeted PARP13.1 to membranes by the analysis of a PARP13 mutant that lacked the cysteine required for the farnesyl modification. Interestingly, Charron and colleagues also discovered that farnesylation enhanced PARP13's antiviral activity against Sindbis virus (Charron et al., 2013). In this context, the authors suggested that farnesylation of PARP13 might direct the protein to endocytic membranes, where it could encounter the viral RNA upon entry. Consistent with this model, the long PARP13 isoform (that can be farnesylated) shows enhanced antiviral activity against certain viruses relative to the shorter unfarnesylated PARP13 isoform, suggesting that the farnesyl modification.

PARP13 functions

Since the discovery of its antiviral activity 13 years ago, studies of PARP13 functions have establish it as a *bona fide* cellular posttranscriptional mRNA regulator

in physiological and stress conditions. Below I will discuss some of these functions in detail.

MicroRNA silencing pathway regulation

PARP13 has been shown to have a role in microRNA silencing during cytoplasmic stress conditions (Leung et al., 2011). MicroRNAs (miRNAs) are ~22 nucleotide short noncoding RNAs that mediate RNA interference (RNAi) (Fabian et al., 2010). During RNAi, the RNA-induced silencing complex, or RISC, incorporates one strand of a miRNA or small interfering RNA (siRNA) that acts as a template for the RISC complex to recognize mRNA transcripts. Transcript recognition by the RISC complex results in posttranscriptional repression by translation inhibition or degradation of the target mRNA (Bartel, 2009; Pratt and MacRae, 2009). The endonuclease Argonaute 2 (Ago2) is responsible for the cleavage of recognized mRNAs, which leads to their subsequent degradation. Ago2 activity, and thus miRNA cleavage-mediated silencing, can be modulated by multiple mechanisms including post-translational modifications (Meister, 2013).

Ago2 is poly(ADP-ribosyl)ated during cytoplasmic stress, leading to a significant decrease in Ago2-mediated miRNA silencing (Leung et al., 2011). It is not known which PARP poly(ADP-ribosyl)ates Ago2, but the catalytically inactive PARP13 facilitates pADPr modification of Ago2 through a yet unknown mechanism. Leung and colleagues showed that overexpression of PARP13 increased the pADPr modification on Ago2, resulting in inhibition of its activity and concomitant decreased miRNA cleavage (Leung et al., 2011). In addition, PARP13-dependent poly(ADP-

ribosyl)ation of Ago2 has also been shown to inhibit miRNA-cleavage upon viral infection, during which miRNA pathways are usually suppressed (Seo et al., 2013). PARP13 is thought to anchor the activity of the catalytically active PARPs to Ago2 through its mRNA-binding domains, and thus serve to target Ago2 for poly(ADP-ribosyl)ation. By regulating Ago2 activity, PARP13 establishes itself as a posttranscriptional regulator of cellular RNAs.

Retrotransposition inhibition by PARP13

Recent studies show that PARP13 inhibits retrotransposition in human cells (Goodier et al., 2015; Moldovan and Moran, 2015). Retrotransposons are mobile DNA elements that replicate and integrate themselves into the genome using an RNA intermediate. Long INterspersed Element-1 (LINE-1 or L1) is the only active autonomous retrotransposon left in the human genome and its retrotransposition poses a threat to genome integrity and appropriate cell function (Lander et al., 2001). Therefore, the cell has evolved mechanisms to limit replication of mobile DNA. For example, PARP13 inhibits retrotransposition of L1 in human cells (Goodier et al., 2015; Moldovan and Moran, 2015). HeLa or 293T cells expressing PARP13 show decreased L1 retrotransposition and, consistent with a mechanism where PARP13 binds to L1 RNA to inhibit it, the zinc-finger domain of PARP13 alone was sufficient to elicit the same inhibitory effects (Goodier et al., 2015; Moldovan and Moran, 2015). In addition, PARP13 co-localizes with both *L1* RNA and L1's protein product, ORF1p, in cytoplasmic stress granules. Although the exact mechanism is currently unknown,

this finding suggests that the inhibition by PARP13 could take place at these foci rich in cellular factors involved in RNA metabolism.

Antiviral response

PARP13's most studied function is its antiviral activity. The first account of its antiviral activity was described by Gao and colleagues, who screened a cDNA library to identify mammalian genes that prevented retroviral infection. Expression of PARP13 or its N-terminus, which contains CCCH RNA-binding zinc fingers, caused a significant loss of viral mRNA in the cytoplasm (Gao et al., 2002). It was later demonstrated that PARP13 requires its RNA-binding zinc fingers to bind viral mRNA and thus for its antiviral activity (Guo et al., 2004). This first account of PARP13's antiviral activity led to the discovery of many other viruses that are downregulated by PARP13, including Sindbis virus (SINV), Semliki Forest virus (SFV), Ross River virus (RRV), Venezuelan Equine Encephalitis virus (VEEV), Ebola virus (EBOV), Marburg virus (MARV), Human Immunodeficiency virus 1 (HIV-1), Xenotropic Murine Leukemia virus (XMRV), Murid herpesvirus 68 (MHV-68) and Hepatitis B virus (HBV) (Bick et al., 2003; Müller et al., 2007; Zhu et al., 2011; Wang et al., 2012; Xuan et al., 2013). Although expression of PARP13 resulted in the decreased infectivity of many viruses, Bick and colleagues showed that PARP13 expression did not inhibit all viruses, because vesicular stomatitis virus, herpes simplex virus and yellow fever virus were not affected by PARP13 expression (Bick et al, 2003).

One important tool to study PAPR13's antiviral activity is to determine where PARP13 binds to its mRNA viral targets. Studies aimed at identifying RNA-binding

sites on viral mRNAs determined that PARP13 binds to the 3' long terminal repeat of MMLV, the 5' UTR of multiply spliced HIV-1, the 3' UTR of XMRV, the gene coding for the filovirus L protein in EBOV and the terminal redundancy sequences of HBV (Guo et al., 2004; Mao et al., 2013; Müller et al., 2007; Zhu et al., 2011). Given that there is no sequence homology between these RNA-binding sites and the shortest target sequence is 500 nucleotides, it was suggested that PARP13 recognizes a secondary or tertiary RNA structure (Guo et al., 2004). Consistent with this idea, X-ray crystallization studies of PARP13's CCCH-zinc fingers demonstrated that PARP13's target RNA contains specific secondary or tertiary structure in order to interact with residues in two RNA-binding cavities (Chen et al., 2012). As a result, PARP13 binding has to be tested experimentally for each putative RNA target.

PARP13's antiviral activity was shown to take place in the cytoplasm, suggesting that viral transcription initiation and elongation are not affected by PARP13 (Gao et al., 2002). This observation along with the fact that PARP13 has no exo- or endonuclease activity suggested that PARP13 is a trans-acting factor that regulates the decay of viral mRNA in the cytoplasm.

Most cytoplasmic mRNAs are degraded by exonucleases acting at their 3' or 5' end. Exonuclease decay starts with shortening of the poly(A) tail of the transcript by PARN, CCR4-NOT or PAN2/3 deadenylases. After poly(A) removal, the exposed 3' end of mRNA can be degraded by the cytoplasmic exosome complex. For 5'-3' mRNA degradation, decapping enzymes DCP1a and DCP2 remove the 5' cap of the target mRNA and subsequently the exoribonuclease XRN1 degrades the transcript in the 5'-3' direction (Figure 7) (reviewed in Schoenberg and Maquat, 2012).

FIGURE 7

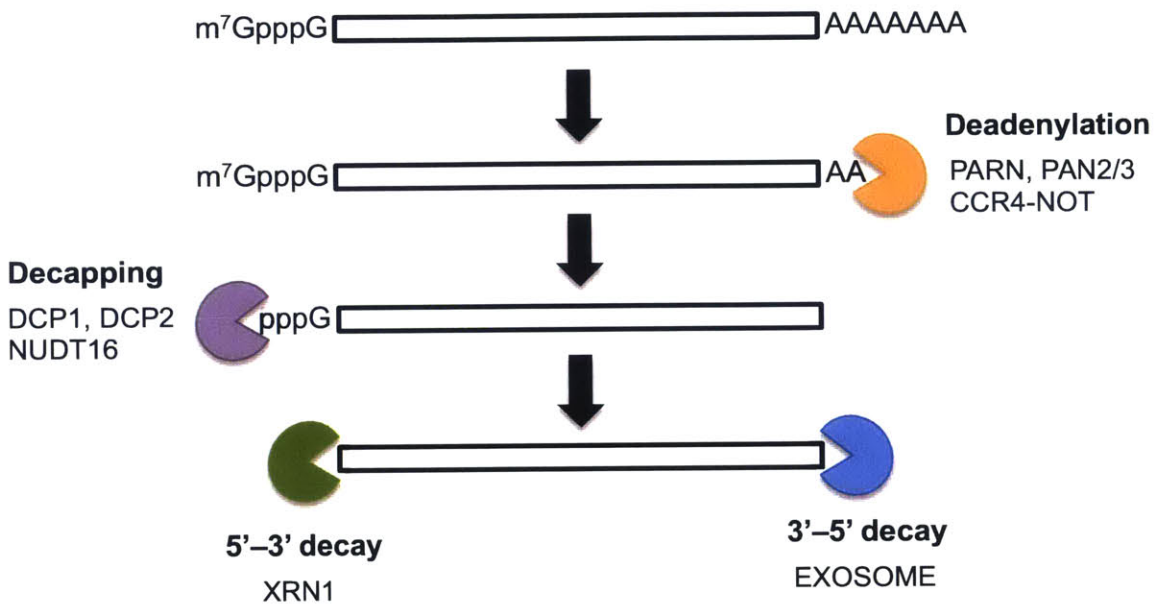

Figure 7. Exonuclease-mediated cytoplasmic mRNA decay pathway. Depiction of the major factors involved in the exonuclease mRNA decay. mRNA degradation begins by the removal of the poly(A) tail of transcripts by deadenylases PAN2/3 complex, PARN and the CCR4-NOT complex. Once deadenylated exosome complex can degrade the mRNA from 3' end. For 5'-3' mRNA decay, first decapping enzymes DCP1, DCP2 and/or NUDT16 remove the m^7G cap from the 5' end of the followed by degradation by the exonuclease XRN1 in the 5'-3' direction. Figure adapted from (Schoenberg and Maquat, 2012).

PARP13 binds directly to viral targets and recruits both the poly(A) specific ribonuclease PARN to remove the poly(A) tail and the 3'-5' exosome complex to degrade the mRNA body from the 3' end (Guo et al., 2004,2007; Zhu et al., 2011). PARP13's antiviral function requires the activity of the p72 RNA helicase, which unwinds mRNA structures for efficient degradation (Chen et al., 2008). RNA helicase p72 also recruits decapping enzymes DCP1a and DCP2 to remove the 5' cap of the target transcript, and subsequently, XRN1 is able to degrade the mRNA from 5' end (Zhu et al., 2011). The RNA helicase DHX30 has also been identified as a cofactor required for PARP13's antiviral activity, although it is unclear how it is involved (Ye et al., 2010).

PARP13 has also been implicated in translational repression of the HIV-1 viral mRNA (Zhu et al., 2012). PARP13 was shown to interact with eukaryotic initiation factor eIF4A and thus interfere with the interaction between eIF4A and eIF4G that is required for translation initiation (Zhu et al., 2012). Zhu and colleagues hypothesized that PARP13 interferes with the interaction between eIF4A-eIF4G that are associated with the target mRNA, therefore affecting viral mRNA translation only. Further studies with other viral targets have not been performed. Thus, it is still unclear if the translational repression by PARP13 is an antiviral response to all mRNA targets.

Evidence suggests that PARP13 works in concert with other host factors, like interferon-stimulated genes, to confer maximal protection against certain viral infections. Interferon proteins are secreted in response to pathogen-associated molecular patterns and trigger a signaling cascade that stimulates antiviral responses (reviewed in Samuel, 2001). In this context, PARP13 expression is induced by

treatment with interferons (IFN)-α/β/λ and also by viral infection (Ryman et al., 2005; Marcello et al., 2006; DeFilippis et al., 2006). Knockdown of PARP13 during IFN-α/β treatment decreases the interferon response to create an antiviral state against SINV virus (MacDonald et al., 2007). Furthermore, interferon regulatory factor 3 (IRF-3) induces PARP13 expression and the short isoform of PARP13, PARP13.2, interacts with retinoic-acid inducible gene-I (RIG-I) to increase RIG-I activity and thus activation of downstream antiviral response (Hayakawa et al., 2010). Taken together, these results suggest that PARP13 is also involved in the initiation of a host immune response during viral infections.

Overall, PARP13 is a key component in the cell's antiviral response, playing roles in the degradation of viral mRNA, the repression of viral mRNA translation, and the activation of the host antiviral state.

Cellular mRNA regulation

Recent studies from our lab show that PARP13 can also regulate cellular mRNAs in the absence of viral infection (Todorova et al., 2014). Both knockdown and knockout of PARP13 in several cell lines causes a significant upregulation of ER-translated transcripts, including *TRAIL-R4*. The upregulation of *TRAIL-R4* was shown to be dependent on the lack of PARP13 and its RNA binding activity, suggesting that inhibition of *TRAIL-R4* requires PARP13 RNA-binding activity. Consistent with this hypothesis, PARP13 was shown to bind to *TRAIL-R4*'s 3' UTR and target it for degradation in an exosome complex and Xrn1 exoribonuclease dependent manner.

TRAIL-R4 is a plasma membrane receptor involved in TRAIL-mediated cell death. TNF-related apoptosis-inducing ligand (TRAIL) is a protein functioning as a ligand that induces cellular apoptosis upon binding to corresponding death receptors (Wiley et al., 1995; Pitti et al., 1996). Two of the four TRAIL receptors in humans, TRAIL-R1 and TRAIL-R2, are apoptosis-inducing receptors. In contrast, the other two receptors, TRAIL-R3 and TRAIL-R4, lack functional domains necessary for apoptotic signaling. They thus act as pro-survival receptors by sequestering TRAIL ligand away from apoptotic receptors and/or by the formation of an impaired TRAIL-R4/TRAIL-R2 signaling complex (LeBlanc and Ashkenazi, 2003; Mérino et al, 2006). Consistent with TRAIL-R4's role in the apoptotic response, PARP13 depletion in several cell lines demonstrated resistance to TRAIL-mediated apoptosis by disrupting the death-inducing signaling complex (DISC) assembly and consequently its caspase-8 activation (Todorova et al., 2014). This study provided evidence of PARP13's regulation of mRNA independent of viral infection and demonstrated that the mechanism of downregulation of cellular transcripts could be similar to that of viral mRNAs. More importantly, this study proved the biological significance of PARP13's mRNA regulation and highlighted the importance of identifying other cellular targets of PARP13.

In my thesis, I identify new cellular targets of PARP13 in HeLa cells and focus on one of them for further functional assays. In the section below I provide background information about its gene product.

Delta/Notch-like epidermal growth factor-related protein (DNER)

The *DNER* gene encodes a transmembrane protein with 10 EGF-like repeats that is strongly expressed in neuronal cells, where it localizes to the plasma membrane and endosomes (Eiraku et al., 2002). DNER was identified as a non-canonical ligand of Notch and regulates many Notch-dependent functions. DNER has been shown to promote the development of Bergmann glia, regulate glioblastoma-derived neurosphere cell differentiation and tumor propagation (Eiraku et al., 2005; Sun et al., 2009). Notch signaling-independent functions of DNER include neural progenitor proliferation in zebrafish and modulation of adipogenesis of human adipose tissue-derived mesenchymal stem cells (hAMSC) (Hsieh et al., 2013, Park et al., 2010).

In Bergmann glial differentiation, the Notch receptor binds to its ligands, triggering the cleavage of the Notch intracellular domain, NICD. NICD then enters the nucleus, where it interacts with DNA-binding proteins to activate transcription of target genes (Louvi and Artavanis-Tsakonas, 2006). Eiraku and colleagues showed that DNER trans-activated Notch1 signaling, in turn regulating Bergmann glial development *in vitro* and *in vivo*. $DNER^{-/-}$ mice demonstrated abnormal glial development, suggesting that DNER regulates morphogenesis of glia during normal development of the cerebellum *in vivo* (Eiraku et al., 2005). Validating these results, recent studies have also demonstrated the same Notch-dependent role of DNER in zebrafish glial development (Hsieh et al., 2013). In addition, the same zebrafish study also showed that overexpression of DNER inhibited the proliferation of neural

progenitors through a Notch-independent mechanism (Hsieh et al., 2013). Thus, DNER has Notch-dependent and Notch-independent roles in neural development.

Notch signaling is not only essential in neuronal development, but also in pathogenesis of cancer and genetic disorders (Roy et al., 2007). Sun and colleagues identified *DNER* as a histone deacetylase inhibitor (HDAC)-induced gene that acts as a tumor suppressor and differentiating factor in glioblastoma-derived neurosphere cells (Sun et al., 2009). It was also determined that these functions of DNER were dependent on non-canonical Notch signaling through transcription factor Deltex-1 (Sun et al., 2009). The tumor-suppressive effects of DNER in this study contrast with the well-documented oncogenic role for classical Notch signaling in certain cancers. However, Notch has also been reported as a tumor suppressor in certain cell types. Therefore, it is possible that DNER acts as a tumor suppressor through the less-studied non-canonical Notch pathways (Ayaz and Osborne, 2014; Nicolas et al., 2003).

Park and colleagues identified a function for DNER in human cells by studying its role in the differentiation of human adipose tissue-derived mesenchymal stem cells (hAMSC) (Park et al., 2010). The group determined that knockdown of *DNER* altered cell morphology, inhibited proliferation and increased frequency and efficiency of adipogenesis in hAMSC (Park et al., 2010). The mechanism behind DNER's Notch-independent role in adipogenesis has yet to be identified (Park et al., 2010).

Lastly, DNER has been implicated in the regulation of neuritogenesis through the signaling of Protein Tyrosine Phosphatase ζ (PTPζ) and its ligand Pleiotrophin (PTN) (Fukazawa et al., 2008). PTPζ-PTN signaling has been previously shown to

control neurite extension and migration processes (Maeda et al., 1996; Maeda and Noda, 1998). Fukazawa and colleagues demonstrated that PTPζ associates with DNER and regulates the endocytic trafficking of the protein by showing that overexpressed DNER in Neuro-2A cells was actively endocytosed and inhibited neurite outgrowth, whereas PTN stimulation suppressed DNER's endocytosis and allowed neurite extension (Fukazawa et al., 2008). The authors speculate that DNER overexpression might activate Notch1 signaling and inhibit differentiation by *cis*-interaction (Fukazawa et al., 2008). Overall, studies of DNER function have implicated the protein in important cellular signaling pathways controlling development, differentiation and cancer pathogenesis; therefore, it seems imperative that the cell should have a mechanism to regulate its levels.

Conclusion

Recent studies of PARP13's functions under physiological conditions clearly demonstrate the biological relevance of PARP13 in mRNA regulation. Therefore, there is an increasing need to understand the mechanism by which PARP13 regulates mRNAs in the cell. My thesis seeks to identify the key PARP13 cellular targets and expand the knowledge of the requirements for their regulation in human cells. Furthermore, the appendix of this thesis presents another important aspect of PARP13 function, a novel role of the protein during endoplasmic reticulum stress. Together, these data will contribute to build a network of PARP13 targets and determine how PARP13 regulation affects the function of the transcripts' gene products.

REFERENCES

Aguiar, R.C., Yakushijin, Y., Kharbanda, S., Salgia, R., Fletcher, J.A., and Shipp, M.A. (2000). BAL is a novel risk-related gene in diffuse large B-cell lymphomas that enhances cellular migration. Blood *96*, 4328-4334.

Ahmed, S., Bott, D., Gomez, A., Tamblyn, L., Rasheed, A., Cho, T., MacPherson, L., Sugamori, K.S., Yang, Y., Grant, D.M., et al. (2015). Loss of the Mono-ADP-ribosyltransferase, Tiparp, Increases Sensitivity to Dioxin-induced Steatohepatitis and Lethality. J Biol Chem *290*, 16824-16840.

Alvarez-Gonzalez, R., and Jacobson, M.K. (1987). Characterization of polymers of adenosine diphosphate ribose generated in vitro and in vivo. Biochemistry *26*, 3218-3224.

Amé, J.C., Spenlehauer, C., and de Murcia, G. (2004). The PARP superfamily. Bioessays *26*, 882-893.

Aravind, L. (2001). The WWE domain: a common interaction module in protein ubiquitination and ADP ribosylation. Trends Biochem Sci *26*, 273-275.

Atasheva, S., Akhrymuk, M., Frolova, E.I., and Frolov, I. (2012). New PARP gene with an anti-alphavirus function. J Virol *86*, 8147-8160.

Ayaz, F., and Osborne, B.A. (2014). Non-canonical notch signaling in cancer and immunity. Front Oncol *4*, 345.

Barbarulo, A., Iansante, V., Chaidos, A., Naresh, K., Rahemtulla, A., Franzoso, G., Karadimitris, A., Haskard, D.O., Papa, S., and Bubici, C. (2013). Poly(ADP-ribose) polymerase family member 14 (PARP14) is a novel effector of the JNK2-dependent pro-survival signal in multiple myeloma. Oncogene *32*, 4231-4242.

Barrowman, J., Hamblet, C., George, C.M., and Michaelis, S. (2008). Analysis of prelamin A biogenesis reveals the nucleus to be a CaaX processing compartment. Mol Biol Cell *19*, 5398-5408.

Bartel, D.P. (2009). MicroRNAs: target recognition and regulatory functions. Cell *136*, 215-233.

Berger, W., Steiner, E., Grusch, M., Elbling, L., and Micksche, M. (2009). Vaults and the major vault protein: novel roles in signal pathway regulation and immunity. Cell Mol Life Sci *66*, 43-61.

Bernhard, E.J., McKenna, W.G., Hamilton, A.D., Sebti, S.M., Qian, Y., Wu, J.M., and

Muschel, R.J. (1998). Inhibiting Ras prenylation increases the radiosensitivity of human tumor cell lines with activating mutations of ras oncogenes. Cancer Res *58*, 1754-1761.

Bick, M.J., Carroll, J.W., Gao, G., Goff, S.P., Rice, C.M., and MacDonald, M.R. (2003). Expression of the zinc-finger antiviral protein inhibits alphavirus replication. J Virol *77*, 11555-11562.

Carballo, E., Lai, W.S., and Blackshear, P.J. (1998). Feedback inhibition of macrophage tumor necrosis factor-alpha production by tristetraprolin. Science *281*, 1001-1005.

Carrick, D.M., Lai, W.S., and Blackshear, P.J. (2004). The tandem CCCH zinc finger protein tristetraprolin and its relevance to cytokine mRNA turnover and arthritis. Arthritis Res Ther *6*, 248-264.

Chang, P., Coughlin, M., and Mitchison, T.J. (2005). Tankyrase-1 polymerization of poly(ADP-ribose) is required for spindle structure and function. Nat Cell Biol *7*, 1133-1139.

Chang, P., Coughlin, M., and Mitchison, T.J. (2009). Interaction between Poly(ADP-ribose) and NuMA contributes to mitotic spindle pole assembly. Mol Biol Cell *20*, 4575-4585.

Charron, G., Li, M.M., MacDonald, M.R., and Hang, H.C. (2013). Prenylome profiling reveals S-farnesylation is crucial for membrane targeting and antiviral activity of ZAP long-isoform. Proc Natl Acad Sci U S A *110*, 11085-11090.

Chen, S., Xu, Y., Zhang, K., Wang, X., Sun, J., Gao, G., and Liu, Y. (2012). Structure of N-terminal domain of ZAP indicates how a zinc-finger protein recognizes complex RNA. Nat Struct Mol Biol *19*, 430-435.

Cox, A.D., and Der, C.J. (1997). Farnesyltransferase inhibitors and cancer treatment: targeting simply Ras? Biochim Biophys Acta *1333*, F51-71.

Daugherty, M.D., Young, J.M., Kerns, J.A., and Malik, H.S. (2014). Rapid evolution of PARP genes suggests a broad role for ADP-ribosylation in host-virus conflicts. PLoS Genet *10*, e1004403.

De Vos, M., Schreiber, V., and Dantzer, F. (2012). The diverse roles and clinical relevance of PARPs in DNA damage repair: current state of the art. Biochem Pharmacol *84*, 137-146.

DeFilippis, V.R., Robinson, B., Keck, T.M., Hansen, S.G., Nelson, J.A., and Fruh, K.J. (2006). Interferon regulatory factor 3 is necessary for induction of antiviral genes

during human cytomegalovirus infection. J Virol *80*, 1032-1037.

Di Paola, S., Micaroni, M., Di Tullio, G., Buccione, R., and Di Girolamo, M. (2012). PARP16/ARTD15 is a novel endoplasmic-reticulum-associated mono-ADP-ribosyltransferase that interacts with, and modifies karyopherin-ss1. PLoS One *7*, e37352.

Diani-Moore, S., Ram, P., Li, X., Mondal, P., Youn, D.Y., Sauve, A.A., and Rifkind, A.B. (2010). Identification of the aryl hydrocarbon receptor target gene TiPARP as a mediator of suppression of hepatic gluconeogenesis by 2,3,7,8-tetrachlorodibenzo-p-dioxin and of nicotinamide as a corrective agent for this effect. J Biol Chem *285*, 38801-38810.

Downward, J. (2003). Targeting RAS signalling pathways in cancer therapy. Nat Rev Cancer *3*, 11-22.

Eiraku, M., Hirata, Y., Takeshima, H., Hirano, T., and Kengaku, M. (2002). Delta/notch-like epidermal growth factor (EGF)-related receptor, a novel EGF-like repeat-containing protein targeted to dendrites of developing and adult central nervous system neurons. J Biol Chem *277*, 25400-25407.

Eiraku, M., Tohgo, A., Ono, K., Kaneko, M., Fujishima, K., Hirano, T., and Kengaku, M. (2005). DNER acts as a neuron-specific Notch ligand during Bergmann glial development. Nat Neurosci *8*, 873-880.

Fabian, M.R., Sonenberg, N., and Filipowicz, W. (2010). Regulation of mRNA translation and stability by microRNAs. Annu Rev Biochem *79*, 351-379.

Font, J., and Mackay, J.P. (2010). Beyond DNA: zinc finger domains as RNA-binding modules. Methods Mol Biol *649*, 479-491.

Fukazawa, N., Yokoyama, S., Eiraku, M., Kengaku, M., and Maeda, N. (2008). Receptor type protein tyrosine phosphatase zeta-pleiotrophin signaling controls endocytic trafficking of DNER that regulates neuritogenesis. Mol Cell Biol *28*, 4494-4506.

Gao, G., Guo, X., and Goff, S.P. (2002). Inhibition of retroviral RNA production by ZAP, a CCCH-type zinc finger protein. Science *297*, 1703-1706.

Gao, J., Liao, J., and Yang, G.Y. (2009). CAAX-box protein, prenylation process and carcinogenesis. Am J Transl Res *1*, 312-325.

Gelb, M.H., Brunsveld, L., Hrycyna, C.A., Michaelis, S., Tamanoi, F., Van Voorhis, W.C., and Waldmann, H. (2006). Therapeutic intervention based on protein prenylation and associated modifications. Nat Chem Biol *2*, 518-528.

Gibbs, J.B., and Oliff, A. (1997). The potential of farnesyltransferase inhibitors as cancer chemotherapeutics. Annu Rev Pharmacol Toxicol *37*, 143-166.

Gibson, B.A., and Kraus, W.L. (2012). New insights into the molecular and cellular functions of poly(ADP-ribose) and PARPs. Nat Rev Mol Cell Biol *13*, 411-424.

Glasker, S., Toller, M., and Kummerer, B.M. (2014). The alternate triad motif of the poly(ADP-ribose) polymerase-like domain of the human zinc finger antiviral protein is essential for its antiviral activity. J Gen Virol *95*, 816-822.

Goenka, S., Cho, S.H., and Boothby, M. (2007). Collaborator of Stat6 (CoaSt6)-associated poly(ADP-ribose) polymerase activity modulates Stat6-dependent gene transcription. J Biol Chem *282*, 18732-18739.

Gomperts, M., Pascall, J.C., and Brown, K.D. (1990). The nucleotide sequence of a cDNA encoding an EGF-inducible gene indicates the existence of a new family of mitogen-induced genes. Oncogene *5*, 1081-1083.

Goodier, J.L., Pereira, G.C., Cheung, L.E., Rose, R.J., and Kazazian, H.H., Jr. (2015). The Broad-Spectrum Antiviral Protein ZAP Restricts Human Retrotransposition. PLoS Genet *11*, e1005252.

Guo, X., Carroll, J.W., Macdonald, M.R., Goff, S.P., and Gao, G. (2004). The zinc finger antiviral protein directly binds to specific viral mRNAs through the CCCH zinc finger motifs. J Virol *78*, 12781-12787.

Guo, X., Ma, J., Sun, J., and Gao, G. (2007). The zinc-finger antiviral protein recruits the RNA processing exosome to degrade the target mRNA. Proc Natl Acad Sci U S A *104*, 151-156.

Hancock, J.F., Magee, A.I., Childs, J.E., and Marshall, C.J. (1989). All ras proteins are polyisoprenylated but only some are palmitoylated. Cell *57*, 1167-1177.

Hata, M., and Ohtsuka, K. (2000). Murine cDNA encoding a novel type I HSP40/DNAJ homolog, mmDjA4(1). Biochim Biophys Acta *1493*, 208-210.

Hayakawa, S., Shiratori, S., Yamato, H., Kameyama, T., Kitatsuji, C., Kashigi, F., Goto, S., Kameoka, S., Fujikura, D., Yamada, T., et al. (2011). ZAPS is a potent stimulator of signaling mediated by the RNA helicase RIG-I during antiviral responses. Nat Immunol *12*, 37-44.

He, F., Tsuda, K., Takahashi, M., Kuwasako, K., Terada, T., Shirouzu, M., Watanabe, S., Kigawa, T., Kobayashi, N., Guntert, P., et al. (2012). Structural insight into the interaction of ADP-ribose with the PARP WWE domains. FEBS Lett *586*, 3858-3864.

Herzog, N., Hartkamp, J.D., Verheugd, P., Treude, F., Forst, A.H., Feijs, K.L., Lippok, B.E., Kremmer, E., Kleine, H., and Luscher, B. (2013). Caspase-dependent cleavage of the mono-ADP-ribosyltransferase ARTD10 interferes with its pro-apoptotic function. FEBS J *280*, 1330-1343.

Hottiger, M.O., Hassa, P.O., Luscher, B., Schuler, H., and Koch-Nolte, F. (2010). Toward a unified nomenclature for mammalian ADP-ribosyltransferases. Trends Biochem Sci *35*, 208-219.

Hougland, J.L., Hicks, K.A., Hartman, H.L., Kelly, R.A., Watt, T.J., and Fierke, C.A. (2010). Identification of novel peptide substrates for protein farnesyltransferase reveals two substrate classes with distinct sequence selectivities. J Mol Biol *395*, 176-190.

Hsieh, F.Y., Ma, T.L., Shih, H.Y., Lin, S.J., Huang, C.W., Wang, H.Y., and Cheng, Y.C. (2013). Dner inhibits neural progenitor proliferation and induces neuronal and glial differentiation in zebrafish. Dev Biol *375*, 1-12.

Huang, S.M., Mishina, Y.M., Liu, S., Cheung, A., Stegmeier, F., Michaud, G.A., Charlat, O., Wiellette, E., Zhang, Y., Wiessner, S., et al. (2009). Tankyrase inhibition stabilizes axin and antagonizes Wnt signalling. Nature *461*, 614-620.

Huang, Z., Wang, X., and Gao, G. (2010). Analyses of SELEX-derived ZAP-binding RNA aptamers suggest that the binding specificity is determined by both structure and sequence of the RNA. Protein Cell *1*, 752-759.

Hussein, D., and Taylor, S.S. (2002). Farnesylation of Cenp-F is required for G2/M progression and degradation after mitosis. J Cell Sci *115*, 3403-3414.

Jackson, J.H., Cochrane, C.G., Bourne, J.R., Solski, P.A., Buss, J.E., and Der, C.J. (1990). Farnesol modification of Kirsten-ras exon 4B protein is essential for transformation. Proc Natl Acad Sci U S A *87*, 3042-3046.

Jankevicius, G., Hassler, M., Golia, B., Rybin, V., Zacharias, M., Timinszky, G., and Ladurner, A.G. (2013). A family of macrodomain proteins reverses cellular mono-ADP-ribosylation. Nat Struct Mol Biol *20*, 508-514.

Juszczynski, P., Kutok, J.L., Li, C., Mitra, J., Aguiar, R.C., and Shipp, M.A. (2006). BAL1 and BBAP are regulated by a gamma interferon-responsive bidirectional promoter and are overexpressed in diffuse large B-cell lymphomas with a prominent inflammatory infiltrate. Mol Cell Biol *26*, 5348-5359.

Jwa, M., and Chang, P. (2012). PARP16 is a tail-anchored endoplasmic reticulum protein required for the PERK- and IRE1alpha-mediated unfolded protein response.

Nat Cell Biol *14*, 1223-1230.

Karlberg, T., Klepsch, M., Thorsell, A.G., Andersson, C.D., Linusson, A., and Schuler, H. (2015). Structural basis for lack of ADP-ribosyltransferase activity in poly(ADP-ribose) polymerase-13/zinc finger antiviral protein. J Biol Chem *290*, 7336-7344.

Kerns, J.A., Emerman, M., and Malik, H.S. (2008). Positive selection and increased antiviral activity associated with the PARP-containing isoform of human zinc-finger antiviral protein. PLoS Genet *4*, e21.

Kickhoefer, V.A., Siva, A.C., Kedersha, N.L., Inman, E.M., Ruland, C., Streuli, M., and Rome, L.H. (1999). The 193-kD vault protein, VPARP, is a novel poly(ADP-ribose) polymerase. J Cell Biol *146*, 917-928.

Kleine, H., Poreba, E., Lesniewicz, K., Hassa, P.O., Hottiger, M.O., Litchfield, D.W., Shilton, B.H., and Luscher, B. (2008). Substrate-assisted catalysis by PARP10 limits its activity to mono-ADP-ribosylation. Mol Cell *32*, 57-69.

Krietsch, J., Rouleau, M., Pic, E., Ethier, C., Dawson, T.M., Dawson, V.L., Masson, J.Y., Poirier, G.G., and Gagne, J.P. (2013). Reprogramming cellular events by poly(ADP-ribose)-binding proteins. Mol Aspects Med *34*, 1066-1087.

Lai, W.S., Carballo, E., Thorn, J.M., Kennington, E.A., and Blackshear, P.J. (2000). Interactions of CCCH zinc finger proteins with mRNA. Binding of tristetraprolin-related zinc finger proteins to Au-rich elements and destabilization of mRNA. J Biol Chem *275*, 17827-17837.

Lander, E.S., Linton, L.M., Birren, B., Nusbaum, C., Zody, M.C., Baldwin, J., Devon, K., Dewar, K., Doyle, M., FitzHugh, W., et al. (2001). Initial sequencing and analysis of the human genome. Nature *409*, 860-921.

LeBlanc, H.N., and Ashkenazi, A. (2003). Apo2L/TRAIL and its death and decoy receptors. Cell Death Differ *10*, 66-75.

Lerner, E.C., Qian, Y., Blaskovich, M.A., Fossum, R.D., Vogt, A., Sun, J., Cox, A.D., Der, C.J., Hamilton, A.D., and Sebti, S.M. (1995). Ras CAAX peptidomimetic FTI-277 selectively blocks oncogenic Ras signaling by inducing cytoplasmic accumulation of inactive Ras-Raf complexes. J Biol Chem *270*, 26802-26806.

Lerner, E.C., Qian, Y., Hamilton, A.D., and Sebti, S.M. (1995). Disruption of oncogenic K-Ras4B processing and signaling by a potent geranylgeranyltransferase I inhibitor. J Biol Chem *270*, 26770-26773.

Leung, A.K., Vyas, S., Rood, J.E., Bhutkar, A., Sharp, P.A., and Chang, P. (2011). Poly(ADP-ribose) regulates stress responses and microRNA activity in the

cytoplasm. Mol Cell *42*, 489-499.

Liang, J., Song, W., Tromp, G., Kolattukudy, P.E., and Fu, M. (2008). Genome-wide survey and expression profiling of CCCH-zinc finger family reveals a functional module in macrophage activation. PLoS One *3*, e2880.

Lin, W., Ame, J.C., Aboul-Ela, N., Jacobson, E.L., and Jacobson, M.K. (1997). Isolation and characterization of the cDNA encoding bovine poly(ADP-ribose) glycohydrolase. J Biol Chem *272*, 11895-11901.

Liu, L., Chen, G., Ji, X., and Gao, G. (2004). ZAP is a CRM1-dependent nucleocytoplasmic shuttling protein. Biochem Biophys Res Commun *321*, 517-523.

Louvi, A., and Artavanis-Tsakonas, S. (2006). Notch signalling in vertebrate neural development. Nat Rev Neurosci *7*, 93-102.

MacDonald, M.R., Machlin, E.S., Albin, O.R., and Levy, D.E. (2007). The zinc finger antiviral protein acts synergistically with an interferon-induced factor for maximal activity against alphaviruses. J Virol *81*, 13509-13518.

MacPherson, L., Tamblyn, L., Rajendra, S., Bralha, F., McPherson, J.P., and Matthews, J. (2013). 2,3,7,8-Tetrachlorodibenzo-p-dioxin poly(ADP-ribose) polymerase (TiPARP, ARTD14) is a mono-ADP-ribosyltransferase and repressor of aryl hydrocarbon receptor transactivation. Nucleic Acids Res *41*, 1604-1621.

Maeda, N., Nishiwaki, T., Shintani, T., Hamanaka, H., and Noda, M. (1996). 6B4 proteoglycan/phosphacan, an extracellular variant of receptor-like protein-tyrosine phosphatase zeta/RPTPbeta, binds pleiotrophin/heparin-binding growth-associated molecule (HB-GAM). J Biol Chem *271*, 21446-21452.

Maeda, N., and Noda, M. (1998). Involvement of receptor-like protein tyrosine phosphatase zeta/RPTPbeta and its ligand pleiotrophin/heparin-binding growth-associated molecule (HB-GAM) in neuronal migration. J Cell Biol *142*, 203-216.

Mao, R., Nie, H., Cai, D., Zhang, J., Liu, H., Yan, R., Cuconati, A., Block, T.M., Guo, J.T., and Guo, H. (2013). Inhibition of hepatitis B virus replication by the host zinc finger antiviral protein. PLoS Pathog *9*, e1003494.

Marcello, T., Grakoui, A., Barba-Spaeth, G., Machlin, E.S., Kotenko, S.V., MacDonald, M.R., and Rice, C.M. (2006). Interferons alpha and lambda inhibit hepatitis C virus replication with distinct signal transduction and gene regulation kinetics. Gastroenterology *131*, 1887-1898.

Maske, C.P., Hollinshead, M.S., Higbee, N.C., Bergo, M.O., Young, S.G., and Vaux, D.J. (2003). A carboxyl-terminal interaction of lamin B1 is dependent on the CAAX

endoprotease Rce1 and carboxymethylation. J Cell Biol *162*, 1223-1232.

Meister, G. (2013). Argonaute proteins: functional insights and emerging roles. Nat Rev Genet *14*, 447-459.

Merino, D., Lalaoui, N., Morizot, A., Schneider, P., Solary, E., and Micheau, O. (2006). Differential inhibition of TRAIL-mediated DR5-DISC formation by decoy receptors 1 and 2. Mol Cell Biol *26*, 7046-7055.

Meyer-Ficca, M.L., Ihara, M., Bader, J.J., Leu, N.A., Beneke, S., and Meyer, R.G. (2015). Spermatid head elongation with normal nuclear shaping requires ADP-ribosyltransferase PARP11 (ARTD11) in mice. Biol Reprod *92*, 80.

Moldovan, J.B., and Moran, J.V. (2015). The Zinc-Finger Antiviral Protein ZAP Inhibits LINE and Alu Retrotransposition. PLoS Genet *11*, e1005121.

Moores, S.L., Schaber, M.D., Mosser, S.D., Rands, E., O'Hara, M.B., Garsky, V.M., Marshall, M.S., Pompliano, D.L., and Gibbs, J.B. (1991). Sequence dependence of protein isoprenylation. J Biol Chem *266*, 14603-14610.

Muller, S., Moller, P., Bick, M.J., Wurr, S., Becker, S., Gunther, S., and Kummerer, B.M. (2007). Inhibition of filovirus replication by the zinc finger antiviral protein. J Virol *81*, 2391-2400.

Nicolae, C.M., Aho, E.R., Vlahos, A.H., Choe, K.N., De, S., Karras, G.I., and Moldovan, G.L. (2014). The ADP-ribosyltransferase PARP10/ARTD10 interacts with proliferating cell nuclear antigen (PCNA) and is required for DNA damage tolerance. J Biol Chem *289*, 13627-13637.

Nicolas, M., Wolfer, A., Raj, K., Kummer, J.A., Mill, P., van Noort, M., Hui, C.C., Clevers, H., Dotto, G.P., and Radtke, F. (2003). Notch1 functions as a tumor suppressor in mouse skin. Nat Genet *33*, 416-421.

Oka, S., Kato, J., and Moss, J. (2006). Identification and characterization of a mammalian 39-kDa poly(ADP-ribose) glycohydrolase. J Biol Chem *281*, 705-713.

Otto, H., Reche, P.A., Bazan, F., Dittmar, K., Haag, F., and Koch-Nolte, F. (2005). In silico characterization of the family of PARP-like poly(ADP-ribosyl)transferases (pARTs). BMC Genomics *6*, 139.

Park, J.R., Jung, J.W., Seo, M.S., Kang, S.K., Lee, Y.S., and Kang, K.S. (2010). DNER modulates adipogenesis of human adipose tissue-derived mesenchymal stem cells via regulation of cell proliferation. Cell Prolif *43*, 19-28.

Philips, M.R. (2005). Compartmentalized signalling of Ras. Biochem Soc Trans *33*,

657-661.

Pitti, R.M., Marsters, S.A., Ruppert, S., Donahue, C.J., Moore, A., and Ashkenazi, A. (1996). Induction of apoptosis by Apo-2 ligand, a new member of the tumor necrosis factor cytokine family. J Biol Chem *271*, 12687-12690.

Pratt, A.J., and MacRae, I.J. (2009). The RNA-induced silencing complex: a versatile gene-silencing machine. J Biol Chem *284*, 17897-17901.

Roberts, P.J., Mitin, N., Keller, P.J., Chenette, E.J., Madigan, J.P., Currin, R.O., Cox, A.D., Wilson, O., Kirschmeier, P., and Der, C.J. (2008). Rho Family GTPase modification and dependence on CAAX motif-signaled posttranslational modification. J Biol Chem *283*, 25150-25163.

Rosenthal, F., Feijs, K.L., Frugier, E., Bonalli, M., Forst, A.H., Imhof, R., Winkler, H.C., Fischer, D., Caflisch, A., Hassa, P.O., et al. (2013). Macrodomain-containing proteins are new mono-ADP-ribosylhydrolases. Nat Struct Mol Biol *20*, 502-507.

Roy, M., Pear, W.S., and Aster, J.C. (2007). The multifaceted role of Notch in cancer. Curr Opin Genet Dev *17*, 52-59.

Ryman, K.D., Meier, K.C., Nangle, E.M., Ragsdale, S.L., Korneeva, N.L., Rhoads, R.E., MacDonald, M.R., and Klimstra, W.B. (2005). Sindbis virus translation is inhibited by a PKR/RNase L-independent effector induced by alpha/beta interferon priming of dendritic cells. J Virol *79*, 1487-1499.

Samuel, C.E. (2001). Antiviral actions of interferons. Clin Microbiol Rev *14*, 778-809, table of contents.

Schoenberg, D.R., and Maquat, L.E. (2012). Regulation of cytoplasmic mRNA decay. Nat Rev Genet *13*, 246-259.

Seo, G.J., Kincaid, R.P., Phanaksri, T., Burke, J.M., Pare, J.M., Cox, J.E., Hsiang, T.Y., Krug, R.M., and Sullivan, C.S. (2013). Reciprocal inhibition between intracellular antiviral signaling and the RNAi machinery in mammalian cells. Cell Host Microbe *14*, 435-445.

Slade, D., Dunstan, M.S., Barkauskaite, E., Weston, R., Lafite, P., Dixon, N., Ahel, M., Leys, D., and Ahel, I. (2011). The structure and catalytic mechanism of a poly(ADP-ribose) glycohydrolase. Nature *477*, 616-620.

Smith, S., Giriat, I., Schmitt, A., and de Lange, T. (1998). Tankyrase, a poly(ADP-ribose) polymerase at human telomeres. Science *282*, 1484-1487.

Sun, J., Blaskovich, M.A., Knowles, D., Qian, Y., Ohkanda, J., Bailey, R.D., Hamilton,

A.D., and Sebti, S.M. (1999). Antitumor efficacy of a novel class of non-thiol-containing peptidomimetic inhibitors of farnesyltransferase and geranylgeranyltransferase I: combination therapy with the cytotoxic agents cisplatin, Taxol, and gemcitabine. Cancer Res *59*, 4919-4926.

Sun, P., Xia, S., Lal, B., Eberhart, C.G., Quinones-Hinojosa, A., Maciaczyk, J., Matsui, W., Dimeco, F., Piccirillo, S.M., Vescovi, A.L., et al. (2009). DNER, an epigenetically modulated gene, regulates glioblastoma-derived neurosphere cell differentiation and tumor propagation. Stem Cells *27*, 1473-1486.

Todorova, T., Bock, F.J., and Chang, P. (2014). PARP13 regulates cellular mRNA post-transcriptionally and functions as a pro-apoptotic factor by destabilizing TRAILR4 transcript. Nat Commun *5*.

Tuncel, H., Tanaka, S., Oka, S., Nakai, S., Fukutomi, R., Okamoto, M., Ota, T., Kaneko, H., Tatsuka, M., and Shimamoto, F. (2012). PARP6, a mono(ADP-ribosyl) transferase and a negative regulator of cell proliferation, is involved in colorectal cancer development. Int J Oncol *41*, 2079-2086.

Verheugd, P., Forst, A.H., Milke, L., Herzog, N., Feijs, K.L., Kremmer, E., Kleine, H., and Luscher, B. (2013). Regulation of NF-kappaB signalling by the mono-ADP-ribosyltransferase ARTD10. Nat Commun *4*, 1683.

Vyas, S., Chesarone-Cataldo, M., Todorova, T., Huang, Y.H., and Chang, P. (2013). A systematic analysis of the PARP protein family identifies new functions critical for cell physiology. Nat Commun *4*, 2240.

Vyas, S., Matic, I., Uchima, L., Rood, J., Zaja, R., Hay, R.T., Ahel, I., and Chang, P. (2014). Family-wide analysis of poly(ADP-ribose) polymerase activity. Nat Commun *5*, 4426.

Wahlberg, E., Karlberg, T., Kouznetsova, E., Markova, N., Macchiarulo, A., Thorsell, A.G., Pol, E., Frostell, Å., Ekblad, T., Öncü, D., Kull, B., Robertson, G.M., Pellicciari, R., Schüler, H., Weigelt, J. et al. (2012). Family-wide chemical profiling and structural analysis of PARP and tankyrase inhibitors. Nat. Biotechnol. *30*, 283–288.

Wang, X., Tu, F., Zhu, Y., and Gao, G. (2012). Zinc-finger antiviral protein inhibits XMRV infection. PLoS One *7*, e39159.

Wiley, S.R., Schooley, K., Smolak, P.J., Din, W.S., Huang, C.P., Nicholl, J.K., Sutherland, G.R., Smith, T.D., Rauch, C., Smith, C.A., et al. (1995). Identification and characterization of a new member of the TNF family that induces apoptosis. Immunity *3*, 673-682.

Willumsen, B.M., Christensen, A., Hubbert, N.L., Papageorge, A.G., and Lowy, D.R.

(1984). The p21 ras C-terminus is required for transformation and membrane association. Nature *310*, 583-586.

Xuan, Y., Gong, D., Qi, J., Han, C., Deng, H., and Gao, G. (2013). ZAP inhibits murine gammaherpesvirus 68 ORF64 expression and is antagonized by RTA. J Virol *87*, 2735-2743.

Ye, P., Liu, S., Zhu, Y., Chen, G., and Gao, G. (2010). DEXH-Box protein DHX30 is required for optimal function of the zinc-finger antiviral protein. Protein Cell *1*, 956-964.

Yu, M., Schreek, S., Cerni, C., Schamberger, C., Lesniewicz, K., Poreba, E., Vervoorts, J., Walsemann, G., Grotzinger, J., Kremmer, E., et al. (2005). PARP-10, a novel Myc-interacting protein with poly(ADP-ribose) polymerase activity, inhibits transformation. Oncogene *24*, 1982-1993.

Zhang, F.L., and Casey, P.J. (1996). Protein prenylation: molecular mechanisms and functional consequences. Annu Rev Biochem *65*, 241-269.

Zhang, Y., Liu, S., Mickanin, C., Feng, Y., Charlat, O., Michaud, G.A., Schirle, M., Shi, X., Hild, M., Bauer, A., et al. (2011). RNF146 is a poly(ADP-ribose)-directed E3 ligase that regulates axin degradation and Wnt signalling. Nat Cell Biol *13*, 623-629.

Zhu, Y., Chen, G., Lv, F., Wang, X., Ji, X., Xu, Y., Sun, J., Wu, L., Zheng, Y.T., and Gao, G. (2011). Zinc-finger antiviral protein inhibits HIV-1 infection by selectively targeting multiply spliced viral mRNAs for degradation. Proc Natl Acad Sci U S A *108*, 15834-15839.

Zhu, Y., Wang, X., Goff, S.P., and Gao, G. (2012). Translational repression precedes and is required for ZAP-mediated mRNA decay. EMBO J *31*, 4236-4246.

CHAPTER 2

FARNESYLATION-DEPENDENT REGULATION OF TRANSCRIPTS BY PARP13

Lilen Uchima and Paul Chang

LU and PC designed experiments. LU performed experiments.

INTRODUCTION

PARP13, also known as zinc finger antiviral factor, is a member of the poly(ADP-ribose) polymerase (PARP) family of human proteins. PARPs synthesize ADP-ribose modifications onto acceptor protein targets using NAD^+ as substrate and their function is important in many cellular processes (Vyas et al., 2013). PARP13 has two splice isoforms, the full length PARP13.1 and the short isoform PARP13.2. Both isoforms of PARP13 have the same N-terminal sequence, which includes four CCCH RNA-binding zinc fingers, a poly(ADP-ribose)-binding WWE domain and a nuclear localization and export sequence (Gao et al., 2004, Guo et al., 2004). This nuclear localization sequence allows PARP13 to shuttle to the nucleus, but its steady-state localization is to the cytoplasm and endoplasmic reticulum (Gao et al., 2004, Vyas et al., 2013; Todorova et al., 2014). Interestingly, both isoforms of PARP13 lack ADP-ribosylation activity due to the absence of key catalytic residues in the PARP domain of PARP13.1 and the lack of a PARP domain in PARP13.2. The PARP domain also contains a CaaX motif that targets PARP13.1 for farnesylation (Charron et al., 2013).

Farnesylation is the addition of a 15-carbon farnesyl group to a conserved cysteine residue in a C-terminal CaxX motif by the enzyme farnesyltransferase. Farnesylation modification of proteins is critical for their localization to the plasma membrane or other intracellular membranes and is essential for the function of proteins such as Ras (Gao J. et al., 2009; Gelb et al., 2006).

PARP13 was initially identified as a host antiviral factor (Gao et al, 2002). PARP13 binds to several viral mRNAs through its CCCH zinc fingers, and targets them for degradation by the cytoplasmic mRNA decay machinery (Bick et al., 2003, Guo et al., 2007; Zhu et al., 2011). Structural and functional studies have shown that PARP13 binds selectively to mRNA targets that have a certain secondary structure and does not recognize a particular linear sequence (Chen et al., 2012).

Later studies of PARP13 function in the absence of viral infection demonstrated that PARP13 also regulates cellular mRNAs. Thus far, it has three such known roles: (i) regulating miRNA silencing by targeting Argonaute2 for ADP-ribosylation; (ii) inhibiting the retrotransposition of the LINE-1 human retrotransposon by reducing L1 RNA levels and (iii) binding to the cellular mRNA *TRAIL-R4* and targeting it for degradation (Leung et al., 2011; Goodier et al., 2015; Moldovan and Moran, 2015; Todorova et al., 2014). In this last study, depletion of PARP13 caused an upregulation in membrane-associated mRNAs (including the membrane receptor *TRAIL-R4*), suggesting that PARP13 could be preferentially regulating membrane-associated transcripts.

In this chapter, I demonstrate that PARP13 localizes to the endoplasmic reticulum through RNA and farnesylation-dependent interactions and show that the farnesylation of PARP13.1 is important for the regulation of its cellular mRNA targets. Furthermore, I validate the regulation of *CERK* and *DNER*, two membrane-associated mRNAs identified in this study, and confirm that PARP13-dependent regulation of *DNER* mRNA affects one of its functions in human U87-MG cells.

RESULTS

PARP13 localizes to the membrane, where it binds RNA

Previous work from our lab showed that both isoforms of PARP13 localize to the cytoplasm as well as to the membranes of HeLa cells. Furthermore, transcriptome analysis using microarrays demonstrated an enrichment of membrane-associated and secreted transcripts that are significantly upregulated upon PARP13 knockdown in HeLa cells. To determine if PARP13 localization is both cytoplasmic and membrane-associated, HeLa cells attached to coverslips were pre-permeabilized with digitonin, fixed with 4% formaldehyde, stained with antibodies against PARP13 or organelle markers and immunofluorescence analyzed by confocal microscopy. The mild digitonin treatment permeabilized the plasma membrane, extracting all cytoplasmic proteins from the cell but leaving membrane-bound organelles intact. The release of all cytoplasmic content was confirmed by staining of the cytoplasmic protein GAPDH (Figure 1A, top left panel). In contrast, membrane-bound proteins were not released by the digitonin treatment, since membrane-bound organelles such as mitochondria (MTCO2), endoplasmic reticulum (calnexin) and Golgi apparatus (p230) were not affected by the treatment (Figure 1A). Although a subset of the PARP13 signal was extracted by digitonin treatment, significant residual signal overlapped with several membrane markers in the digitonin-treated samples. This finding suggests that PARP13 is both a cytoplasmic and a membrane-localized protein. PARP13 overlapped strongly with calnexin signal (Figure 1A top right panel),

FIGURE 1

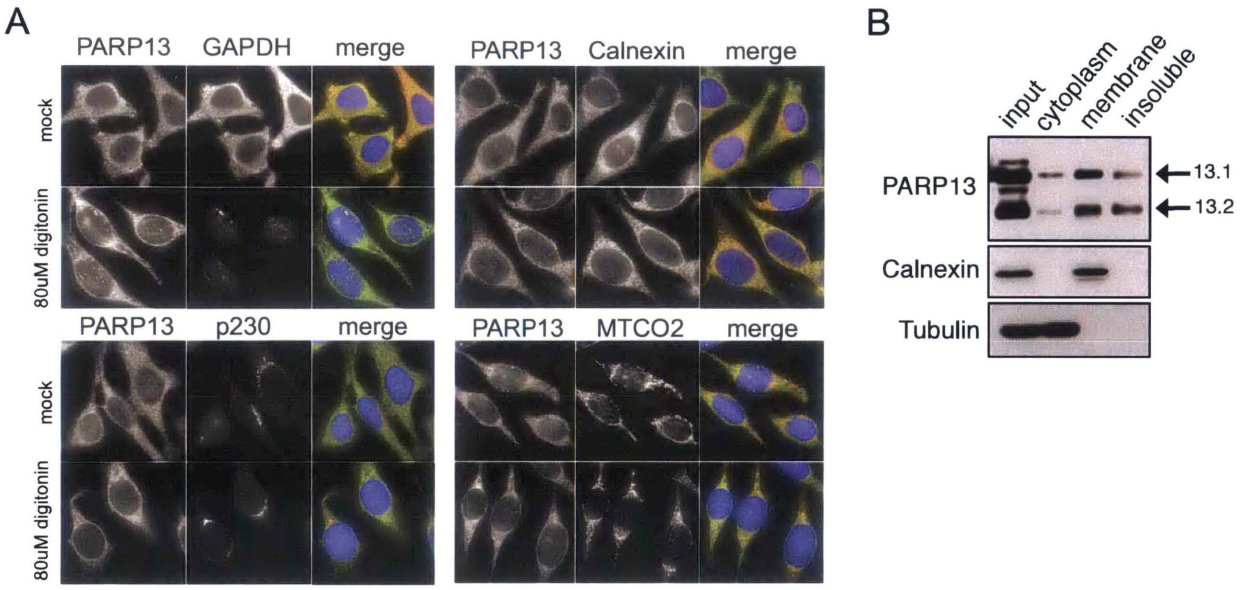

Figure 1. **PARP13 isoforms localize to cytoplasm and membranes in HeLa cells**. **(A)** Untransfected HeLa cells were extracted with 80μM digitonin for 90 seconds or mock treated and stained for PARP13 (green) and the different organelle markers (red) GAPDH (cytoplasm), calnexin (endoplasmic reticulum), p230 (Golgi) and MTCO2 (mitochondria). Nuclear staining by Hoechst (blue). **(B)** Immunoblot of 0.05% digitonin extracted (cytoplasm), 0.5% Triton X-100 extracted (membrane) and pellet of detergent extracted (insoluble) fractions of untransfected HeLa cells.

in agreement with our previous results, which identified PARP13 as an endoplasmic reticulum (ER)-localized protein.

To validate the immunofluorescence results, cells were treated with digitonin and the cytoplasmic and membrane fractions analyzed using immunoblot (Figure 1B). In addition to the cytoplasmic and membrane-associated fractions of PARP13, a subset of both PARP13.1 and 13.2 were found in the insoluble fraction, suggesting that PARP13 also localizes to the nucleus. This localization is consistent with previously published results that identified a nuclear localization sequence in PARP13 (Liu et al, 2004).

The antiviral function of PARP13 requires exosome complex activity to degrade RNA (Guo et al, 2007, Ye et al, 2010). Since we had shown that PARP13 binds to and regulates cellular mRNAs, with a strong enrichment for those that encode membrane-bound or secreted transcripts such as *TRAIL-R4* (Todorova et al, 2014), we sought to determine if membrane-associated PARP13 binds RNA. We therefore overexpressed PARP13.1 and 13.2 as streptavidin binding protein (SBP)-tagged proteins in HeLa cells and performed cross-linking immunoprecipitation (CLIP) analysis of cytoplasmic and membrane-associated fractions. As shown in Figure 2A, both isoforms of PARP13 bind RNA in the cytoplasm and membrane fractions, as demonstrated by the incorporation of ^{32}P at the molecular weight of each protein. A mock transfection control suggests that the assigned bands denoted by arrows are due to the binding of RNA to PARP13 isoforms and not to non-specific binding to the streptavidin beads. Immunoblot analysis of the samples with antibodies against PARP13 shows that these bands are SBP-PARP13 (Figure 2A, bottom).

FIGURE 2

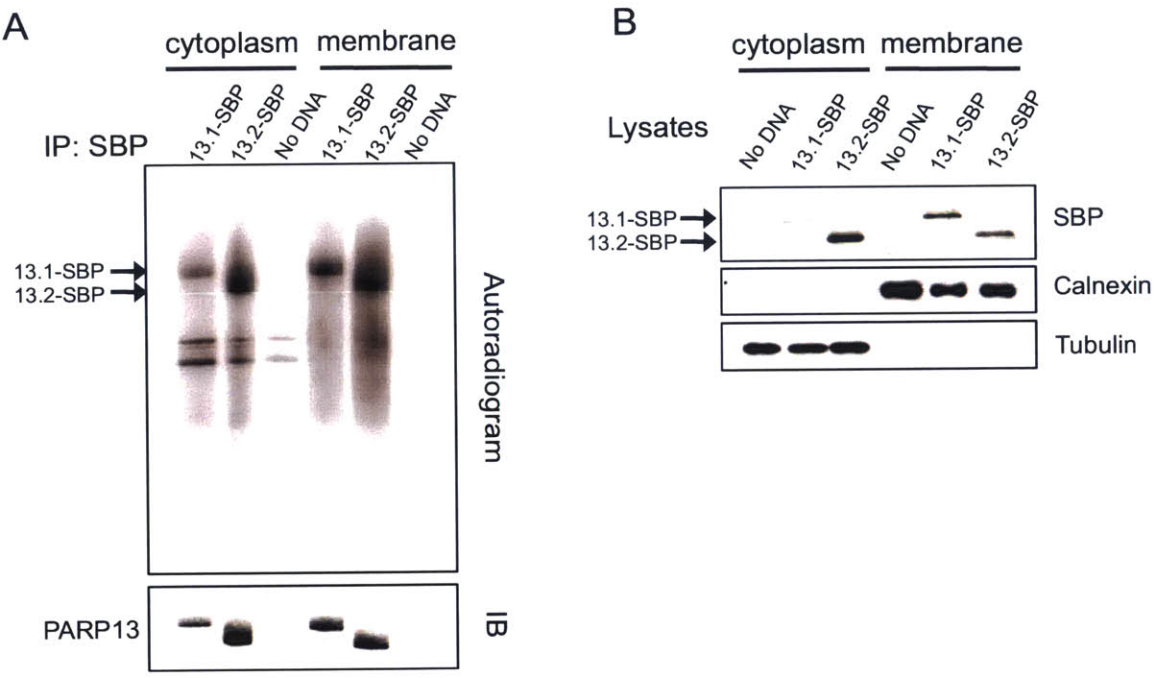

Figure 2. PARP13 binds RNA in the cytoplasm and at the membranes of HeLa cells. **(A)** CLIP assays were performed on cytoplasmic and membrane fractions of 13.1-SBP, 13.2-SBP or mock transfected HeLa cells. Immunoprecipitates containing PARP13-RNA complexes were loaded on 10% SDS PAGE and the incorporation of ^{32}P was assayed by autoradiogram (top). PARP13 immunoblot (IB) for the same samples shown below. **(B)** Immunoblots for lysates used in part **(A)** showing localization of PARP13.1-SBP and PARP13.2-SBP and cytoplasmic extraction.

Interestingly, anti-SBP immunoblots of the extracted fractions suggest that overexpressed PARP13.1-SBP is enriched at the membrane fraction, whereas overexpressed PARP13.2-SBP is enriched in the cytoplasm of HeLa cells (Figure 2B). This localization is consistent with a possible function of the PARP13.1 PARP domain in membrane localization by posttranslational modifications or interactions mediated through the domain. Furthermore, PARP13.2, which lacks the PARP domain, localizes mainly to the cytoplasm but also to the membrane fraction, suggesting that membrane localization is not entirely dependent on the presence of a PARP domain. Given that both PARP13 isoforms bind RNA in membranes, we hypothesize that RNA-binding could play a role in targeting PARP13 to membranes.

PARP13 association with membranes is dependent on farnesylation and RNA binding

To test the possibility that RNA binding targets PARP13 to membranes, we determined the subcellular localization of endogenous PARP13 by a fractionation assay in which cells were mechanically homogenized and the cytoplasm and membrane fractions were sequentially isolated by high-speed centrifugation. To determine if PARP13 association with membranes was RNA-dependent, homogenized cell fractions were split in half and either treated with 20µg/ml RNAse A or mock treated for 20 minutes and subsequently subjected to high-speed centrifugation to separate the membrane and cytoplasmic fractions. RNase A is an endoribonuclease that specifically cleaves single-stranded RNA at pyrimidine nucleotides (Raines, 1998) and thus should degrade any RNA tethering PARP13 to the membrane. Immunoblot analysis of the samples shows that upon treatment with

RNAse A, PARP13.1 and PARP13.2 are released from the membrane fraction into the cytoplasm, suggesting that the PARP13 membrane localization is RNA-dependent (Figure 3). Interestingly, a subpopulation of PARP13.1 remained associated with membranes upon RNAse A treatment, suggesting this pool of PARP13.1 is targeted to the membrane by another mechanism. Alternatively, it is possible that insufficient amounts of RNAse A were used to untether all the PARP13 protein from the membrane. Overall, this result suggests that PARP13 isoforms can localize to the membrane through a RNA-mediated interaction.

Previous work demonstrated that farnesyl modification of the C terminus of PARP13.1 targets the protein to membranes, including endolysosomes (Charron et al., 2013). To determine if PARP13 localization to the membrane is mediated primarily by binding to membrane-localized RNAs or by farnesylation, we analyzed the localization of several PARP13.1 mutants. These include an RNA-binding mutant, PARP13.1^{VYFHR}, a newly cloned farnesylation mutant of PARP13.1 (PARP13.1^{C899S}) that alters the human farnesylation site equivalent to that previously found in mouse PARP13.1, and a double mutant containing both mutations (PARP13.1^{VYFHR,C899S}) (Todorova et al., 2014; Charron et al., 2013). Clones were generated as both SBP fusions and untagged cDNAs. SBP-tagged proteins were expressed in PARP13$^{-/-}$ HeLa cells and their localization assayed by immunofluorescence after either cytoplasmic extraction or cytoplasmic extraction combined with RNAse A treatment (Figure 4). Digitonin extraction of cells expressing each of the wild type SBP-PARP13 isoforms suggests that SBP-PARP13.1 and 13.2 localize to both the cytoplasm and the membrane in HeLa cells. Cytoplasmic extraction together with

FIGURE 3

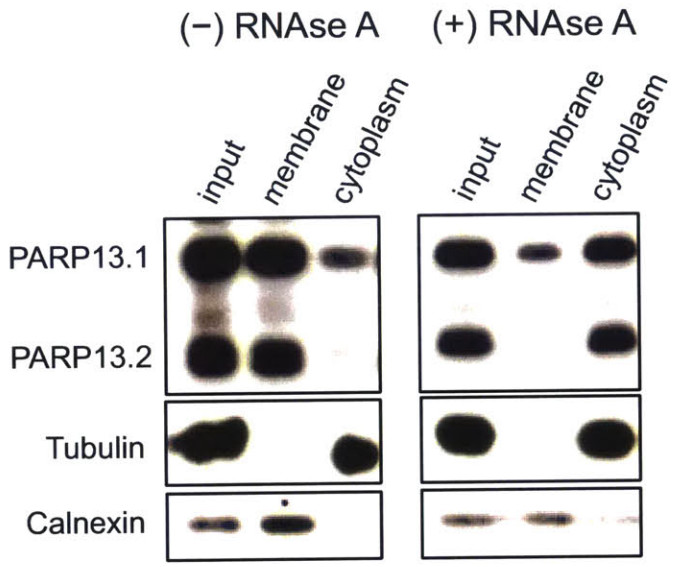

Figure 3. PARP13.1 localizes to the membrane through RNA-dependent and RNA-independent interactions. Immunoblots of input, membrane or cytoplasm fractions obtained from sequential subcellular fractionation of HeLa cells pretreated with or without RNAse A (20µg/ml) suggest PARP13.1 associates with cellular membranes through both RNA-independent and dependent interactions.

FIGURE 4

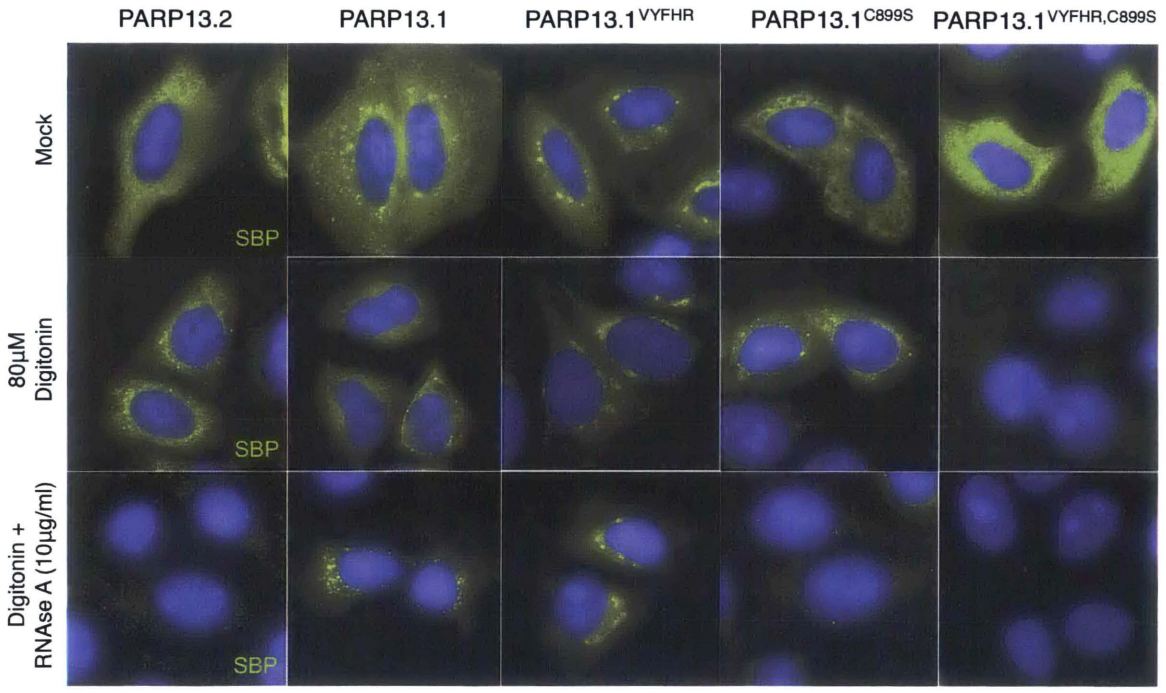

Figure 4. PARP13.1 localizes to the membrane through farnesylation and RNA-dependent interactions. **(A)** SBP-tagged PARP13 constructs were overexpressed in PARP13$^{-/-}$ cells. Cells were either mock treated (top row), extracted with 80μM digitonin for 90s (middle row) or treated with digitonin and subsequently RNAse A (10μg/ml) (bottom row). Immunofluorescent analysis was performed using SBP antibody (green) and Hoechst nuclear staining (blue). Confocal microscopy at 60X.

RNAse A treatment demonstrates that SBP-PARP13.2 localization to membranes is completely RNA-dependent, whereas SBP-PARP13.1 localization to membranes is only partially RNA-dependent, confirming our previous results (shown in Figure 3). Analysis of the RNA-binding mutant PARP13.1^{VYFHR} also suggests that localization to the membrane is not completely dependent on RNA binding, since under conditions of digitonin extraction, a portion of SBP-PARP13.1^{VYFHR} associates with the membrane. A subset of farnesylation mutant PARP13.1^{C899S} still localized to membranes upon cytoplasmic extraction. However, RNAse A treatment released nearly all of the PARP13.1^{C899S} membrane-associated signal, suggesting that PARP13.1 membrane localization is dependent on RNA binding. This was further confirmed by analysis of the double mutant SBP-PARP13.1^{VYFHR,C899S}, which displayed predominantly cytoplasmic localization, as digitonin extraction resulted in little to no membrane signal after treatment. Taken together, these data suggest that PARP13.1 localizes to membranes via both RNA and farnesylation-dependent interactions.

Expression of PARP13.1 and PARP13.1^{VYFHR} resulted in the appearance of a vesicle-like localization pattern in a subset of cells expressing high amounts of the protein. Previous work describing the farnesylation of murine PARP13.1 reported that overexpression of HA-tagged PARP13.1 in mouse embryonic fibroblasts resulted in localization to lysosomes and late endosomes. This localization was not observed when cysteine farnesylation was abrogated by mutation to serine, suggesting that localization to the lysosomes and late endosomes is due to farnesylation (Charron et al, 2013). Our analysis of highly overexpressed PARP13.1 mutants containing an

intact CaaX sequence (PARP13.1 and PARP13.1^{VYFHR}) displayed a similar lysosome and late endosome localization, as shown by co-staining of PARP13 (green) and lysosomal protein LAMP2 (red) (Figure 5, top two rows). In contrast, the PARP13 farnesylation mutants (PARP13.1^{C899S} and PARP13.1^{VYFHR,C899S}) showed no such localization (Figure 5, bottom two rows), further suggesting that the lysosomal localization was due to the farnesylation modification on cysteine 899 of PARP13.1.

Our immunofluorescence analysis suggests that PARP13 localization to the membrane is at least in part dependent on farnesylation. We confirmed this biochemically using two approaches: 1) expression of PARP13.1 mutants and 2) treatment with a farnesylation inhibitor, both followed by cytoplasmic extraction using digitonin and immunoblot analysis. The digitonin extractions performed in this study isolate cytoplasmic proteins away from membrane-bound organelle and nuclear-localized proteins. Thus, we determined the de-localization of PARP13.1 mutants from membranes by comparing the amount of cytoplasmic-localized mutant protein to cytoplasmic-localized full length PARP13.1. Immunoblot analysis of input, cytoplasmic and membrane fractions of expressed PARP13.1, PARP13.1^{C899S}, and PARP13.1^{VYFHR} mutants showed that all proteins localize to both cytoplasm and membranes, although the cytoplasmic-associated signal of the farnesylation mutant PARP13.1^{C899S} is higher relative to the other constructs (Figure 6, left). Since the levels of GAPDH (cytoplasmic protein) and calnexin (ER protein) are very similar between all samples, this disparity suggests that the farnesylation mutant PARP13.1^{C899S} did not localize as well to the membrane, and that farnesylation of expressed PARP13.1 drives membrane targeting. Mutant PARP13.1^{VYFHR} does not

FIGURE 5

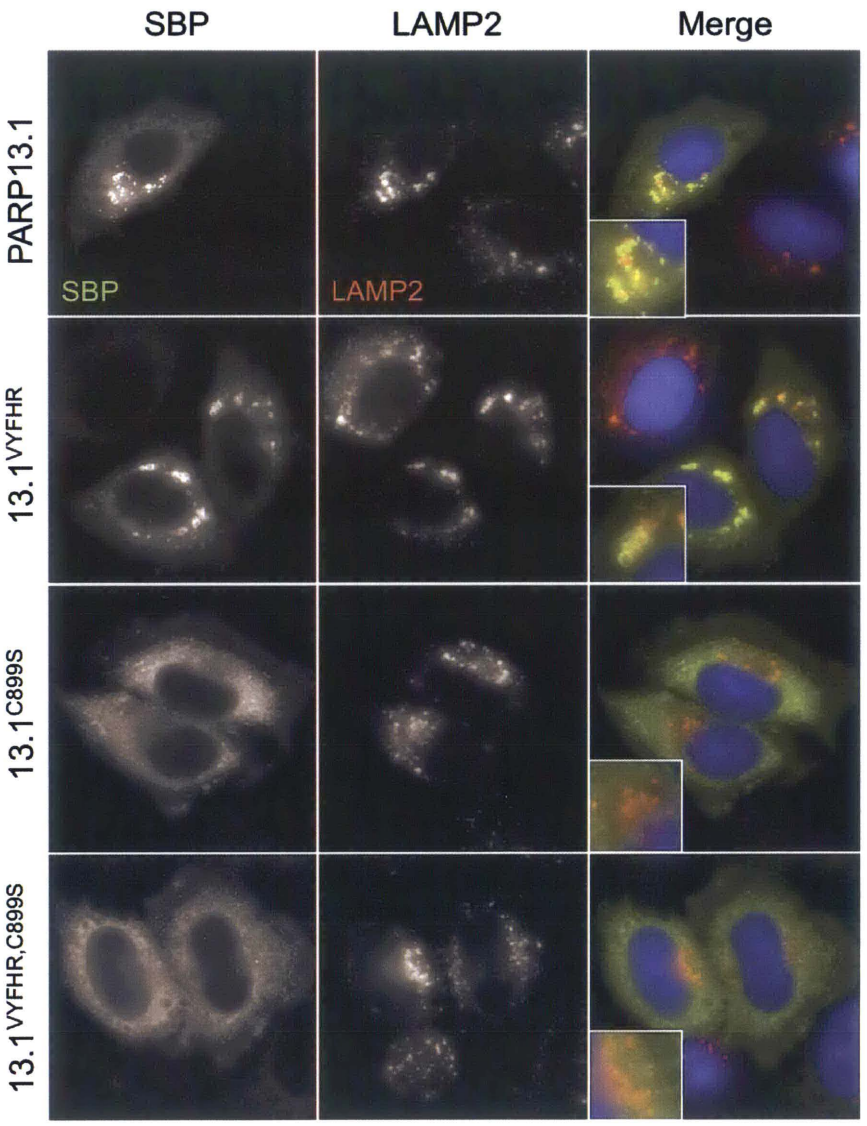
SBP
LAMP2
Merge
PARP13.1
13.1VYFHR
13.1C899S
13.1VYFHR,C899S
SBP
LAMP2

Figure 5. A subset of exogenous PARP13.1 and PARP13.1^{VYFHR} localizes to lysosomal vesicles. SBP-tagged PARP13.1 mutant and wild type constructs were expressed in PARP13$^{-/-}$ cells and immunofluorescent analysis was performed with antibodies against SBP (green), lysosomal protein LAMP2 (red) and nuclear staining with Hoechst (blue).

FIGURE 6

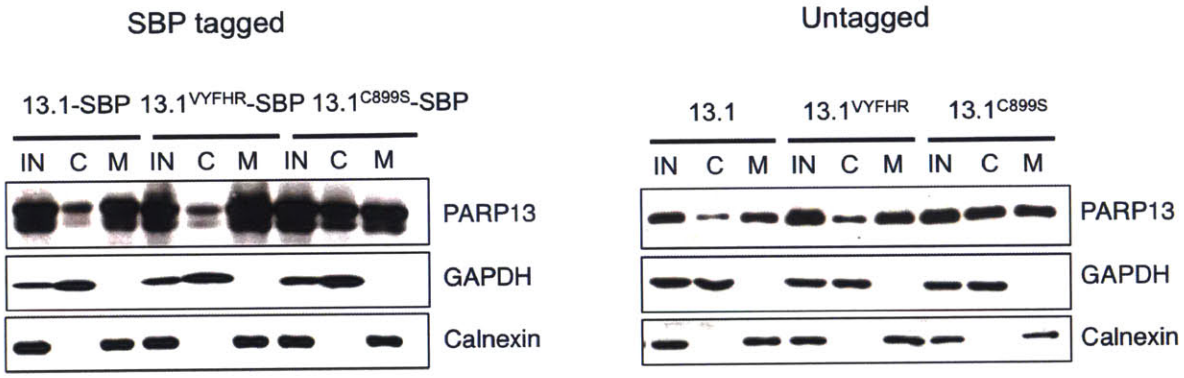

Figure 6. Farnesylation mutant SBP-PARP13.1^{C899S} or untagged PARP13.1^{C899S} show increased cytoplasmic localization. HeLa cells expressing SBP-tagged (left) or untagged (right) PARP13.1 constructs were extracted with 0.05% digitonin and the cytoplasm (supernatant) and membrane fraction (pellet) recovered by centrifugation. Immunoblot for each fraction was performed against PARP13, GAPDH (cytoplasm marker) and calnexin (ER marker).

show the same degree of release from membrane in this particular assay, suggesting that the subset of RNA-dependent localization to membrane is smaller than the farnesylation-dependent pool. Expression of untagged versions of each mutant yields the same result, suggesting that the small SBP tag does not interfere with PARP13.1 localization (Figure 6, right).

To inhibit farnesylation we used FTI-277, a potent farnesyltranferase inhibitor that acts as mimetic of the CaaX peptide, the recognition sequence for the enzyme. FTI-277 binds to the enzyme and inhibits the farnesylation of substrates such as pre-lamin A (Adjei et al, 2000). Lamin A is first synthesized as the precursor protein pre-lamin A, which must be targeted to the membrane by farnesylation at its C-terminal CaaX domain prior to maturation (Beck et al, 1990, Hennekes and Niggs, 1994). FTI-277 inhibits farnesylation of pre-lamin A and, as a consequence, unprocessed and higher molecular weight pre-lamin A accumulates (Adjei et al, 2000). We determined the inhibitory activity of FTI-277 in HeLa cells by treating cells with different concentrations of the drug for 24 hours and assaying the accumulation of pre-lamin A by immunoblot (Figure 7A). Treatment of HeLa cells with 10μM FTI-277 demonstrated ~50% accumulation of unprocessed pre-lamin A, whereas 20μM and 50μM treatment for 24 hours showed a ~92% and 98% accumulation of pre-lamin A respectively, suggesting that FTI-277 is capable of inhibiting farnesylation in HeLa cells at these concentrations. Since a complete inhibition of global cellular farnesylation could cause deleterious effects, we used 20μM FTI-277 for 24 hours to inhibit farnesylation in our experiments.

FIGURE 7

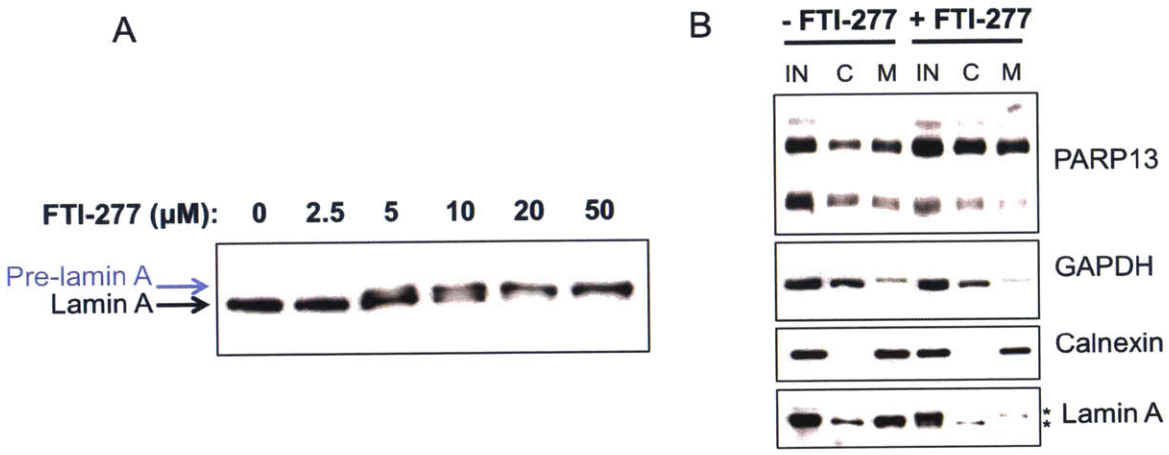

Figure 7. Farnesyltransferase inhibitor FTI-277 inhibits farnesylation and releases PARP13.1 from the membrane. (A) HeLa cells were treated with farnesylation inhibitor FTI-277 at 0, 2.5, 5, 10, 20 and 50μM for 24 hours. Lysates were then probed against Lamin A by immunoblot to assay the accumulation of unfarnesylated pre-lamin A (blue arrow). **(B)** Untransfected HeLa cells were either mock or 20μM FTI-277 treated for 24hrs. Cells were extracted with 0.05% digitonin and the cytoplasm and membrane fractions were recovered by centrifugation. Immunoblots of each fraction were probed with antibodies against PARP13, GAPDH, calnexin and lamin A.

We next performed digitonin extraction of HeLa cells with or without the addition of 20μM FTI-277 for 24 hours. The immunoblot of extracted fractions in Figure 7B demonstrates a strong enrichment of cytoplasmic PARP13.1 after FTI-277 treatment that was not seen in mock-treated cells (lane 2 vs. lane 5). Quantification of PARP13.1 protein normalized to total cytoplasmic GAPDH by ImageJ software analysis demonstrates a ~2.8-fold enrichment of PARP13.1 in the cytoplasm upon FTI-277 treatment compared to untreated fractions. Together with our mutation analysis, this result suggests that the localization of endogenous PARP13.1 to membrane is in part farnesylation-dependent.

To further confirm these results, we assayed the localization of expressed PARP13.1 and PARP13.1^{C899S} upon treatment with FTI-277. PARP13.1 or PARP13.1^{C899S} were expressed in PARP13$^{-/-}$ cells and then treated with 20μm FTI-277 for 24 hours. Cells were then analyzed by cytoplasmic extraction or immunofluorescence assays. Cytoplasmic extraction of cells using digitonin demonstrated an increased cytoplasmic SBP-PARP13.1 signal upon FTI-277 treatment, whereas no appreciable enrichment of cytoplasmic PARP13.1^{C899S} was identified (Figure 8A). This supports the hypothesis that the effect of FTI-277 on PARP13.1 membrane localization is due to the inhibition of PARP13 farnesylation at Cys899. Furthermore, and consistent with the above results, the cytoplasmic proportion of PARP13.1^{C899S} is higher than that of full-length PARP13.1 in untreated samples (Figure 8A, lane 2 vs. lane 8).

To confirm that the PARP13 localization to lysosomal vesicles observed upon PARP13.1 overexpression was due to farnesylation modification, we assayed its

FIGURE 8

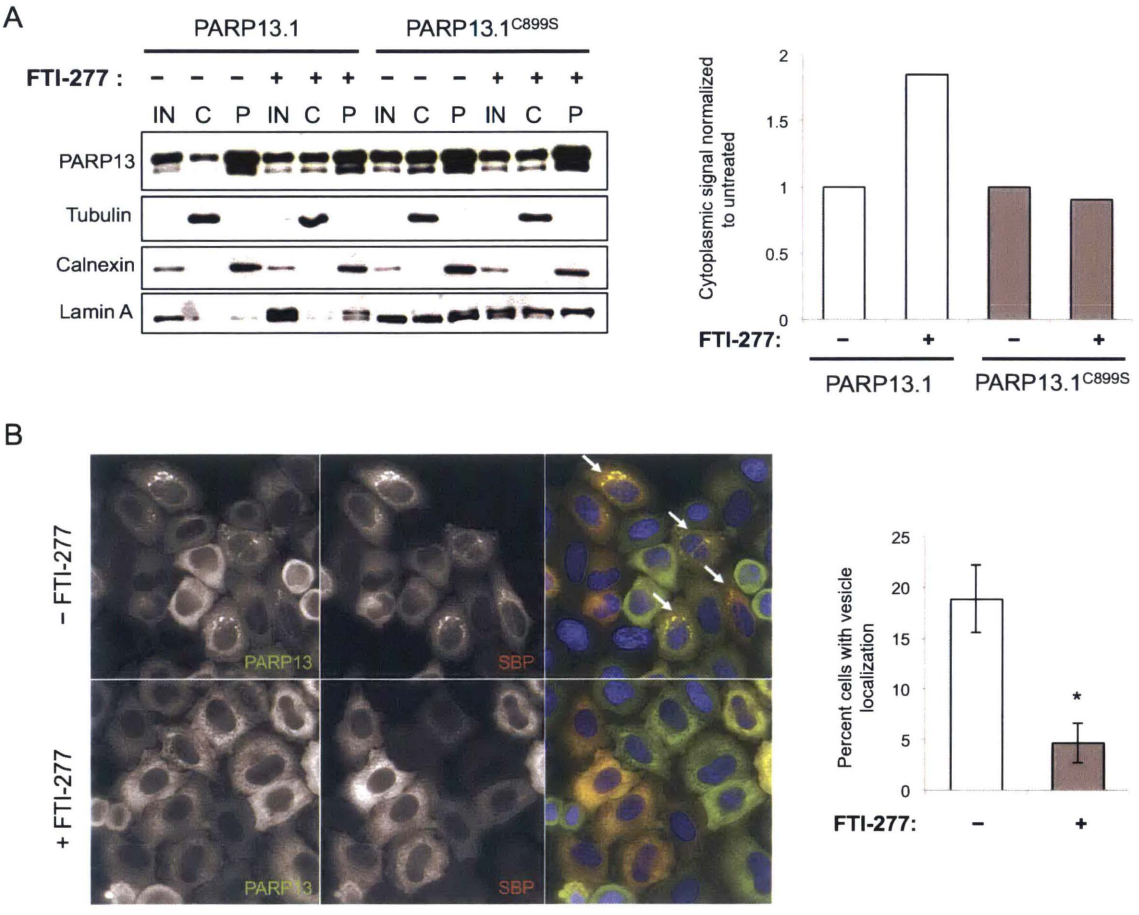
A
PARP13.1
PARP13.1C899S
FTI-277 : – – – + + + – – – + + +
IN C P IN C P IN C P IN C P
PARP13
Tubulin
Calnexin
Lamin A
Cytoplasmic signal normalized to untreated
2
1.5
1
0.5
0
FTI-277: – + – +
PARP13.1
PARP13.1C899S
B
– FTI-277
+ FTI-277
PARP13
SBP
PARP13
SBP
Percent cells with vesicle localization
25
20
15
10
5
0
*
FTI-277: – +

Figure 8. Farnesyltransferase inhibitor FTI-277 releases exogenous PARP13.1 from membranes and lysosomal vesicles. (A) (Left) PARP13$^{-/-}$ cells expressing either SBP-tagged PARP13.1 or farnesylation mutant PARP13.1^{C899S} were either mock treated or treated with 20μM FTI-277 for 24hrs. Cytoplasmic and membrane fractions were isolated by centrifugation after 0.05% digitonin treatment. Samples were probed by western blot against PARP13, tubulin, calnexin and lamin A. (Right) Quantification of the cytoplasmic signal of PARP13 normalized to tubulin signal in either FTI-277 treated or mock treated cells. **(B)** (Left) Immunofluorescence analysis of HeLa cells expressing SBP-tagged PARP13.1 either mock or treated with 20μM FTI-277 for 24hrs were stained for PARP13 (green), SBP (red) and nuclear staining Hoechst (blue). White arrows mark cells with vesicle localization. Images taken at 40X. (Right) Quantification of cells with vesicle localization upon PARP13.1 expression from either mock or FTI-277 treatment (n=2, two-sided t-test * p-value<0.05, error bars represent S.D.)

localization by immunofluorescence. HeLa cells expressing SBP-PARP13.1 treated with 20μm FTI-277 inhibitor for 24 hours or mock treated were stained for PARP13 (green) or SBP (red) and cells showing PARP13 lysosomal vesicle localization were counted (Figure 8B). Farnesylation inhibition significantly reduced the number of cells exhibiting vesicular localization of PARP13 relative to untreated cells (two tailed t-test, * p-value<0.05, n=2) (Figure 8B, right), confirming that farnesylation of overexpressed PARP13.1 causes lysosomal vesicle localization. We predict that a subset of farnesylated endogenous PARP13.1 also localizes to these structures. However, wild type cells stained for PARP13 do not exhibit significant localization to lysosomal vesicles. This observation, taken together with the fact that overexpressed HA-tagged PARP13.1 also showed a similar overexpression-related localization (Charron et al: 2013), suggests that the lysosomal localization observed when PARP13.1 is exogenously expressed is likely to be an overexpression artifact.

Given the lysosomal localization of overexpressed PARP13.1, we sought to use biochemical methods to confirm the presence of PARP13 at the endoplasmic reticulum (ER), as suggested by previous cell staining experiments. To enrich for ER membranes, we followed a well-established ER microsome isolation protocol (Stephens et al, 2008). Briefly, HeLa cells were mechanically homogenized and ER membranes were separated by density centrifugation using a discontinuous sucrose gradient. The isolate of ER membranes from HeLa cells was enriched in ER transmembrane proteins such as calnexin and devoid of cytoplasmic proteins like GAPDH as assayed by immunoblot (Figure 9A). Furthermore, the ER membrane fraction was devoid of proteins found in other membrane-bound organelles, such as

FIGURE 9

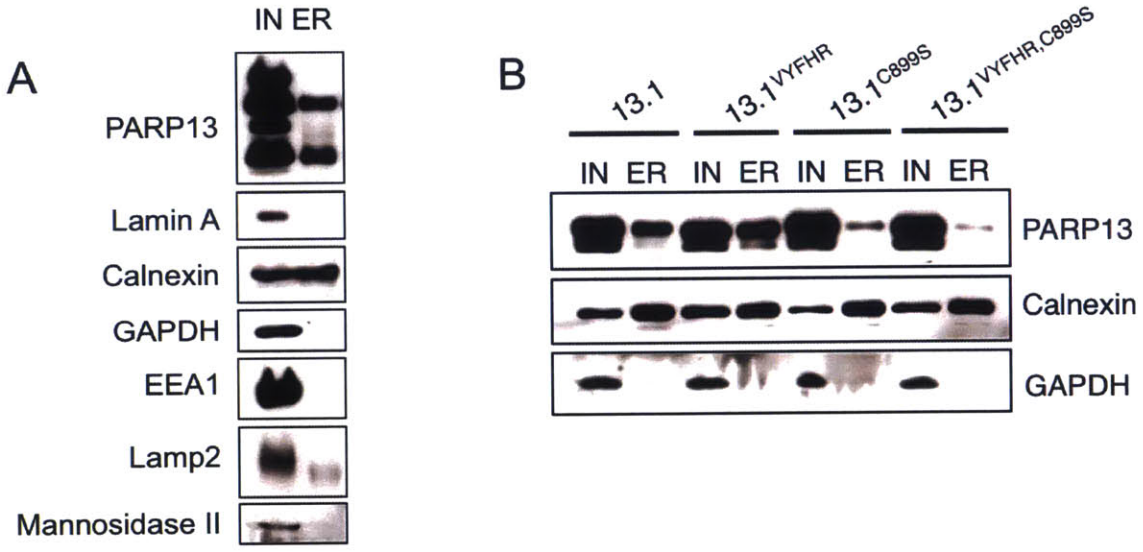

Figure 9. PARP13.1 localizes to ER through farnesylation and RNA-dependent interactions. **(A)** ER microsomes were prepared from untransfected HeLa cells by density centrifugation of discontinuous sucrose gradients and the input (IN) and ER fractions were probed for the purity of the ER isolation by organelle markers: Lamin A (nucleus), calnexin (ER), GAPDH (cytoplasm), EEA1 (endosomes), LAMP2 (lysosomes) and mannosidase II (Golgi apparatus). **(B)** ER microsomes were prepared in the same manner as A from PARP13$^{-/-}$ cells transfected with SBP tagged PARP13 mutants.

the nuclear protein lamin A, Golgi apparatus protein mannosidase II, the endosomal protein EEA1, and the lysosomal protein LAMP2 (Figure 9A), suggesting that the ER membrane fraction consisted of highly purified ER microsomes. Consistent with cell staining, these ER microsomes contained a significant amount of PARP13, confirming an ER membrane localization for PARP13.

ER microsomes were then isolated from cells expressing SBP-PARP13.1 and PARP13.1 mutants to identify the molecular requirements for localization to the ER (Figure 9B). Similar levels of PARP13.1 and the RNA-binding mutant PARP13.1^{VYFHR} were isolated from ER microsomes, whereas the farnesylation mutant PARP13.1^{C899S} demonstrated a significantly decreased localization to ER microsomes. The ER microsome signal of PARP13.1^{C899S} and double mutant PARP13.1^{VYFHR,C899S} was only ~40% and ~15%, respectively, of full-length PARP13.1, as normalized by calnexin signal. Decreased localization of PARP13.1^{C899S} to the ER microsomes suggests that farnesylation of expressed PARP13.1 is important for ER membrane targeting and the main targeting mechanism to the ER compared to RNA-binding. Double mutant PARP13.1^{VYFHR,C899S} showed less ER localization than PARP13.1^{C899S} confirming that a subset of ER-localized PARP13.1 is due to RNA-dependent interactions. Given that the expression of double mutant PARP13.1^{VYFHR,C899S} showed considerable but not complete reduction in ER localization, we hypothesize that it is possible that other factors such as protein-protein interactions could localize PARP13.1 to ER membranes.

Farnesylation is important for PARP13-dependent downregulation of transcripts

Charron and colleagues have previously shown that farnesylation is important for regulation of Sindbis viral mRNA by PARP13 (Charron et al., 2013). We therefore sought to determine if farnesylation is also important for the regulation of cellular RNAs by PARP13. To do so, we performed next-generation sequencing of total cellular mRNA in wild type HeLa cells and in PARP13$^{-/-}$ HeLa cell lines we previously generated (Todorova et al., 2014). To identify the transcripts that are regulated by PARP13 activity, specifically those that require PARP13's RNA binding activity, farnesylation activity, or both, we sequenced total RNA purified from PARP13$^{-/-}$ cells expressing wild type PARP13.1, PARP13.1^{VYFHR}, PARP13.1^{C899S} or PARP13.1^{VYFHR,C899S}. To avoid sequencing untransfected cells, cells were co-transfected with GFP and sorted for GFP signal using fluorescence-activated cell sorting (FACS). Wild type HeLa cells and PARP13$^{-/-}$ HeLa cells that were either mock-transfected or GFP-transfected were used as RNA sequencing controls. Prior to cDNA sequencing, we verified that each of the GFP sorted PARP13 $^{-/-}$ HeLa cells expressed similar amounts of PARP13.1 protein via immunoblot (Figure 10A) and that *TRAIL-R4* mRNA was regulated in a manner consistent with PARP13 RNA binding using real-time quantitative polymerase chain reaction (RT-qPCR) (Figure 10B).

Expression of full-length PARP13.1 in PARP13$^{-/-}$ cells significantly reduced the levels of *TRAIL-R4* transcript compared to PARP13$^{-/-}$ cells, whereas expression of the RNA-binding mutant PARP13^{VYFHR} did not (two tailed t-test, * p-value<0.05 ** p-

FIGURE 10

A

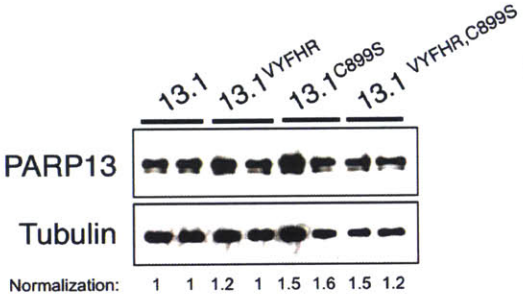

B

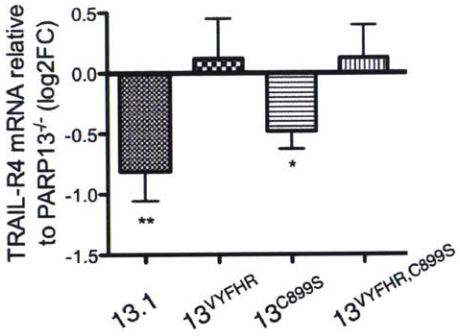

C

Sample	Total Reads	% Mapped
WT mock	2.09E+07	85.20
	2.31E+07	85.09
PARP13$^{-/-}$ mock	1.93E+07	85.01
	2.54E+07	85.01
WT + GFP	2.04E+07	85.21
	2.70E+07	84.91
PARP13$^{-/-}$ + GFP	2.15E+07	84.80
	2.49E+07	84.59
PARP13.1 + GFP	2.82E+07	84.35
	1.89E+07	85.75
PARP13^{VYFHR} + GFP	2.08E+07	84.29
	2.46E+07	84.44
PARP13^{C899S} + GFP	3.29E+07	83.75
	2.63E+07	84.31
PARP13^{VYFHR,C899S} + GFP	1.96E+07	83.70
	1.72E+07	84.75

Figure 10. RNAseq of PARP13.1 mutants. Full-length PARP13.1 and the mutants PARP13.1^{C899S,} PARP13.1^{VYFHR} and PARP13.1^{VYFHR,C899S} were expressed in PARP13$^{-/-}$ cells along with GFP. Cells were sorted by GFP expression and RNA was extracted from each and sequenced. **(A)** Immunoblot of samples from two replicates of PARP13 mutants after GFP sorting. Numbers below blots represent normalization to tubulin. **(B)** Samples for RNASeq were tested for PARP13 rescue by assaying the levels of *TRAIL-R4* mRNA by RT-qPCR. Shown are Log2 fold change *TRAIL-R4* mRNA levels compared to PARP13$^{-/-}$ cells for each expressed construct (n=3, two-sided t-test, * p-value<0.05, ** p-value<0.001, error bars represent S.D.) **(C)** Two biological replicates of PARP13.1 mutants as well as controls expressing GFP or mock transfected were submitted for RNASeq. Shown are the total number of reads for each replicate and the percent of reads that mapped to human genome Hg19.

value<0.01, n=3). Interestingly, expression of the farnesylation mutant PARP13^{C899S} also significantly reduced *TRAIL-R4* transcript levels, suggesting that farnesylation modification on PARP13 is not required for the downregulation of *TRAIL-R4*. However, the double mutant PARP13^{VYFHR,C899S} was unable to rescue *TRAIL-R4* levels, further confirming an RNA-binding requirement for PARP13 in *TRAIL-R4* mRNA regulation. Taken together these results confirm that *TRAIL-R4* is regulated by the RNA-binding activity of PARP13 and reveal that the mechanism of PARP13 regulation of *TRAIL-R4* does not require the farnesylation of PARP13.

Samples that exhibited similar expression levels of the PARP13.1 proteins and rescue of PARP13 activity were used to purify total RNA. Following these controls, RNA from two biological replicates of the following samples were submitted for sequencing: WT mock transfected, PARP13$^{-/-}$ mock transfected, WT + GFP, PARP13$^{-/-}$ + GFP, PARP13$^{-/-}$ + GFP + PARP13.1, PARP13$^{-/-}$ + GFP + PARP13^{C899S}, PARP13$^{-/-}$ + GFP + PARP13^{VYFHR} and PARP13$^{-/-}$ + GFP + PARP13^{VYFHR,C899S}. cDNAs were sequenced using Illumina's HiSeq 2000 system. As shown in Figure 10C, samples contained between 1.7 and 3.2 x10^{7} total reads, with 84-85% of reads mapping to human genome Hg19. This is sufficient to carry out differential expression analysis.

We used DESeq software to test for differential expression among our samples. From the list of genes generated by DESeq, we focused on transcripts that were differentially expressed by Log2FC(fold change)>0.5 or Log2FC<-0.5 when compared to the two sets of controls: mock wild type HeLa cells to mock PARP13$^{-/-}$ cells, and GFP transfected wild type HeLa to GFP transfected PARP13$^{-/-}$. This cutoff,

which includes both GFP and mock-transfected cells, allows us to discard genes that are differentially expressed due to GFP transfection alone. We found 2,816 differentially expressed genes using this selection criterion. Of these, 1,432 genes were upregulated and 1,384 were downregulated in PARP13$^{-/-}$ cells as compared to wild type (Figure 11A). To distinguish only the significantly up- and downregulated genes, we set our significance threshold at adjusted p-value<0.05. The use of this stringent selection criterion yields 247 significantly upregulated and 382 significantly downregulated genes in PARP13$^{-/-}$ cells relative to control cells (shown as orange dots in Figure 11B). To focus on PARP13 function in regulating the stability of cellular mRNAs, we examined the 247 transcripts that were significantly upregulated upon PARP13 depletion more carefully. The presence of downregulated transcripts in our study suggests that PARP13 could have a role in mRNA stabilization, or that their downregulation results from the misregulation of direct PARP13 targets.

To identify transcripts that are likely to be regulated by PARP13 RNA-binding, we selected those whose expression levels were rescued by expression of wild type PARP13.1 but not by expression of the RNA-binding mutant PARP13.1^{VYFHR} (downregulated in PARP13$^{-/-}$ vs. PARP13.1, adjusted p-value<0.05). Although we note that PARP13 could have RNA-independent functions, we chose to focus specifically on RNA-binding dependent transcripts. By implementing this stringent cutoff, we identified 16 transcripts that are likely to be directly regulated by PARP13. These are represented as blue dots in Figure 11B. One of these transcripts is the known PARP13 target *TRAIL-R4* providing confidence in the validity of our analyses.

FIGURE 11

A

Cutoff	# of genes	% of total	Upregulated	Downregulated
Log2FC > 0.5	2,816	9.2	1,432	1,384
Log2FC > 0.5 and FDR < 0.05	629	2	247	382
Rescued by PARP13.1 expression and not by PARP13.1^{VYFHR}	39	<1	16	23

B

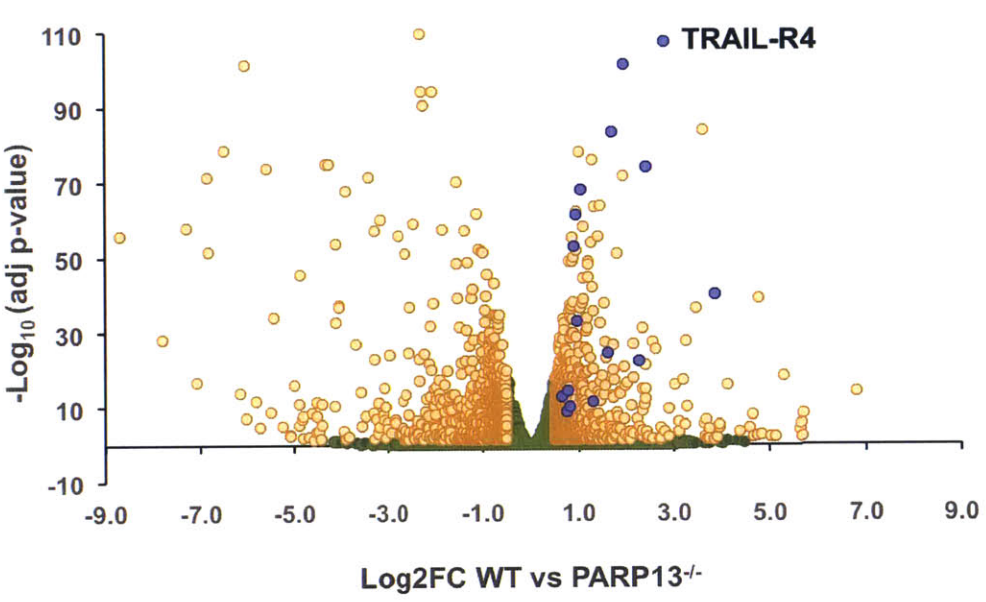

Figure 11. Genes are differentially expressed in wild type and PARP13$^{-/-}$ cells. **(A)** Number of differentially expressed transcripts in PARP13 knockout cells at different thresholds. **(B)** Volcano plot of –Log10 adjusted p-value vs Log2 fold change between wild type cells and PARP13$^{-/-}$ cells (both GFP and mock transfected) differential expression analysis. Green dots represent all non-significant differentially expressed transcripts. Orange dots denote transcripts with a Log2 fold change > 0.5 (upregulated) or Log2 fold change < -0.5 (downregulated) with adjusted p-value<0.05. Blue dots represent the 16 significantly upregulated genes that are rescued upon exogenous expression of full length PARP13.1 but not by RNA-binding mutant PARP13.1^{VYFHR}. Blue dot representing TRAIL-R4 is labeled.

To determine if the 16 PARP13-regulated transcripts are influenced by farnesylation, we examined the Log2FC and adjusted p-values of each transcript when rescued by the various PARP13 mutants. These values are listed in Figure 12A and depicted in Figure 12B, where the Log2FC for each mutant is plotted in bar graphs and asterisks represent an adjusted p-value<0.05. Interestingly, *TRAIL-R4* is the only transcript significantly rescued by farnesylation mutant PARP13.1^{C899S} in this group. This result suggests that farnesylation of PARP13.1 is not required for the regulation of *TRAIL-R4* transcript. In addition, given that the other 15 transcripts are not rescued by PARP13.1^{C899S}, it suggests that farnesylation of PARP13 is important to regulate the stability of the majority of its RNA targets.

We sought to identify the function of the additional transcripts regulated by PARP13, and to determine if there is an enrichment for those that are targeted to the membrane. To do so, we performed MetaCore and GO localization analyses. MetaCore™ uses manually curated databases to perform enrichment analysis for high-throughput data. Shown in Figure 13A are the cellular process network enrichment categories for the set of 247 significantly upregulated genes with an adjusted p-value<0.05. The top hit was for inflammation, with enrichment in complement immunity. Regulation of genes involved in the immune response is expected, since PARP13 is involved in the innate antiviral immune response (reviewed in Todorova et al, 2015). Other enriched cellular categories were in cell adhesion, cytoskeletal rearrangement and development suggesting that PARP13 could affect these cellular processes. When we performed the same enrichment

FIGURE 12

A

	Gene	Log2FC WTv13$^{-/-}$	adj p-value	Log2FC 13$^{-/-}$ v13.1	adj p-value	Log2FC 13$^{-/-}$ v 13.1^{VYFHR}	adj p-value	Log2FC 13$^{-/-}$ v 13.1^{C899S}	adj p-value	Log2FC 13$^{-/-}$ v 13.1^{VYFHR,C899S}	adj p-value
*	TRAIL-R4	2.79	4.1E-108	-0.88	2.6E-10	-0.01	1	-0.42	0.02	0.05	1
*	FAM172A	2.41	7.0E-75	-1.05	2.0E-12	-0.25	0.68	-0.32	0.53	-0.04	1
*	PRKCA	1.62	3.8E-25	-0.49	2.2E-02	-0.31	0.35	-0.39	0.17	-0.03	1
*	IFITM3	0.90	1.5E-53	-0.37	1.4E-03	-0.11	1	-0.12	1	-0.08	1
	ARNT	0.96	1.3E-33	-0.33	3.1E-02	-0.11	1	-0.05	1	0.01	1
	DDX60	0.95	5.6E-62	-0.29	1.6E-02	-0.12	1	-0.09	1	-0.09	1
	EPAS1	1.06	1.0E-68	-0.29	1.9E-02	0.04	1	-0.09	1	0.05	1
*	CERK	1.95	4.0E-102	-0.57	2.2E-06	0.02	1	-0.11	1	-0.03	1
*	DNER	1.71	3.7E-84	-0.50	3.3E-05	-0.04	1	-0.07	1	-0.06	1
	NFIX	3.86	6.7E-41	-0.69	4.4E-03	0.10	1	0.07	1	0.12	1
*	SH3BGRL	1.31	3.6E-12	-0.67	3.1E-02	-0.10	1	-0.15	1	-0.09	1
*	CHMP1B	0.66	1.4E-13	-0.34	3.6E-02	-0.06	1	-0.05	1	0.04	1
	RPL37	0.78	3.3E-15	-0.37	1.3E-03	-0.06	1	-0.09	1	0.03	1
*	LGSN	2.27	4.7E-23	-1.03	1.6E-04	-0.50	0.44	-0.48	0.95	-0.63	1
*	PLD1	0.82	8.0E-11	-0.45	3.1E-02	-0.30	0.47	-0.25	1	0.01	1
*	RAB27A	0.75	1.3E-09	-0.50	1.3E-02	-0.26	0.88	-0.22	1	-0.05	1

B

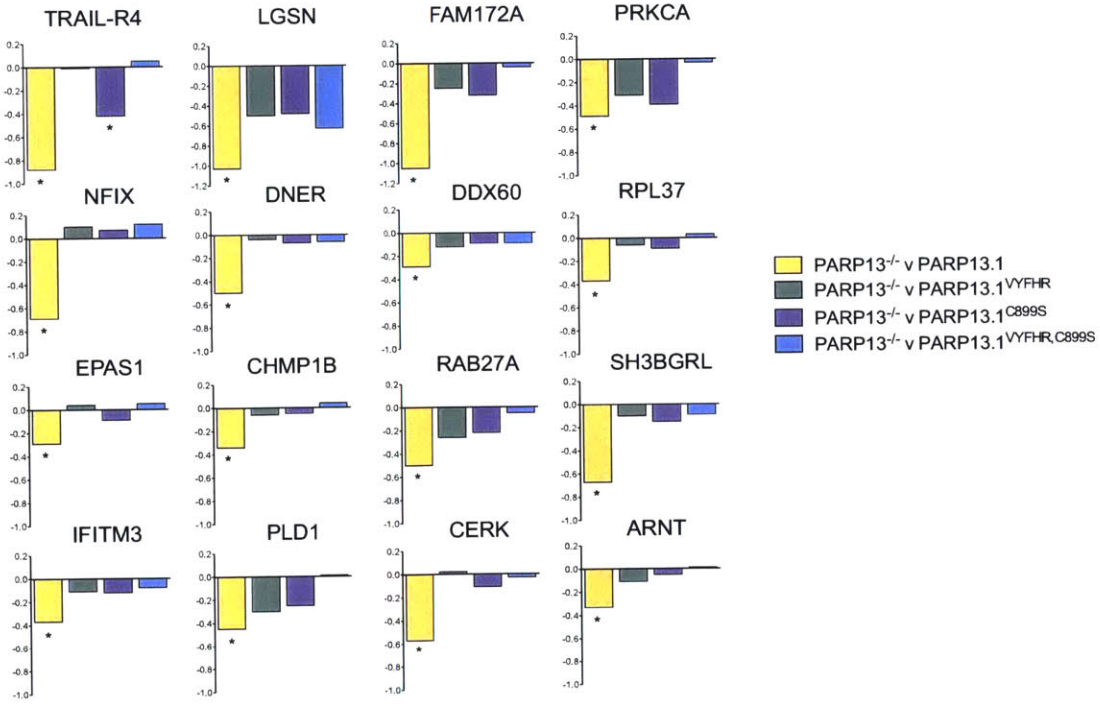

Figure 12. Sixteen significantly upregulated PARP13-dependent genes. (A) Table showing the significantly upregulated genes rescued by wild type PARP13.1 but not PARP13.1^{VYFHR} expression. Listed are the Log2 fold change values and p-adjusted values for comparisons between: wildtype vs PARP13$^{-/-}$, PARP13$^{-/-}$ vs PARP13.1, PARP13$^{-/-}$ vs PARP13.1^{VYHFR,} PARP13$^{-/-}$ vs PARP13.1^{C899S} and PARP13$^{-/-}$ vs PARP13.1^{VYHFR,C899S}. Asterisks denote gene products that localize to membranes. **(B)** Graphical representation of information depicted in table in part **(A)** (* adj p-value<0.05).

analysis on the subset of 16 genes, however, we did not find any significantly enriched cellular processes.

We also performed enrichment analysis for GO localization terms with adjusted p-value<0.05 (Figure 13B). As with previous microarray data (Todorova et al., 2014) we found that most of the GO localization terms for the 247 upregulated genes were membrane-related, such as secreted (extracellular region) and membrane associated (vesicle, cell periphery, plasma membrane, lysosome) (Figure 13B, top). Similarly, localization enrichment analysis of the set of 16 RNA binding competent PARP13-dependent upregulated genes was significantly enriched for membrane-related GO localization terms, particularly for endosomal localized gene products (Figure 13B, bottom). Furthermore, upon inspection of the annotated localization of each gene we found that 11 out of 16 (69%) have membrane-related localizations, including plasma membrane, Golgi, secreted, endosomal and lysosomal localizations (Figure 13C).

Taken together, the enrichment analyses of genes upregulated upon PARP13 knockout suggest that PARP13-regulated transcripts are more likely to be regulated based on their localization than their functional activity in the cell. Furthermore, it confirms that a considerable subset of PARP13-regulated transcripts is associated to membranes.

Validation of two farnesylation-dependent PARP13 regulated transcripts: *CERK* and *DNER*

We next validated a subset of the putative PARP13 regulated transcripts by RT-qPCR. We focused on transcripts that demonstrated high Log2FC in wild type

FIGURE 13

A

Process Network (247 genes)	p-value	Adj p-val	# of proteins
Inflammation_Complement system	2.5E-05	1.8E-03	7
Cell adhesion_Integrin-mediated cell-matrix adhesion	4.6E-05	1.8E-03	11
Development_Neurogenesis_Synaptogenesis	5.4E-05	1.8E-03	10
Cytoskeleton_Regulation of cytoskeleton rearrangement	6.2E-05	1.8E-03	10
Development_Neurogenesis_Axonal guidance	4.1E-04	9.4E-03	10
Cell adhesion_Platelet aggregation	5.9E-04	1.1E-02	8
Reproduction_Feeding and Neurohormone signaling	9.2E-04	1.3E-02	9
Cell adhesion_Cell-matrix interactions	9.2E-04	1.3E-02	9
Cell adhesion_Attractive and repulsive receptors	1.2E-03	1.5E-02	8
Development_Neuromuscular junction	1.9E-03	2.2E-02	7

B

GO Localization (247 genes)	p-value	Adj p-val	# of proteins
extracellular region	6.2E-07	4.6E-05	96
vesicle	1.4E-06	8.5E-05	76
membrane-bounded vesicle	1.6E-06	8.5E-05	74
cell periphery	2.1E-05	7.6E-04	98
plasma membrane	2.8E-05	8.8E-04	96
neuron projection	2.8E-04	5.0E-03	26
lysosome	5.3E-04	7.7E-03	16
cytoplasmic part	9.0E-04	1.2E-02	125
apical part of cell	1.6E-03	1.8E-02	13
membrane-bounded organelle	2.3E-03	2.4E-02	178

GO Localization (16 genes)	p-value	Adj p-val	# of proteins
late endosome membrane	3.16E-06	3.86E-04	4
late endosome	5.21E-05	3.17E-03	4
endosome membrane	5.22E-04	1.52E-02	5
apical part of cell	6.11E-04	1.52E-02	2
endosomal part	6.22E-04	1.52E-02	4
endosome	8.15E-03	1.66E-02	5
photoreceptor outer segment	1.81E-03	2.79E-02	2
Glucosidase II complex	1.83E-03	2.79E-02	1

C

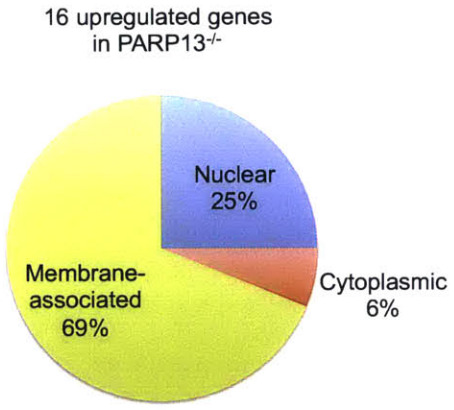

Figure 13. Enriched cellular process and localization terms in upregulated genes in PARP13$^{-/-}$ cells suggest role of localization in regulation by PARP13. **(A)** Significantly (adj p-value<0.05) enriched cellular process terms for the 247 significantly upregulated transcripts in PARP13$^{-/-}$ cells. No cellular process terms were enriched for the set of 16 PARP13 rescued transcripts. **(B)** Same analysis as in **(A)** except for GO localization terms. **(C)** Graphical representation of the localization of the gene products of the 16 transcripts significantly rescued by PARP13.1 expression but not PARP13.1^{VYFHR}.

vs. PARP13$^{-/-}$ cells, minimal Log2FC change upon PARP13^{VYFHR} mutant expression, robust expression levels in HeLa cells (count > 200), and had known biological significance. Based on these criteria, we tested ceramide kinase (CERK) and Delta and Notch-like epidermal growth factor-related (DNER), both of which are involved in important cellular functions. CERK phosphorylates ceramide, generating the signaling lipid ceramide 1-phosphate (reviewed in Bornancin, 2011), and DNER induces glial development and regulates neuroblast outgrowths (Eiraku et al., 2005; Fukazawa et al., 2008).

To validate the upregulation of *CERK* and *DNER* mRNAs, transcript levels were measured by RT-qPCR. For this assay we used the same two sets of GFP-sorted samples submitted for RNAseq along with a third set to yield three biological replicates. RT-qPCR analyses of these samples for *CERK* and *DNER* transcripts confirmed our RNAseq results. Both transcripts are only significantly rescued (One way ANOVA, ** p-value<0.01, *** p-value<0.001) by full-length PARP13.1 and not by the farnesylation, RNA-binding or double mutants when compared to PARP13$^{-/-}$ cells (Figure 14).

To confirm the farnesylation requirement for transcript regulation by PARP13, we tested the effect of the farnesylation inhibitor FTI-277 on the regulation of *CERK*, *DNER* and *TRAIL-R4* (as control) transcript levels. Wild-type PARP13.1 or farnesylation mutant PARP13.1^{C899S} were expressed in PARP13$^{-/-}$ cells that were treated with 20μm FTI-277 or mock treated for 24 hours. RT-qPCR was performed for each sample and results of two independent experiments are shown in Figure 15. Consistent with RNASeq results, *TRAIL-R4* transcript levels are rescued by

FIGURE 14

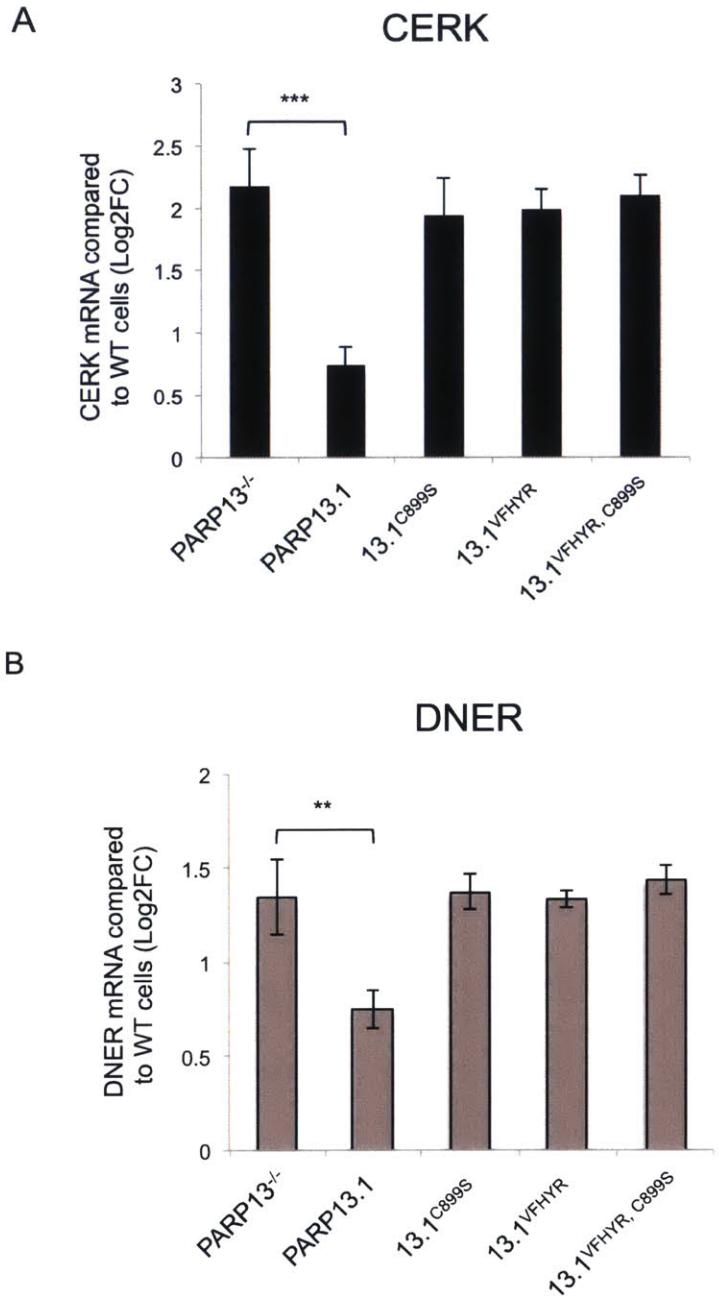
A
CERK
CERK mRNA compared to WT cells (Log2FC)
***
3
2.5
2
1.5
1
0.5
0
PARP13-/-
PARP13.1
13.1C899S
13.1VFHYR
13.1VFHYR, C899S
B
DNER
DNER mRNA compared to WT cells (Log2FC)
**
2
1.5
1
0.5
0
PARP13-/-
PARP13.1
13.1C899S
13.1VFHYR
13.1VFHYR, C899S

Figure 14. RT-qPCR validation of PARP13 regulation of CERK and DNER transcripts. PARP13$^{-/-}$ cells were expressed with SBP-tagged PARP13.1 or mutants PARP13.1^{VYFHR}, PARP13.1^{C899S} or PARP13.1^{VYFHR,C899S} along with GFP. Wild type and PARP13$^{-/-}$ cells transfected with GFP were used as controls. All samples were GFP sorted by FACS and RNA was extracted for RT-qPCR. Shown are the results for qPCR for *CERK* **(A)** and *DNER* **(B)** transcripts. (n=3, mean Log2FC compared to PARP13$^{-/-}$. One way ANOVA with Bonferroni posttest, ** p=value <0.01, *** p-value<0.001, error bars denote S.D.)

expression of both full-length PARP13.1 and PARP13.1^{C899S}, irrespective of treatment with FTI-277 (Two way ANOVA, Bonferroni posttest, ** p-value<0.01). In contrast, *CERK* and *DNER* transcript levels in PARP13.1-expressing cells are only significantly rescued in the absence of the farnesylation inhibitor and not in either treated or untreated PARP13.1^{C899S} expressing cells (Two way ANOVA, Bonferroni posttest, ** p-value<0.01). This experiment confirms the results of our differential expression analysis of the RNASeq data for these transcripts and is consistent with the hypothesis that farnesylation of PARP13.1 is important for the regulation of 15 out of 16 of its targets, including *CERK* and *DNER*.

Upregulation of *DNER* mRNA upon PARP13 depletion causes astrocytic outgrowth inhibition in U87-MG cells

To determine if PARP13 plays a role in regulating the function of transcripts that are regulated by farnesylation, we assayed DNER function. Overexpression of DNER in the mouse neuroblastoma cells line Neuro-2A, results in the decreased neurite outgrowth and causes a rounder cell morphology compared to mock transfected cells, even in the presence of the known neurite growth inducer retinoic acid (Fukazawa et al., 2008). Based on this result, we assayed the morphology of PARP13 knockdown cells in the human glioblastoma cell line U87-MG. Since *DNER* mRNA levels are upregulated upon PARP13 depletion, we expected to see a phenotype similar to DNER overexpression. First, we assayed the knockdown efficiency of PARP13 in U87-MG cells. As shown in Figure 16A, PARP13 siRNA

FIGURE 15

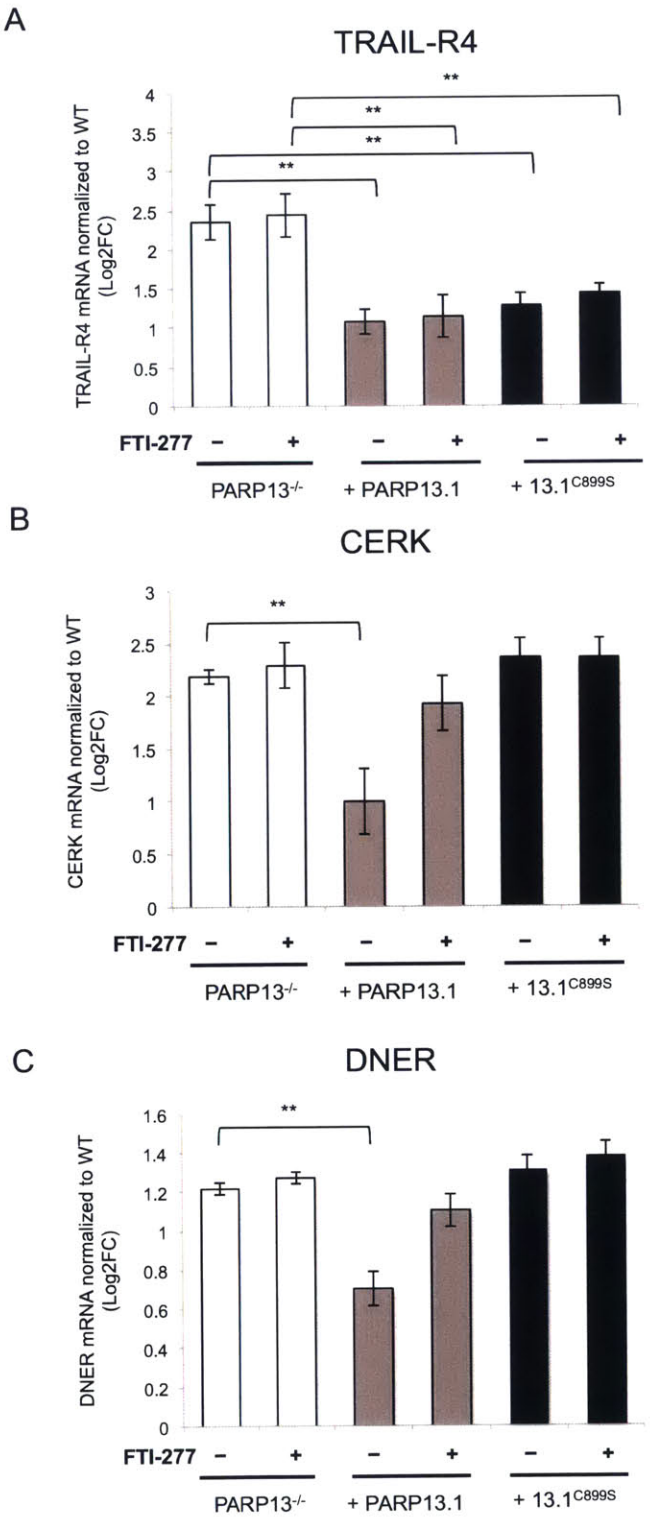
A
TRAIL-R4
TRAIL-R4 mRNA normalized to WT (Log2FC)
**
**
**
**
4
3.5
3
2.5
2
1.5
1
0.5
0
FTI-277 – + – + – +
PARP13-/-
+ PARP13.1
+ 13.1C899S
B
CERK
CERK mRNA normalized to WT (Log2FC)
**
3
2.5
2
1.5
1
0.5
0
FTI-277 – + – + – +
PARP13-/-
+ PARP13.1
+ 13.1C899S
C
DNER
DNER mRNA normalized to WT (Log2FC)
**
1.6
1.4
1.2
1
0.8
0.6
0.4
0.2
0
FTI-277 – + – + – +
PARP13-/-
+ PARP13.1
+ 13.1C899S

Figure 15. Treatment with farnesyltransferase inhibitor FTI-277 prevents the rescue of farnesylation-dependent PARP13.1 regulated transcripts. PARP13$^{-/-}$ cells were mock, PARP13.1 or PARP13.1^{C899S} transfected and either mock treated or treated with 20μM FTI-277 for 24hrs. RNA was extracted and used for RT-qPCR to determine the levels of *TRAIL-R4* **(A)**, *CERK* **(B)** and *DNER* transcripts **(C)**. (n=2, Two way ANOVA with Bonferroni posttest, mean Log2FC compared to treated or untreated PARP13$^{-/-}$, error bars show S.D. ** p-value<0.01)

knockdown in this cell line showed 70% reduction in PARP13 levels compared to control siRNA transfected cells. Furthermore, PARP13-depleted U87-MG cells showed a significant upregulation of ~1.8 fold increase (~0.8 Log2FC) in *DNER* mRNA levels (Figure 16B). To correlate the increase of *DNER* mRNA levels to protein levels, we performed immunoblot analysis with 3 different commercial antibodies raised against DNER. However, we identified no specific reactivity towards the protein in either U87-MG or HeLa cells. As an alternative, we assayed protein level by immunostaining of DNER in control, PARP13 or DNER siRNA transfected cells using wide-field quantitative microscopy. We found increased DNER immunostaining upon PARP13 knockdown and reduced signal in DNER siRNA knockdown cells as compared to control knockdown (Figure 16C). Additionally, RT-qPCR of the samples confirmed that both *PARP13* and *DNER* mRNA levels were significantly decreased upon their respective knockdowns. Furthermore, a co-knockdown of *PARP13* and *DNER* showed a similar magnitude of mRNA downregulation compared to PARP13 or DNER knockdown alone (Figure 16D). Taken together, these results suggest that knockdown of PARP13 in U87-MG cells results in increased *DNER* mRNA and protein levels.

To determine if upregulation of *DNER* in PARP13 knockdown U87-MG cells results in a phenotype similar to the one observed under DNER overexpression in Neuro-2A cells, we examined the morphology of PARP13 knockdown, DNER knockdown and PARP13-DNER co-knockdowns in U87-MG cells using differential phase contrast microscopy. Figures 17A and 17B (a higher magnification view of

FIGURE 16

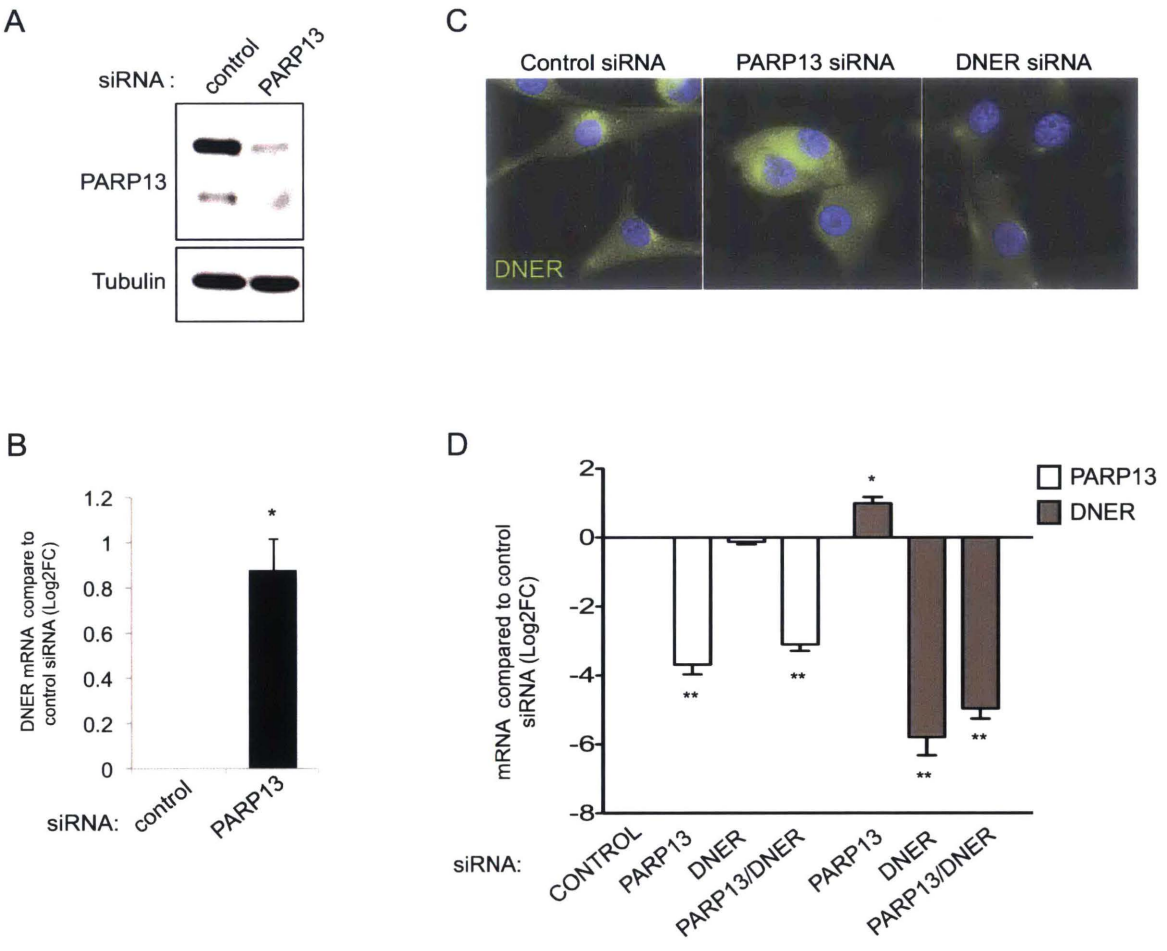
A
siRNA :
control
PARP13
PARP13
Tubulin
C
Control siRNA
PARP13 siRNA
DNER siRNA
DNER
B
DNER mRNA compare to control siRNA (Log2FC)
1.2
1
0.8
0.6
0.4
0.2
0
siRNA:
control
PARP13
D
mRNA compared to control siRNA (Log2FC)
2
0
-2
-4
-6
-8
PARP13
DNER
siRNA:
CONTROL
PARP13
DNER
PARP13/DNER
PARP13
DNER
PARP13/DNER

Figure 16. PARP13 regulates DNER mRNA levels in U87-MG cells. (A) Immunoblot for U87-MG cells transfected with control and PARP13 siRNA. **(B)** PARP13 knockdown in U87-MG cells shows increased levels of DNER mRNA compared to control siRNA as assayed by RT-qPCR (n=2, two-sided t-test, * $p<0.05$, error bar represent S.D.) **(C)** Immunofluorescent staining of DNER (green) and nucleus by Hoechst (blue) in U87-MG cells upon transfection of control, PARP13 or DNER siRNA. **(D)** RT-qPCR analysis of relative mRNA levels of *PARP13* (white bars) and *DNER* (grey bars) in PARP13, DNER, and both PARP13 and DNER knockdowns in U87-MG cells. (n=2, average Log2FC relative to control siRNA, two-sided t-test, error bars show S.D. * p-value<0.05, ** p-value<0.01).

17A) show representative images of each siRNA transfection. U87-MG cells that were depleted of PARP13 by siRNA transfection displayed a rounder cell morphology and shorter astrocytic outgrowths than control siRNA cells. In contrast, DNER-depleted cells showed no appreciable change in outgrowth length relative to those transfected with control siRNA. To determine if the phenotype seen in PARP13 knockdown cells was due to the increase in *DNER* mRNA and protein levels, we performed a double knockdown of PARP13 and *DNER* to assay the morphology of the cells. Double knockdown cells displayed similar morphology to control siRNA cells, suggesting that the phenotypic change seen in PARP13 knockdown cells is due to the increase in *DNER* levels, not the possible misregulation of other PARP13 targets. To determine the significance of the morphological change, we used the microscopy analysis software Nikon NIS-Elements to measure the length of astrocytic outgrowths from each knockdown experiment. We measured the length of outgrowths extending from the cell body to the end of the outgrowth (as shown by the colored lines in Figure 17C). Statistical analysis by two-tailed t test of two independent experiments demonstrates that astrocytic outgrowths from *PARP13* knockdown (mean=13.1μm ± 0.8, p-value=0.01) cells are significantly shorter than that of control knockdown (mean=24.4μm ± 0.9). The mean length of outgrowths in *DNER* knockdown (mean=23.5μm ± 0.4) and *PARP13* and *DNER* co-knockdown (mean=24.3μm ± 0.2) are not significantly different from control knockdowns. Taken together, these results suggest that PARP13-dependent regulation of *DNER* transcript levels affects at least one of its biological roles in human U87-MG cells.

FIGURE 17

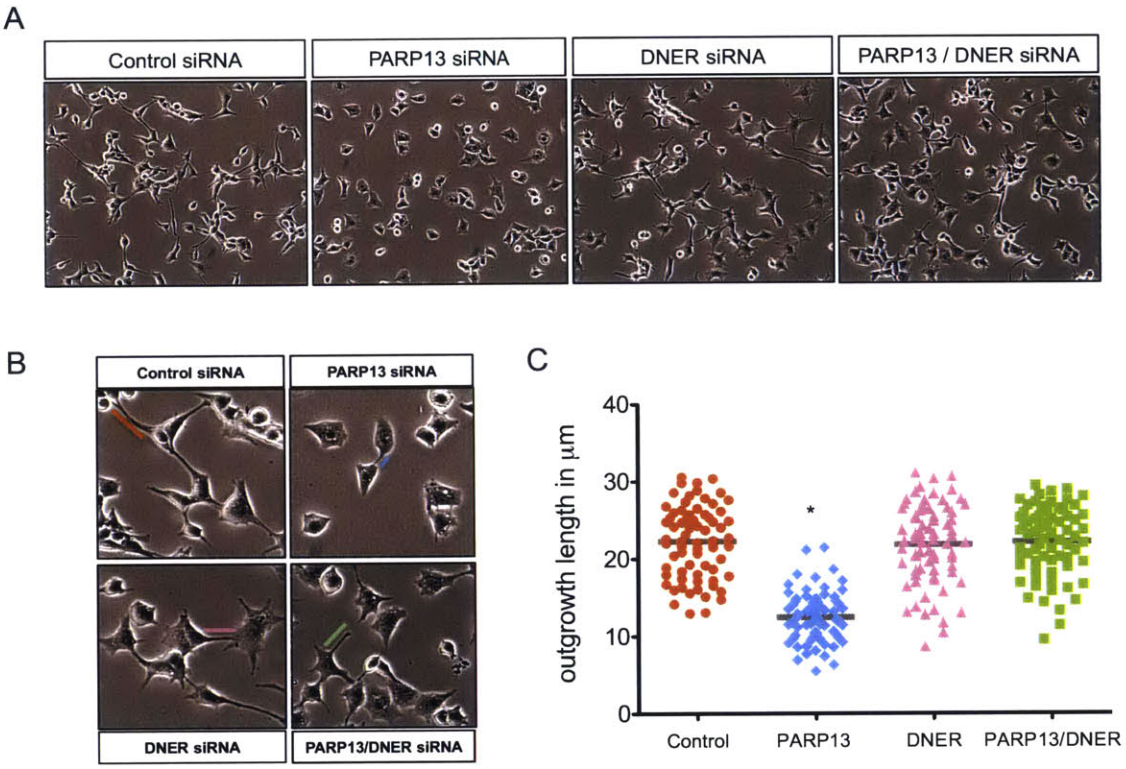
A
Control siRNA
PARP13 siRNA
DNER siRNA
PARP13 / DNER siRNA
B
Control siRNA
PARP13 siRNA
DNER siRNA
PARP13/DNER siRNA
C
outgrowth length in µm
40
30
20
10
0
*
Control
PARP13
DNER
PARP13/DNER

Figure 17. Upregulation of DNER upon PARP13 knockdown causes shorter astrocytic outgrowths in U87-MG cells. (A) PARP13, DNER and PARP13 together with DNER were knocked down with specific siRNAs in U87-MG cells. Cells were imaged with phase contrast microscopy at 20X and images were taken to assess morphological changes upon knockdown. **(B)** Magnified images of cells in **(A)** with colored lines (red= control siRNA, blue=PARP13 siRNA, pink=DNER siRNA, green=PARP13/DNER siRNAs) representing examples of the outgrowth lengths quantified in (C). **(C)** Outgrowth lengths from each knockdown were measured using Nikon NIS Elements software. Plotted are the raw measurements from two independent experiments for each treatment. Statistical significance of two independent experiments was measured by comparing mean length of control siRNA to mean length of knockdowns (n=2, two-sided t test, * p-value<0.05).

DISCUSSION

In this study we used rescue analysis of PARP13$^{-/-}$ cells to identify 16 PARP13-regulated transcripts, the majority of which encode proteins translated at the ER. In addition, we demonstrate the requirement of a farnesylation modification for the PARP13-dependent regulation of cellular mRNA targets. Furthermore, we show that PARP13-dependent regulation of Delta/notch-like EGF-related receptor (DNER) mRNA results in the regulation at the protein level and affects DNER activity in human U87-MG cells.

A previous report found that farnesylation of murine PARP13.1 C terminus targeted the protein to membranes and enhanced its antiviral activity towards Sindbis virus (Charron et al., 2013). Similarly, our results suggest that farnesylation of human PARP13.1 targets the protein to membranes, particularly to the endoplasmic reticulum. In addition, our results show that a smaller subset of PARP13.1 localizes to the ER through RNA-dependent interactions, suggesting that the ER localization is primarily dependent on the farnesylation of PARP13.1 and to a lesser degree to its RNA-binding activity. Although the exact mechanism of RNA-dependent localization of PARP13 to the ER is not known, PARP13 could be interacting with mRNAs on their way to being translated at the ER and thus targeting the protein there, and/or PARP13 could be binding to mRNAs that are already tethered to the ER.

Interestingly, our data shows that farnesylation of PARP13.1 plays an important role in PARP13's physiological function of mRNA regulation. In fact, 15 out of 16 of the putative mRNAs targets identified in this study, require the farnesylation

of PARP13.1 for their regulation. This result, combined with previous data showing that most PARP13 targets are ER-translated, suggest that PARP13 localization to membrane is important for the regulation of membrane-associated mRNA transcripts by PARP13 (Todorova et al., 2014). Our result does not preclude the possibility that non-farnesylated PARP13.1 can regulate the stability of membrane transcripts, as demonstrated by the regulation of *TRAIL-R4* by the farnesylation mutant PARP13.1^{C899S} in our rescue experiments. However, *TRAIL-R4* seems to be the exception rather than the rule, because it is the only transcript identified in our set of 16 to be rescued by PARP13.1^{C899S}. Why farnesylation of PARP13 is not required for the regulation of the membrane-associated *TRAIL-R4* transcript is currently unknown. However, it is possible that the interaction of PARP13 with *TRAIL-R4* mRNA is robust enough that direct membrane targeting of PARP13 via farnesylation is not required for its regulation.

Although our set of putative PARP13 targets are enriched for membrane-associated transcripts, there are five that do not encode secreted or membrane proteins. Our results show that PARP13 binds RNA at membranes, but we and others have shown that PARP13 also binds RNA in the cytoplasm (Gao et al., 2002; Leung et al., 2011; Goodier et al., 2015). Thus, it is possible that PARP13 regulates cytoplasmic-translated transcripts as well. Another possibility is that some of the PARP13 targets found in this study might not necessarily be direct targets of PARP13, but rather misregulated as a downstream consequence of the regulation of a direct PARP13 target. Validation of binding of PARP13 to these mRNAs is required to prove they are indeed PARP13 targets.

How PARP13 regulates transcripts at the membrane is still unknown. Since the regulation of both viral mRNAs and the cellular transcript *TRAIL-R4* is mediated by 3'-5' degradation by the exosome complex and 5'-3' action of XRN1 exonuclease (Guo et al., 2007; Zhu et al., 2011; Todorova et al., 2014), we hypothesize that PARP13 most likely downregulates the newly identified transcripts by serving as a trans-acting factor in a similar manner. An emerging body of evidence demonstrates that RNA-binding proteins, translational regulators, and ribonucleases localize to the ER to carry out their functions (reviewed in Reid and Nicchitta, 2015). For example, recent studies suggest that both miRNA- and siRNA-mediated mRNA silencing take place in association with the ER membrane (Stalder et al., 2013; Li et al., 2013). Furthermore, XRN1 5'-3' exonuclease was also shown to localize to the ER and degrade cleaved mRNA there (Stalder et al., 2013). Therefore, it is plausible that the downregulation of mRNA targets of farnesylated PARP13.1 occurs in association with the ER membrane and is carried out by mRNA decay factors that are localized there, such as XRN1.

How PARP13 recognizes mRNAs targeted to the ER is not known. Structural analysis of PARP13's CCCH zinc fingers shows that RNA binding to PARP13 requires key nucleotides spread along secondary or tertiary RNA structure (Chen et al., 2012). Another study suggested that G-rich aptamers with predicted stem-loop structures containing "GGGUGG" and "GAGGG" motifs in the loop region (also known as Zap responsive elements ZRE) bound to PARP13 (Huang et al., 2010). However, these motifs failed to confer sensitivity against PARP13's antiviral activity, suggesting that they are likely not sufficient for PARP13 binding (Huang et al., 2010).

Recently, work from our lab mapped the binding site of PARP13 to cellular mRNA target *TRAIL-R4* to a 600 nucleotide sequence in its 3'UTR that contains two ZREs and one AU-rich element (ARE). Inspection of the 3'UTR of our two validated PARP13-dependent targets *CERK* and *DNER* shows that *CERK* contains 6 ZREs and multiple AREs, whereas *DNER*'s 3'UTR has only AREs. Inspection of the rest of the transcripts shows that 11 of them have both ZREs and AREs in their 3'UTR, 1 (*SH3BGRL*) has only AREs, and another (*IFITM3*) contains neither (Gruber et al., 2010). Given that the exact sequence/structural feature of the 3'UTR fragment of *TRAIL-R4* that PARP13 binds is not known, it is not possible to predict if ZREs or AREs elements have any role in PARP13 binding. However, we hypothesize that putative PARP13 targets might share a structural feature (which may or may not be related to their membrane association) that is recognized by PARP13. In addition, the targeting of PARP13 to the ER could be an important factor in mRNA recognition. The increase in local concentration of PARP13 at the ER could drive recognition of the mRNAs located there.

Delta/Notch-like EGF-like receptor (DNER) is a non-canonical Notch ligand that regulates the development of glial cells (Eiraku et al., 2005). DNER overexpression in Neuro-2A inhibits neurite outgrowth, resulting in a round cell phenotype (Fukazawa et al., 2008). Our results show that upregulation of *DNER* mRNA and protein levels upon PARP13 knockdown results in a similar phenotype and shorter outgrowths. The reversion to a wildtype phenotype upon co-knockdown of *PARP13* and *DNER* suggests that the PARP13-dependent regulation of *DNER* mRNA affects DNER function and implicates PARP13 in neurite outgrowth in U87-

MG cells. This novel regulation of *DNER* expands the cellular mRNA regulatory function of PARP13 and suggests that the activity of PARP13 can be implicated in a different array of cellular processes largely depending on the gene product of the mRNAs it regulates.

METHODS

Reagents

Digitonin was from Acros Organics. RNAse A was purchased from Fermentas. Hoechst 33342 from Invitrogen. All qPCR primers were pre-designed from Sigma (KiCqStart SYBR Green Primers). Farnesylation inhibitor FTI-277 was from Sigma. Antibodies used: PARP13 (In house HM928 or Genetex, GTX120134), SBP (Millipore, MAB10764), Tubulin (Thermo Scientific, MA1-80017), GAPDH (Genetex, GTX282445), Calnexin (BD Biosciences, 610523), BiP (Cell Signaling, C50B12), MTCO2 (Abcam, ab3298), Lamp2 (Abcam, ab25631), DNER (Abcam, ab113251), Lamin A/C (Abcam, ab8984) and p230 (BD Biosciences, 611280).

Cell lines and transfection conditions

Experiments were performed using HeLa Kyoto cells, U87-MG cells or PARP13 knockout HeLa Kyoto cell line (PARP13$^{-/-\ A}$) described in Todorova et al., 2014. All three cell lines were cultured in Dulbecco's Modified Eagle's Medium (DMEM) containing 10% Fetal Bovine Serum in 5% CO_2 at 37°C. Transfections were performed using Lipofectamine 2000 (Life technologies) as per manufacturer's instructions for 24 hours prior to assay. Knockdowns by RNAi were performed by

double 48 hour transfection using Lipofectamine 2000 and 5nM of Silencer Select siRNAs (Life technologies).

Cloning

SBP-PARP13.1, -13.2 and 13.1^{VYFHR} were previously described in Todorova et al., 2014. SBP-PARP13.1^{C899S} was generated using GeneString (Invitrogen) flanked by Sal/BamH1 sites inserted into SBP-PARP13.1. Double mutant SBP-PARP13.1^{VYFHR,C899S} was generated by SalI/BamHI cuts of SBP-PARP13.1^{C899S} and insertion into SBP-PARP13.1^{VYFHR}. Untagged mutants were generated from previously cloned untagged PARP13.1. Untagged PARP13.1^{VYFHR} was generated using XhoI/BstXI sites in SBP-PARP13.1^{VYFHR} and inserting fragement into untagged PARP13.1. Untagged PARP13.1^{C899S} was generated using SalI/BamHI sites to cut SBP-PARP13.1^{C899S} and inserting fragment into untagged PARP13.1.

Immunofluorescence and confocal microscopy

HeLa cells were split into glass coverslips at least 16 hours prior to imaging. For cytoplasmic extraction assays, cells were treated with EB buffer (50mM HEPES pH 7.4, 50mM KCl, 5mM EGTA, 1mM $MgCl_2$, 1mM DTT) supplemented with 80μM digitonin for 90 seconds and washed once with EB buffer. For digitonin and RNAse A treatments, after digitonin treatment EB buffer + RNAse A (10μg/ml) was added for 5 minutes at room temperature. Coverslips were washed once with PBS and fixated with 4% formaldehyde in PBS for 30 minutes at room temperature, rehydrated with PBS and blocked with Abdil (1X PBS with 4% Bovine serum albumin (BSA) and 0.1% Triton X-100) for 45 minutes. Primary and secondary antibody staining was

performed with antibodies diluted 1:300 in Abdil for 1 hour. For U87-MG, cells were fixed in 4% formaldehyde for 10mins and permeabilized/blocked in 5% BSA and 0.1% Triton X-100 for 1hr. All images were collected on a Nikon TE2000 confocal microscope using Nikon NIS Elements software.

Digitonin extraction assays

Cells were washed in PBS thrice and cytoplasmic proteins were extracted by incubation with permeabilization buffer (25mM KHepes pH 7.4, 110mM KOAc, 2.5mM $Mg(OAc)_2$, 1mM EGTA, 1mM DTT, 0.05% digitonin, protease inhibitor cocktail) for 8 mins at 4°C and subsequently centrifuged at 1000g for 5 mins to collect cytoplasmic fraction. Pellet was washed thrice with wash buffer (permeabilization buffer but with 0.013% digitonin) and centrifuged 7600g for 10 mins to collect membrane fraction. For experiments assaying farnesylation inhibition, 20μM FTI-277 was added to cells 24 hours prior to extraction assay.

Sequential subcellular fractionation

Cells were washed thrice with PBS and homogenized in buffer IB1 (30mM Tris-HCl pH 7.5, 225mM mannitol, 75mM sucrose, 0.1mM EGTA, protease inhibitor cocktail) using a Dounce homogenizer. The lysed cells were pelleted at 600g for 5 minutes twice and the supernatant was further centrifuged at 7000g for 10 minutes at 4°C. Supernatant was further pelleted at 20,000g for 30mins. Collected supernatant was treated with RNAse A (10μg/ml) for 20mins or left untreated. Both samples were further centrifuged at 100,000g using a TLA120.1 rotor for 1hr to yield supernatant (cytoplasm) and pellet (ER membrane).

CLIP

PARP13.1-SBP and PARP13.2-SBP transfected HeLa cells were UV crosslinked at 254 nm with 200mJ/cm^2 (Stratagene Stratalinker). Cells were washed in PBS and cytosolic and membrane fractions were isolated using digitonin (see method section above). Each fraction was treated with RNAse A at 37°C for 10 mins and precipitated for 2hrs at 4°C using streptavidin sepharose beads (GE Healthcare). Beads were washed using wash buffer containing 1M NaCl and bound RNA was labeled with ^{32}P using T4 PNK enzyme (NEB) for 10mins at 37°C. Beads were subsequently washed 5 times and the SBP-tagged protein was eluted using 4mM biotin.

Microsome isolation

Microsome isolation was performed as described previously (Stephens et al., 2008). HeLa cells were washed in PBS twice and homogenized in hypotonic buffer using a Dounce homogenizer (B pestle). Sucrose was added to the homogenate to a final concentration of 2M, loaded on a discontinuous sucrose gradient and centrifuged at 259,000g for 16hrs using a TLS-55 rotor. ER microsomes were manually removed from the 1.3M/1.9M interphase, diluted fourfold and recovered by centrifugation at 259,000g for 40 mins.

RNASeq

HeLa and PARP13$^{-/-}$ cells were transfected with GFP or mock transfected and PARP13$^{-/-}$ cells were transfected with GFP and SBP-PARP13.1, SBP-PARP13.1^{VYFHR}, SBP-PARP13.1^{C899S} or SBP-PARP13.1^{VYFHR,C899S} for 24 hrs. Cells

were sorted for GFP positive cells at the Koch Institute Flow Cytometry facility using a MoFlo sorter (Beckman). RNA from sorted cells was extracted using RNeasy Mini kit (Qiagen) as manufacturer's instructions. RNA libraries were prepared using Illumina's TruSeq method by the Biomicrocenter at MIT. RNAseq data was aligned and summarized using bowtie version 1.0.1, rsem version 1.2.15, samtools/0.1.19 and a UCSC known genes annotation file from the hg19 assembly. Differential expression analysis was done with R version 3.2.0 and DESeq_1.20.0.

RT-qPCR

cDNA was prepared using Prime Script RT reagent (Takara) and random primers. 500ng of total RNA was used per reaction. RT-qPCR reactions were carried out with 100ng of cDNA using Sybr Select master mix reagent (Life Technologies) following manufacturer instructions. RT-qPCR was performed on a Roche 480 Light Cycler. Data analysis was performed using the $\Delta\Delta C_T$ method (Livak and Schmittgen, 2001). PCR efficiencies were measured for ACTB (102%), DNER (96%) and CERK (90%) by serial dilution. Actin-β (ACTB) or GAPDH were used as normalizing controls.

Astrocytic outgrowth measurement

U87-MG cells were plated at least 16hrs prior to visualization. Phase contrast images were taken of U87-MG knockdown cells using Nikon Eclipse Ti microscope. Outgrowth length in μm of ~85 cells from two independent experiments were measured using Nikon NIS Elements software and the mean average length for each experiment was calculated and plotted.

REFERENCES

Adjei, A.A., Davis, J.N., Erlichman, C., Svingen, P.A., and Kaufmann, S.H. (2000). Comparison of potential markers of farnesyltransferase inhibition. Clin Cancer Res *6*, 2318-2325.

Artavanis-Tsakonas, S., Rand, M.D., and Lake, R.J. (1999). Notch signaling: cell fate control and signal integration in development. Science *284*, 770-776.

Beck, L.A., Hosick, T.J., and Sinensky, M. (1990). Isoprenylation is required for the processing of the lamin A precursor. J Cell Biol *110*, 1489-1499.

Berezovska, O., McLean, P., Knowles, R., Frosh, M., Lu, F.M., Lux, S.E., and Hyman, B.T. (1999). Notch1 inhibits neurite outgrowth in postmitotic primary neurons. Neuroscience *93*, 433-439.

Bornancin, F. (2011). Ceramide kinase: the first decade. Cell Signal *23*, 999-1008.

Charron, G., Li, M.M., MacDonald, M.R., and Hang, H.C. (2013). Prenylome profiling reveals S-farnesylation is crucial for membrane targeting and antiviral activity of ZAP long-isoform. Proc Natl Acad Sci U S A *110*, 11085-11090.

Chen, S., Xu, Y., Zhang, K., Wang, X., Sun, J., Gao, G., and Liu, Y. (2012). Structure of N-terminal domain of ZAP indicates how a zinc-finger protein recognizes complex RNA. Nat Struct Mol Biol *19*, 430-435.

Eiraku, M., Hirata, Y., Takeshima, H., Hirano, T., and Kengaku, M. (2002). Delta/notch-like epidermal growth factor (EGF)-related receptor, a novel EGF-like repeat-containing protein targeted to dendrites of developing and adult central nervous system neurons. J Biol Chem *277*, 25400-25407.

Eiraku, M., Tohgo, A., Ono, K., Kaneko, M., Fujishima, K., Hirano, T., and Kengaku, M. (2005). DNER acts as a neuron-specific Notch ligand during Bergmann glial development. Nat Neurosci *8*, 873-880.

Fukazawa, N., Yokoyama, S., Eiraku, M., Kengaku, M., and Maeda, N. (2008). Receptor type protein tyrosine phosphatase zeta-pleiotrophin signaling controls endocytic trafficking of DNER that regulates neuritogenesis. Mol Cell Biol *28*, 4494-4506.

Gao, G., Guo, X., and Goff, S.P. (2002). Inhibition of retroviral RNA production by ZAP, a CCCH-type zinc finger protein. Science *297*, 1703-1706.

Gilbert, C., and Svejstrup, J.Q. (2006). RNA immunoprecipitation for determining

RNA-protein associations in vivo. Curr Protoc Mol Biol *Chapter 27*, Unit 27 24.

Goodier, J.L., Pereira, G.C., Cheung, L.E., Rose, R.J., and Kazazian, H.H., Jr. (2015). The Broad-Spectrum Antiviral Protein ZAP Restricts Human Retrotransposition. PLoS Genet *11*, e1005252.

Gruber, A.R., Fallmann, J., Kratochvill, F., Kovarik, P., and Hofacker, I.L. (2011). AREsite: a database for the comprehensive investigation of AU-rich elements. Nucleic Acids Res *39*, D66-69.

Guo, X., Carroll, J.W., Macdonald, M.R., Goff, S.P., and Gao, G. (2004). The zinc finger antiviral protein directly binds to specific viral mRNAs through the CCCH zinc finger motifs. J Virol *78*, 12781-12787.

Guo, X., Ma, J., Sun, J., and Gao, G. (2007). The zinc-finger antiviral protein recruits the RNA processing exosome to degrade the target mRNA. Proc Natl Acad Sci U S A *104*, 151-156.

Hennekes, H., and Nigg, E.A. (1994). The role of isoprenylation in membrane attachment of nuclear lamins. A single point mutation prevents proteolytic cleavage of the lamin A precursor and confers membrane binding properties. J Cell Sci *107 (Pt 4)*, 1019-1029.

Huang, Z., Wang, X., Gao, G. (2010). Analyses of SELEX-derived ZAP-binding RNA aptamers suggest that the binding specificity is determined by both structure and sequence of the RNA. Protein Cell. *8*, 752-759.

Leung, A.K., Vyas, S., Rood, J.E., Bhutkar, A., Sharp, P.A., and Chang, P. (2011). Poly(ADP-ribose) regulates stress responses and microRNA activity in the cytoplasm. Mol Cell *42*, 489-499.

Li, S., Liu, L., Zhuang, X., Yu, Y., Liu, X., Cui, X., Ji, L., Pan, Z., Cao, X., Mo, B., et al. (2013). MicroRNAs inhibit the translation of target mRNAs on the endoplasmic reticulum in Arabidopsis. Cell *153*, 562-574.

Liu, L., Chen, G., Ji, X., and Gao, G. (2004). ZAP is a CRM1-dependent nucleocytoplasmic shuttling protein. Biochem Biophys Res Commun *321*, 517-523.

Livak, K.J., and Schmittgen, T.D. (2001). Analysis of relative gene expression data using real-time quantitative PCR and the 2(-Delta Delta C(T)) Method. Methods *25*, 402-408.

Moldovan, J.B., and Moran, J.V. (2015). The Zinc-Finger Antiviral Protein ZAP Inhibits LINE and Alu Retrotransposition. PLoS Genet *11*, e1005121.

Raines, R.T. (1998). Ribonuclease A. Chem Rev *98*, 1045-1066.

Reid, D.W., and Nicchitta, C.V. (2015). Diversity and selectivity in mRNA translation on the endoplasmic reticulum. Nat Rev Mol Cell Biol *16*, 221-231.

Rio, D.C. (2012). Filter-binding assay for analysis of RNA-protein interactions. Cold Spring Harb Protoc *2012*, 1078-1081.

Saito, S.Y., and Takeshima, H. (2006). DNER as key molecule for cerebellar maturation. Cerebellum *5*, 227-231.

Stalder, L., Heusermann, W., Sokol, L., Trojer, D., Wirz, J., Hean, J., Fritzsche, A., Aeschimann, F., Pfanzagl, V., Basselet, P., et al. (2013). The rough endoplasmatic reticulum is a central nucleation site of siRNA-mediated RNA silencing. EMBO J *32*, 1115-1127.

Stephens, S.B., Dodd, R.D., Lerner, R.S., Pyhtila, B.M., and Nicchitta, C.V. (2008). Analysis of mRNA partitioning between the cytosol and endoplasmic reticulum compartments of mammalian cells. Methods Mol Biol *419*, 197-214.

Todorova, T., Bock, F.J., and Chang, P. (2015). Poly(ADP-ribose) polymerase-13 and RNA regulation in immunity and cancer. Trends Mol Med *21*, 373-384.

Tohgo, A., Eiraku, M., Miyazaki, T., Miura, E., Kawaguchi, S.Y., Nishi, M., Watanabe, M., Hirano, T., Kengaku, M., and Takeshima, H. (2006). Impaired cerebellar functions in mutant mice lacking DNER. Mol Cell Neurosci *31*, 326-333.

Ule, J., Jensen, K., Mele, A., and Darnell, R.B. (2005). CLIP: a method for identifying protein-RNA interaction sites in living cells. Methods *37*, 376-386.

Yakhnin, A.V., Yakhnin, H., and Babitzke, P. (2012). Gel mobility shift assays to detect protein-RNA interactions. Methods Mol Biol *905*, 201-211.

Ye, P., Liu, S., Zhu, Y., Chen, G., and Gao, G. (2010). DEXH-Box protein DHX30 is required for optimal function of the zinc-finger antiviral protein. Protein Cell *1*, 956-964.

Zhu, Y., Chen, G., Lv, F., Wang, X., Ji, X., Xu, Y., Sun, J., Wu, L., Zheng, Y.T., and Gao, G. (2011). Zinc-finger antiviral protein inhibits HIV-1 infection by selectively targeting multiply spliced viral mRNAs for degradation. Proc Natl Acad Sci U S A *108*, 15834-15839.

CHAPTER 3

CONCLUSION AND FUTURE DIRECTIONS

CONCLUSION AND FUTURE DIRECTIONS

PARP13 functions in cellular processes outside of its antiviral role have only recently started to be uncovered (Leung et al., 2011; Todorova et al., 2014; Moldovan and Moran, 2015; Goodier et al., 2015). These studies implicate PARP13 in important cellular processes that involve the post-transcriptional regulation of mRNAs and include miRNA regulation, retrotransposition and the regulation of cellular mRNAs. In this thesis, I examined the regulation of cellular mRNAs by PARP13, one of the physiological functions of PARP13 recently found in our laboratory (Todorova et al., 2014).

The goals of our study were to expand our understanding of the regulation of membrane-associated transcripts by PARP13, find new putative cellular PARP13 targets, and determine if PARP13-dependent regulation affects the biological function of its gene product. We demonstrated requirements of RNA binding and farnesylation of PARP13 for ER membrane localization, found that farnesylation of PARP13.1 is required for the regulation of the majority of the cellular targets identified in this study, and showed that PARP13 regulation is biologically important for one validated target, *DNER*. Our study opens the possibility of a membrane-specific mRNA regulatory role of PARP13 and expands the list of possible PARP13 cellular targets, thus confirming the protein's relevance in physiological RNA regulation

Validation of PARP13 binding to targets

Future experiments should validate the direct binding of PARP13 to our set of novel targets. Given that PARP13 recognizes RNAs with a specific secondary or

tertiary structure and PARP13 targets found thus far do not share a common nucleotide sequence or regulatory motif, direct binding validation must be performed for the entire target sequence. One approach to narrow down possible interaction sites would be to generate fragments of the target sequence, clone them into reporter vectors and assay each fragment for downregulation by PARP13 (as performed in Todorova et al., 2014). RNA fragments or *in vitro* synthesized RNA can then be tested for binding to PARP13 by RNA Electrophoretic Mobility Shift Assays (RNA-EMSA), filter binding assays, or RNA immunoprecipitation (RIP), among other techniques (Rio, 2012; Yakhnin et al., 2012; Gilbert and Svejstrup, 2006). To identify other direct PARP13 targets, one could perform CLIPSeq or high-throughput sequencing of RNA fragments precipitated in CLIP reactions (Ule et al., 2005). This technique would allow the identification of PARP13 targets as well as their RNA binding sites, and increase our understanding of how PARP13 recognizes its ER-translated targets. In addition, data from this experiment would test whether PARP13 targets are mostly ER-translated and/or identify cytoplasmic targets. In this context, it would be interesting to perform CLIPSeq experiments with either PARP13.1 or PARP13.2 to address the possibility that only farnesylated PARP13 can interact with and regulate ER-translated mRNAs.

Functional effects of PARP13 mRNA regulation

It is important not only to identify mRNAs that are regulated by PARP13 but also determine the functional consequence of their regulation in the cell. A clear example of the importance of PARP13 cellular mRNA regulation is illustrated by the

downregulation of *TRAIL-R4* mRNA, and in turn TRAIL-R4 protein levels, which leads to increased sensitivity to TRAIL-mediated cell death (Todorova et al., 2014). Based on our present study, PARP13 regulates cellular mRNAs whose gene products have roles in different cellular processes such as neurite outgrowth and sphingolipid metabolism. Unfortunately, this makes the study of the effects of PARP13 regulation more complicated, as each functional assay would have to be performed and validated independently. In the particular case of the two transcripts validated in this study, *CERK* and *DNER*, more extensive functional studies are needed to examine the effects of PARP13 regulation. DNER is an important component of the neuron-glia interaction that promotes differentiation of glial cells through Notch signaling (Eiraku et al., 2005). In addition, overexpression of DNER is thought to suppress differentiation of neuroblastoma cells and neurite outgrowth (Fukazawa et al., 2008). In our study, we tested the latter functional activity of DNER and confirmed that upregulation of *DNER* upon PARP13 knockdown caused a similar phenotype in U87-MG cells. In the future it would be important to test both the upregulation of DNER by PARP13 and its inhibitory effect in neurite outgrowth using non-cancerous neuronal cell lines such as Purkinje cells. Future experiments should also focus on other known roles for DNER in cells. For example, it would be of great interest to examine the effect of PARP13 regulation of DNER in Notch1 signaling, which is involved in many important processes like differentiation, proliferation and apoptotic programs. One interesting function to assay would be the differentiation of Bergmann glial cells and determine if, for example, the overexpression of PARP13 causes lower levels of DNER and thus an abnormal glia development.

Mechanism of PARP13 mRNA regulation of ER-translated transcripts

Another avenue left to explore is the mechanism by which PARP13 downregulates ER-translated transcripts. Both viral and cellular (*TRAIL-R4*) mRNA degradation of PARP13 is mediated by 3'- 5' and 5'- 3' degradation factors such as the cytoplasmic exosome, PARN deadenylase, XRN1 exoribonuclease and decapping enzymes DCP1a and DCP2 (Guo et al., 2007; Zhu et al., 2011; Todorova et al., 2014). Thus, future experiments could assay the regulation of PARP13 targets upon depletion of such decay factors in cells. Quantitative experiments could be performed measuring reporter activity (i.e. luciferase reporter) or mRNA levels by RT-qPCR using PARP13 knockout or depleted cells as control. Furthermore, sucrose density fractionation or ER-microsome preparations would help to elucidate which mRNA decay factors are localized to ER-membrane and might mediate the PARP13-dependent post-transcriptional regulation of transcripts.

In summary, future experiments should focus on the validation of direct transcript-PARP13 binding of the targets identified in this study and/or the identification of new PARP13 targets by CLIPseq. In addition, studies of the mechanism by which PARP13 regulates these transcripts should be performed. Mechanistic experiments are of particular interest since we could learn which RNA decay factors are required and furthermore, if this regulation occurs in association with the ER membrane. Finally, functional assays of each of the gene products of PARP13 targets should be carefully performed in order to learn the biological relevance of PARP13's regulation of each transcript in the cell. As a result, these

studies will to continue to uncover the importance of PARP13 function in cellular mRNA regulation.

REFERENCES

Eiraku, M., Tohgo, A., Ono, K., Kaneko, M., Fujishima, K., Hirano, T., and Kengaku, M. (2005). DNER acts as a neuron-specific Notch ligand during Bergmann glial development. Nat Neurosci *8*, 873-880.

Fukazawa, N., Yokoyama, S., Eiraku, M., Kengaku, M., and Maeda, N. (2008). Receptor type protein tyrosine phosphatase zeta-pleiotrophin signaling controls endocytic trafficking of DNER that regulates neuritogenesis. Mol Cell Biol *28*, 4494-4506.

Gilbert, C., and Svejstrup, J.Q. (2006). RNA immunoprecipitation for determining RNA-protein associations in vivo. Curr Protoc Mol Biol *Chapter 27*, Unit 27 24.

Goodier, J.L., Pereira, G.C., Cheung, L.E., Rose, R.J., and Kazazian, H.H., Jr. (2015). The Broad-Spectrum Antiviral Protein ZAP Restricts Human Retrotransposition. PLoS Genet *11*, e1005252.

Guo, X., Ma, J., Sun, J., and Gao, G. (2007). The zinc-finger antiviral protein recruits the RNA processing exosome to degrade the target mRNA. Proc Natl Acad Sci U S A *104*, 151-156.

Leung, A.K., Vyas, S., Rood, J.E., Bhutkar, A., Sharp, P.A., and Chang, P. (2011). Poly(ADP-ribose) regulates stress responses and microRNA activity in the cytoplasm. Mol Cell *42*, 489-499.

Moldovan, J.B., and Moran, J.V. (2015). The Zinc-Finger Antiviral Protein ZAP Inhibits LINE and Alu Retrotransposition. PLoS Genet *11*, e1005121.

Rio, D.C. (2012). Filter-binding assay for analysis of RNA-protein interactions. Cold Spring Harb Protoc *2012*, 1078-1081.

Todorova, T., Bock, F.J., and Chang, P. (2014). PARP13 regulates cellular mRNA post-transcriptionally and functions as a pro-apoptotic factor by destabilizing TRAILR4 transcript. Nat Commun *5*.

Ule, J., Jensen, K., Mele, A., and Darnell, R.B. (2005). CLIP: a method for identifying protein-RNA interaction sites in living cells. Methods *37*, 376-386.

Yakhnin, A.V., Yakhnin, H., and Babitzke, P. (2012). Gel mobility shift assays to detect protein-RNA interactions. Methods Mol Biol *905*, 201-211.

Zhu, Y., Chen, G., Lv, F., Wang, X., Ji, X., Xu, Y., Sun, J., Wu, L., Zheng, Y.T., and

Gao, G. (2011). Zinc-finger antiviral protein inhibits HIV-1 infection by selectively targeting multiply spliced viral mRNAs for degradation. Proc Natl Acad Sci U S A *108*, 15834-15839.

ACKOWLEDGMENTS

I would like to thank Paul Chang and the Chang lab for their assistance, scientific advice and helpful discussions. I offer thanks to Tenzin, Florian, Tanya, Miri, Sejal and Jenny.

I would also like to thank the members of my thesis committee, Stephen P. Bell, Wendy Gilbert and David Bartel, for their thoughtful advice and undivided support with all my research projects. In particular, I would like to acknowledge my thesis supervisor Stephen P. Bell for inspiring me with his passion for biology and for his genuine commitment to my scientific training and personal well being.

I would also like to thank my mentors during my undergraduate studies, Stephen P. Bell, Zarixia Zavala-Ruiz, Eric Schreiter and Gustavo E. López for instilling in me their love for research and inspiring me to continue graduate studies.

Many thanks to all my friends -new and old- that have cheered me all the way through the ups and downs of graduate school. To my puertorican crew: Frances, María Cristina, Javi, José J., Merangelí, Krizia, Rocío and Zunamys. Also, to my biograds2009 colleagues and to the amazing friends I've met in my time at MIT: Jenny, Tenzin, Robert and Lourdes. Especially to Jenny Rood who thoroughly edited this thesis and has been a supportive friend the last six years.

I would also like to thank my amazing family. Thanks also to my mother and father-in-law Deb and David Piccioli, for their unconditional love and support. Especially to my mother-in-law and friend Deb who has been my source of strength and encouragement, I love you. Also to my brother-in-laws, Alex, Michael and Tommy, and my sister-in-law Amy for being hilariously fun to be around and always putting a smile on my face.

I want to say ¡GRACIAS! to my best friend and sister Eluney for being my favorite partner-in-crime, for loving and supporting me at every step of my life and also for blessing me with my brother-in-law Orlando and my niece Ayelen who lights up my world. ¡Te amo!

I would like to dedicate this thesis and degree to my parents Nora Méndez and Ricardo Uchima. Gracias por enseñarme a seguir mis sueños, a ser humilde, respetuosa, y sobretodo agradecida. Ahora, les agradezco yo a ustedes el habérmelo dado TODO para llegar hasta acá. Son mi más grande tesoro y mi mayor orgullo. Los amo y les dedico esta tesis y grado doctoral. ¡Gracias totales!

Finally, I would like to thank my number one fan -my husband Zach. Thanks for supporting me every single day and for always believing in me. Your words of encouragement, your unconditional love and care guided me through tough times and helped me accomplished my biggest dream. I love you my Zachy Pooh.

APPENDIX I

PARP13 DOWNREGULATES *TRAIL-R4* mRNA DURING THE EARLY ER STRESS RESPONSE

Lilen Uchima and Paul Chang

LU and PC designed the experiments and LU performed experiments.

INTRODUCTION

ER stress and the unfolded protein response

The eukaryotic endoplasmic reticulum (ER) is an organelle responsible for the synthesis, modification and delivery of secretory and transmembrane proteins. It also controls the proper folding of ER-translated proteins by molecular chaperones and the degradation of improperly folded proteins by the proteasome (Braakman and Hebert, 2013). Perturbations such as viral infection, oxygen deficiency, glucose starvation and changes in the intracellular stores of Ca^{2+} disrupt ER homeostasis and lead to the accumulation of misfolded and unfolded proteins in the ER. This condition is known as ER stress (reviewed in Chakrabarti et al., 2011). In order to reduce ER stress and restore ER homeostasis, the cell activates an intricate signaling network termed the unfolded protein response (UPR). Activation of the UPR leads to pro-survival mechanisms that attempt to restore ER homeostasis named the adaptive response. If on the contrary, these attempts fail and the ER stress is unable to be mitigated, the UPR triggers apoptosis.

The UPR is mediated by the activation of at least three major stress sensors: inositol-requiring protein 1 (IRE1), activating transcription factor 6 (ATF6) and protein kinase RNA-like ER kinase (PERK) (Ron and Walter, 2007). The adaptive response of the UPR includes three initial responses (i) the inhibition of general protein translation by PERK phosphorylation of eukaryotic translation initiator factor 2α (eIF2α), (ii) the degradation of IRE1 ER-localized mRNA transcripts through regulated IRE1-dependent decay (RIDD) and (iii) the autophagy of damaged proteins

through the IRE1–JUN N-terminal kinase (JNK) pathway (Hollien and Weissman, 2006; Harding et al., 2007; Hollien et al., 2009; Kroemer et al., 2010). These events prevent the influx of proteins to the ER and dispose of structurally compromised proteins thus allowing repair mechanisms to restore ER homeostasis. The adaptive response to ER stress also involves the expression of target genes by UPR-activated transcription factors. Three transcription factors govern this response: activating transcription factor 4 (ATF4), spliced X-box binding protein 1 (XBP1s) and the cytosolic domain fragment of activating transcription factor 6 (ATF6f). Although each transcription factor is activated by a unique mechanism and some of their target genes are stimulus and cell type-dependent, their overall goal is to promote adaptive responses that restore ER function and maintain cell survival.

In the case that these adaptive mechanisms fail, the cell activates intrinsic and extrinsic apoptotic pathways to induce cell death (Danial and Korsmeyer, 2004). Although not all the mediators will be described in detail here, key regulators in this response include (i) PERK/eIF2α-dependent induction of the pro-apoptotic transcriptional factor C/EBP-homologous protein (CHOP), (ii) IRE1-mediated activation of tumor necrosis factor receptor associated factor 2 (TRAF2), which stimulates the ASK1 (apoptosis signal-regulating kinase 1)/JNK (c-Jun amino terminal kinase) kinase cascade, and (iii) Ca^{2+} release from the ER by the action of pro-apoptotic proteins Bax/Bcl2 which sensitize mitochondria to activate apoptosis (reviewed in Sano and Reed, 2013). One of the most important mediators of ER stress-mediated apoptosis is the transcriptional factor CHOP. CHOP upregulates the expression of targets such as growth arrest and DNA damage-inducible 34

(GADD34), trail receptor 2 (TRAIL-R2) and endoplasmic reticulum oxidoreductase-1 (ERO1α). GADD34 activation reverses protein translation inhibition by promoting the dephosphorylation of eIF2α and thus leading to accumulation of unfolded proteins. TRAIL-R2 receptor upregulation induces apoptosis by activation of caspase-8 and ERO1α hyperoxidizes the ER and promotes excessive Ca^{2+} transport from the ER to the mitochondria triggering cell death (Li et al., 2009; reviewed in Oyadomari and Mori, 2004; Lu et al., 2014). As evidenced by the different pathways and players in the complex ER stress-mediated apoptotic response, more studies are needed to uncover all the possible regulators. More importantly, the UPR has important implications in diseases such as cancer, diabetes, and neurodegeneration (reviewed in Wang and Kaufman, 2012). Therefore, understanding the mechanisms that integrate the ER stress responses is fundamental for therapy development in many important human diseases.

TRAIL receptors in ER stress-mediated apoptosis

Tumor necrosis factor-related apoptosis-inducing ligand (TRAIL) is a cytokine that acts as a ligand of TRAIL-receptors to induce apoptosis (Wiley et al., 1995; Pitti et al., 1996). There are four TRAIL receptors in humans; TRAIL-R1/DR4, TRAIL-R2/DR5, TRAIL-R3/DcR1 and TRAIL-R4/DcR2. Although all four receptors bind to TRAIL ligand, only the death domain-containing receptors TRAIL-R1 and TRAIL-R2 are able to induce TRAIL-mediated apoptosis (Sprick et al., 2000; Kischkel et al., 2000). Upon TRAIL-ligand binding, death receptors recruit proteins to their intracellular death domain to form a structure known as the death-inducing signaling

complex (DISC) (Kishkel et al., 1995). The DISC complex subsequently activates the caspase8/10 cascade that leads to apoptosis (Thorburn, 2004). The denominated "decoy" receptors TRAIL-R3 and TRAIL-R4 lack the death domain or contain a truncated non-functional death domain respectively and thus are incapable of inducing a competent DISC complex formation (Marsters et al., 1997; Mérino et al., 2006). Decoy receptors act as pro-survival factors by binding TRAIL ligand away from death signaling receptors and, in addition, TRAIL-R4 is co-recruited with TRAIL-R2 to the DISC complex where it interferes with TRAIL-R2 multimerization inhibiting caspase activation (Mérino et al., 2006).

Recent studies have unveiled the importance of TRAIL-R2 receptor in the ER stress response, by showing that TRAIL-R2 levels are tightly controlled to promote either adaptation or apoptosis during the unfolded protein response (Lu et al., 2014). Upon reversible ER stress, transcription factor CHOP upregulates, whereas RIDD decay suppresses TRAIL-R2 mRNA levels. If ER stress resolves, TRAIL-R2 mRNA return to basal levels. If the ER stress is unmitigable, IRE1-mediated decay of TRAIL-R2 transcript subsides but TRAIL-R2 mRNA levels continue to rise by CHOP upregulation. High levels of TRAIL-R2 trigger its multimerization and assembly of the DISC complex, which leads to initiation of apoptosis by caspase 8 (Lu et al., 2014). This study also demonstrates that the expression of death receptor TRAIL-R3, is not upregulated during the response suggesting that is not essential for ER-stress mediated apoptosis.

Although the importance of decoy receptors during ER stress has not been examined as thoroughly as for TRAIL death receptors, studies suggest that the cell-

type dependent regulation of these receptors during the ER stress response could be relevant for their apoptotic fate. Work from Condamine and colleagues showed that upon ER stress induction by thapsigargin, both decoy receptors TRAIL-R3 and TRAIL-R4 expression is decreased in human polymorphonuclear neutrophils myeloid-derived suppressor cells whereas death receptors expression remains the same (Condamine et al., 2014). Interestingly, lower expression of decoy receptors in these cells correlated with a decreased viability due to ER stress-mediated apoptosis (Condamine et al., 2014). A different study using human giant cell tumor of bone cells revealed that upon ER stress the cells were sensitized to TRAIL-mediated death as compared to TRAIL-treatment alone (Huang et al., 2004). Examination of TRAIL receptors levels upon ER stress treatment demonstrated that TRAIL-R2 expression was upregulated whereas TRAIL-R3 was downregulated (Huang et al., 2004). Together these studies suggest that regulation of TRAIL receptors during ER stress is cell type-dependent and could have relevant consequences in the ER stress response. Neither study examined the mechanism the mechanism of regulation of TRAIL decoy receptors upon ER stress conditions. In this appendix we examine the mRNA regulation of TRAIL receptors during early ER stress response in HeLa cells and demonstrate that mRNA levels of decoy receptor *TRAIL-R4* are regulated by PAR13.

RESULTS

TRAIL-R4 mRNA levels are downregulated during early ER stress response

Our lab previously identified that PARP13 binds and regulates cellular mRNAs such as the decoy TRAIL receptor *TRAIL-R4* (Todorova et al., 2014). In addition, given that PARP13 functions as a posttranscriptional regulator under physiological and stress conditions, such as cytoplasmic stress, we sought to determine if PARP13 also regulated *TRAIL-R4* mRNA levels under cellular stress. In order to examine if *TRAIL-R4* mRNA levels change under stress conditions, we performed real time quantitative polymerase chain reaction (RT-qPCR) to measure *TRAIL-R4* mRNA levels in HeLa cells after treatment with different cellular stressors. HeLa cells were treated with either 1mM Dithiothreitol (DTT), 100μM sodium arsenite or subjected to 42°C for one hour. DTT is a strong reducing agent that blocks disulfide bond formation leading to unfolded protein accumulation and thus triggering ER stress response (Oslowski and Urano, 2011). Sodium arsenite treatment causes oxidative stress and incubation at 42°C leads to heat shock stress. We compared *TRAIL-R4* mRNA levels of treated cells to levels in untreated cells and found a significant change in *TRAIL-R4* mRNA levels only after 1mM DTT treatment (Figure 1). More specifically, 1mM DTT treatment caused a significant decrease in *TRAIL-R4* mRNA levels. This decrease could be due to a specific regulation of *TRAIL-R4* levels upon DTT-induced ER stress or due to a secondary effect of DTT treatment.

FIGURE 1

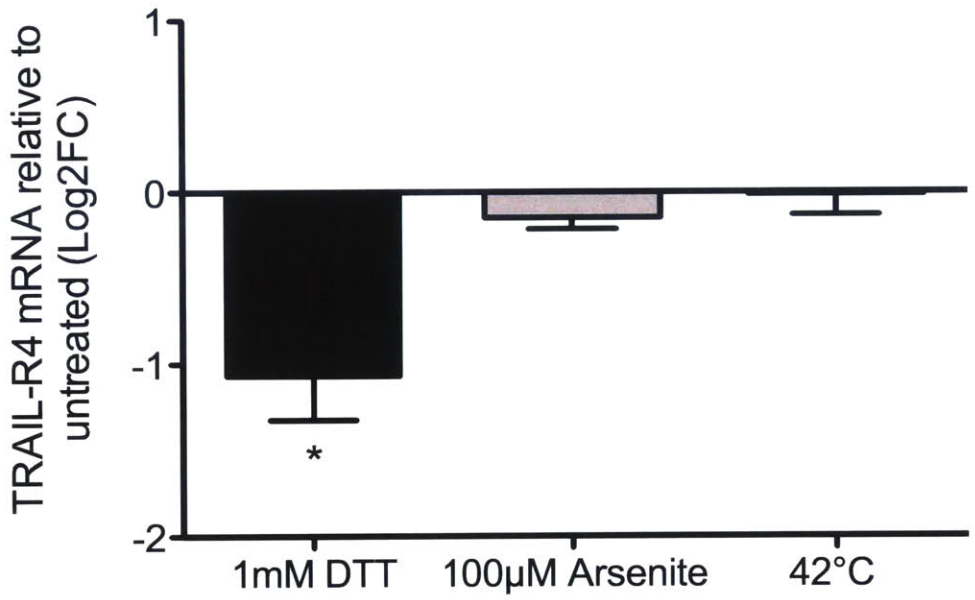

Figure 1. TRAIL-R4 mRNA is downregulated upon DTT treatment. HeLa cells were treated with 1mM DTT, 100µM arsenite or incubated at 42°C for 1 hour. Subsequently, *TRAIL-R4* mRNA levels were measured by RT-qPCR and compared to untreated cells (two-sided t-test, n=2, * p-value <0.05, error bars represent S.D.)

Downregulation of *TRAIL-R4* mRNA during early ER stress is PARP13-dependent

In order to examine if the downregulation of *TRAIL-R4* mRNA was due to a specific response to ER stress and furthermore, if the downregulation was PARP13-dependent, we measured *TRAIL-R4* mRNA levels after treatment of the specific ER stress inducers Brefeldin A (BFA), Tunicamycin (Tm) and Thapsigargin (Tg) in PARP13 siRNA knockdown cells. All three drugs induce ER stress by different mechanisms but result in protein misfolding and thus lead to activation of the unfolded protein response. BFA inhibits the transport of proteins from the ER to the Golgi causing the accumulation of unfolded proteins, Tm inhibits protein N-linked glycosylation and Tg blocks the ER calcium-dependent ATPase pump (Samali et al., 2010). Figure 2 shows that consistent with the previous result, *TRAIL-R4* mRNA levels decreased in control knockdown cells upon treatment with all three ER stress-inducing drugs as compared to mock-treated control knockdown cells, suggesting that *TRAIL-R4* mRNA is downregulated during ER stress. As already characterized by Todorova and colleagues, PARP13 knockdown cells demonstrated upregulation of *TRAIL-R4* mRNA as compared to control knockdown cells (Figure 2). Interestingly, *TRAIL-R4* levels in PARP13 knockdown cells were not affected by the treatment of any of the ER stress-inducing drugs. Together these results suggest that the ER-stress-induced downregulation of *TRAIL-R4* mRNA is dependent on PAPR13.

TRAIL-R4 mRNA levels were downregulated by eight hours after ER stress induction thus we assayed the levels of *TRAIL-R4* mRNA within eight hours of ER stress treatments. Wildtype and PARP13$^{-/-}$ cells were treated with either Tm or BFA

FIGURE 2

A

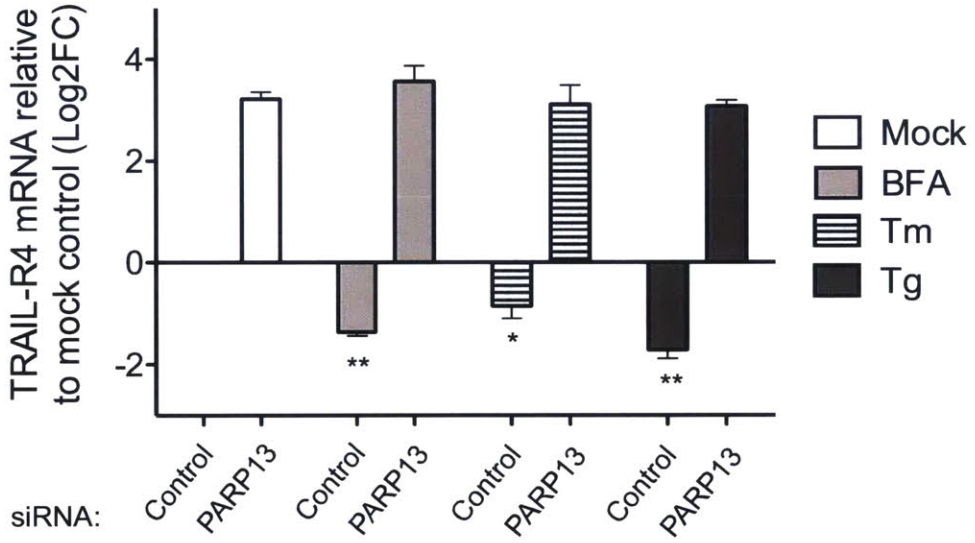
TRAIL-R4 mRNA relative to mock control (Log2FC)
4
2
0
-2
**
*
**
siRNA:
Control
PARP13
Control
PARP13
Control
PARP13
Control
PARP13
Mock
BFA
Tm
Tg

B

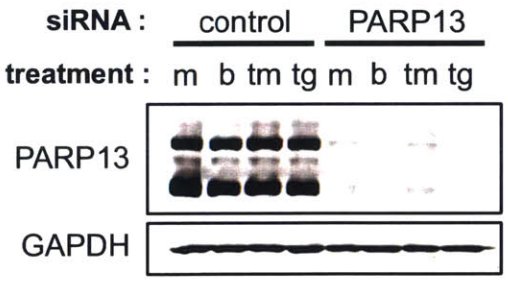
siRNA :
control
PARP13
treatment :
m b tm tg m b tm tg
PARP13
GAPDH

Figure 2. PARP13 downregulates *TRAIL-R4* mRNA upon ER stress. (A) PARP13 or control siRNA depleted HeLa cells were treated with 5μg/ml BFA, 3μg/ml Tm or 0.2μM Tg for 8 hours. *TRAIL-R4* mRNA was quantified by RT-qPCR and compared to mock treated mRNA levels (two-sided t-test, n=3, * p-value<0.05, ** p-value<0.0, error bars represent S.D.) **(B)** Immunoblot of samples in **(A)** for PARP13 and GAPDH (loading control). Treatments labeled as (m) mock, (b) BFA, (tm) Tunicamycin, (tg) Thapsigargin.

for 0, 2, 4, 6 or 8 hours and *TRAIL-R4* mRNA levels were quantified by RT-qPCR (Figure 3). Both BFA and Tm treated wildtype cells demonstrated a time-dependent downregulation of *TRAIL-R4* mRNA that was not observed in PARP13$^{-/-}$ cells, confirming that the downregulation of *TRAIL-R4* is PARP13-dependent. BFA and Tm treatment of wildtype cells demonstrated different *TRAIL-R4* downregulation kinetics. *TRAIL-R4* mRNA levels were lowest after 2-4 hours of Tm treatment whether for BFA treated wildtype cells it was 4-6 hours. This difference suggests that the degree of downregulation of *TRAIL-R4* mRNA is specific to the type of ER stress inducer and/or concentration of the drug. More importantly, this would suggest that *TRAIL-R4* downregulation is specific to the degree of ER stress response being elicited. It is also important to note that the levels of *TRAIL-R4* mRNA increase after 4 hours in the case of Tm and after 6 hours after BFA treatment. This increase is PARP13-independent as PARP13$^{-/-}$ cells also show an increase in *TRAIL-R4* mRNA levels during the same time frame as wildtype cells.

Additionally, we tested the possibility that PARP13 could also regulate other TRAIL receptors during these early time points of the ER stress response. For this, we measured the mRNA levels of TRAIL receptors: *TRAIL-R1*, *TRAIL-R2* and *TRAIL-R3* from wildtype and PARP13$^{-/-}$ cells treated with BFA or mock treated for 0, 2, 4 and 6 hours. As shown in Figure 4, the mRNA levels for each receptor were not significantly different between wildtype and PARP13$^{-/-}$ cells suggesting that gene expression regulation of these TRAIL receptors during ER stress is not dependent on PARP13.

FIGURE 3

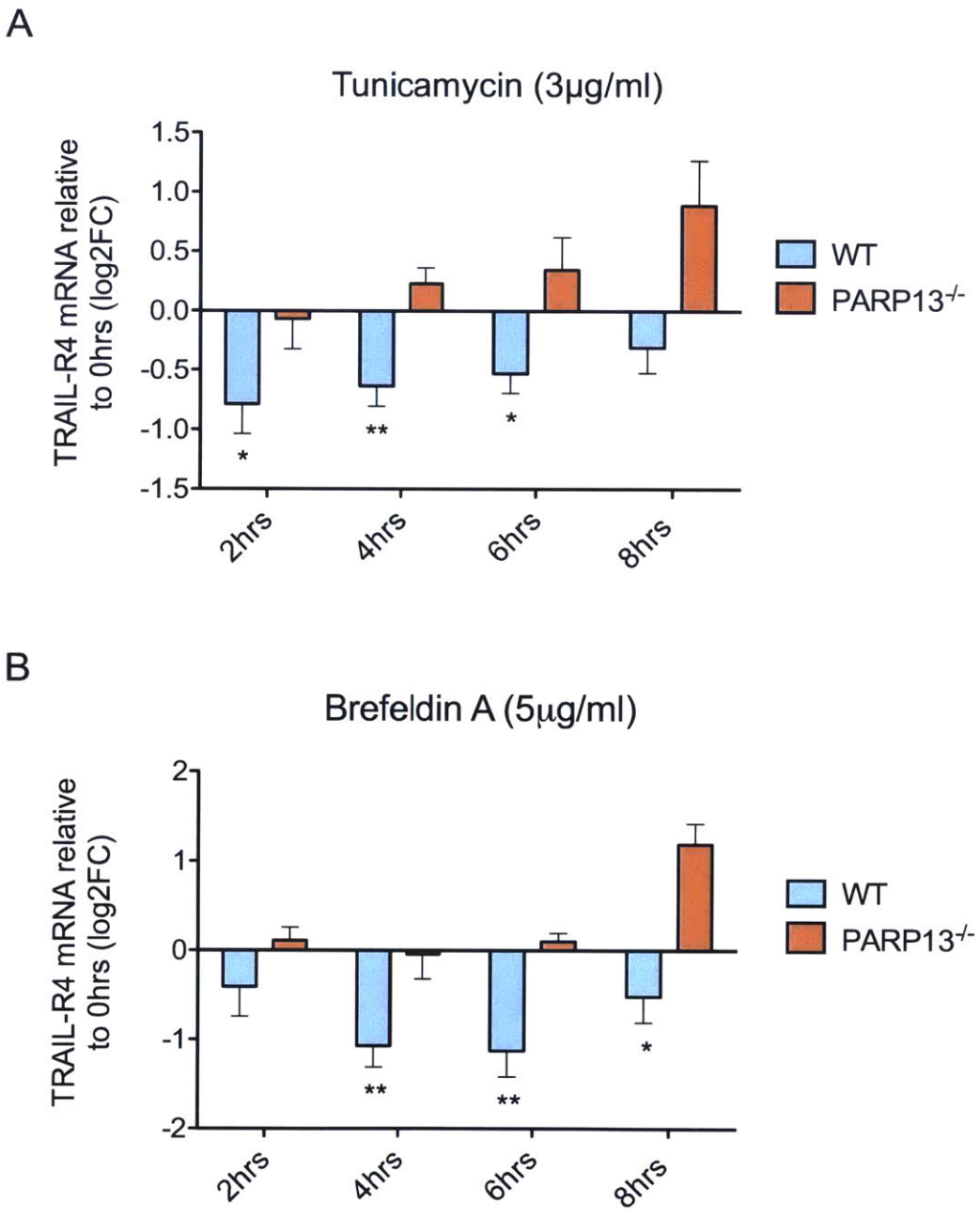
A
Tunicamycin (3µg/ml)
TRAIL-R4 mRNA relative to 0hrs (log2FC)
1.5
1.0
0.5
0.0
-0.5
-1.0
-1.5
*
**
*
2hrs
4hrs
6hrs
8hrs
WT
PARP13-/-
B
Brefeldin A (5µg/ml)
TRAIL-R4 mRNA relative to 0hrs (log2FC)
2
1
0
-1
-2
**
**
*
2hrs
4hrs
6hrs
8hrs
WT
PARP13-/-

Figure 3. PARP13 downregulates *TRAIL-R4* mRNA upon early ER stress response. Wildtype or PARP13$^{-/-}$ cells were treated with either 3μg/ml Tm **(A)** or 5μg/ml BFA **(B)** for 0, 2, 4, 6 or 8 hours. *TRAIL-R4* mRNA levels were measured by RT-qPCR and compared to mRNA levels at 0 hours (two-sided t-test, n=3, * p-value<0.05, ** p-value<0.0, error bars represent S.D.)

FIGURE 4

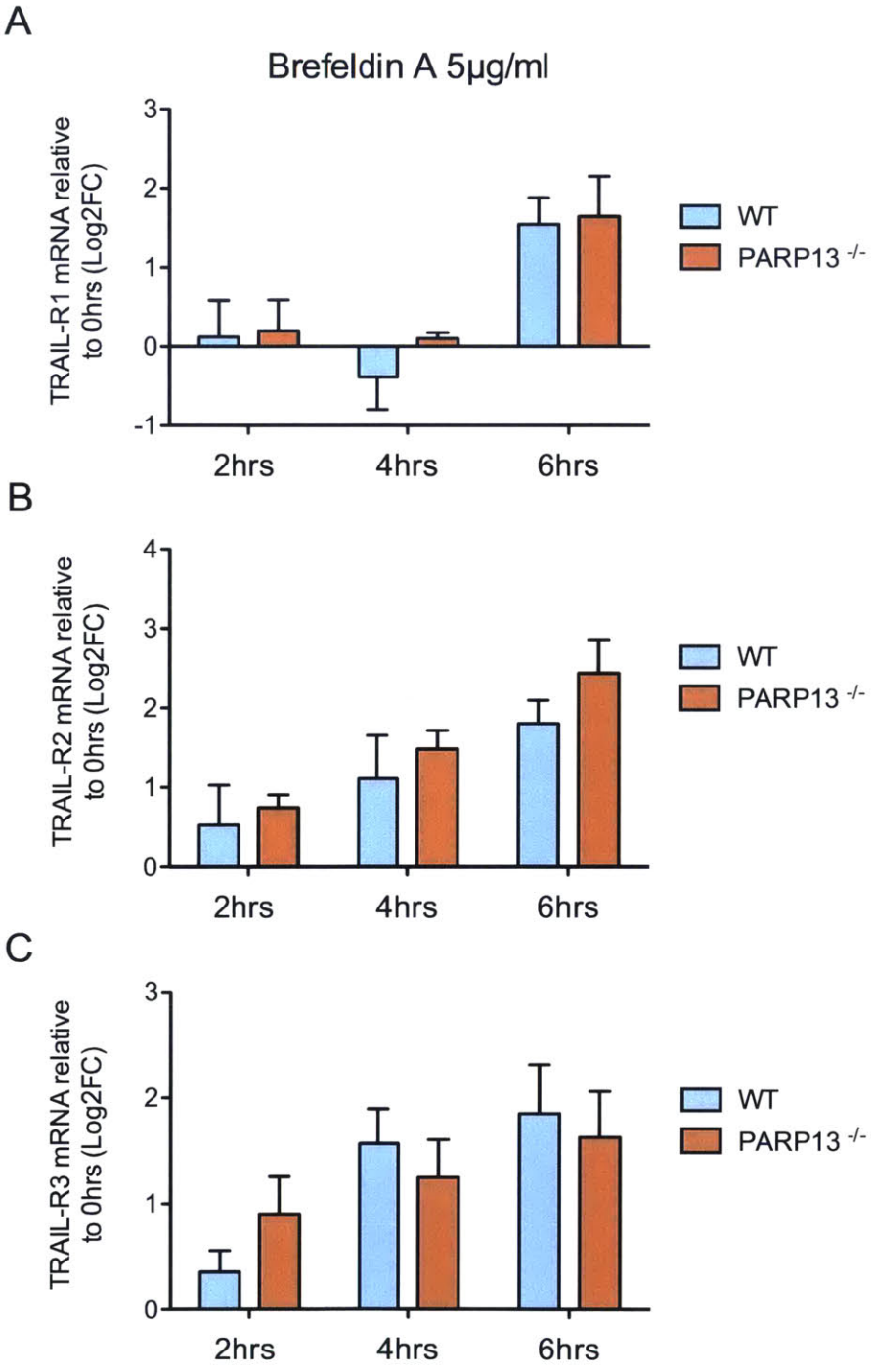
A
Brefeldin A 5µg/ml
TRAIL-R1 mRNA relative to 0hrs (Log2FC)
3
2
1
0
-1
2hrs
4hrs
6hrs
WT
PARP13 -/-
B
TRAIL-R2 mRNA relative to 0hrs (Log2FC)
4
3
2
1
0
2hrs
4hrs
6hrs
WT
PARP13 -/-
C
TRAIL-R3 mRNA relative to 0hrs (Log2FC)
3
2
1
0
2hrs
4hrs
6hrs
WT
PARP13 -/-

Figure 4. PARP13 does not regulate mRNA levels of other TRAIL receotors upon early ER stress. Wildtype or PARP13$^{-/-}$ cells were treated with 5μg/ml BFA for 0, 2, 4, or 6 hours and the mRNA levels of *TRAIL-R1* **(A)** *TRAIL-R2* **(B)** or *TRAIL-R3* **(C)** were measured by RT-qPCR and compared to mRNA levels at 0 hours (two-sided t-test, n=3, error bars represent S.D.)

In order to corroborate that BFA and Tm treatments were indeed triggering an ER stress response, we assayed the *XBP1* mRNA, which is often used as a marker for ER stress (van Schadewjik et al., 2012). Splicing assays for *XBP1* mRNA were performed with wildtype and PARP13$^{-/-}$ cells treated with BFA for 0, 2, 4 or 6 hours (Figure 5A). Induction of ER stress response signaling was detected within 2 hours as evidenced by the splicing of *XBP1* mRNA, suggesting that the ER stress response was activated as early as 2 hours after ER-stress-inducing drug treatment. Furthermore, we measured the levels of ER stress-induced transcription factor *CHOP* mRNA of wildtype and PARP13$^{-/-}$ cells after 0, 2, 4, 6 and 8 hours after BFA and Tm treatment. As expected, *CHOP* mRNA levels were upregulated in a time-dependent manner upon ER stress induction by both drugs. In addition, no significant difference was observed between *CHOP* mRNA levels in wildtype and PARP13$^{-/-}$, suggesting PARP13 does not affects CHOP upregulation (Figure 5B). Another hallmark of unfolded protein response activation is the upregulation of the ER chaperone Binding immunoglobulin Protein (BiP). We tested BiP protein levels by immunoblot upon mock or BFA treatment of wildtype and PARP13$^{-/-}$ cells and found that BiP was ~1.5 fold upregulated in both cell types (Figure 5C). In addition, an immunoblot against PARP13 demonstrated that BFA treatment did not cause a change in PARP13 levels in wildtype cells as compared to mock treated cells. These results suggest that BiP upregulation upon ER stress is not affected by PARP13. Given that PARP13 expression levels do not change upon ER stress, this suggests that the downregulation of *TRAIL-R4* by PARP13 could be due to enhanced activity during ER stress response.

FIGURE 5

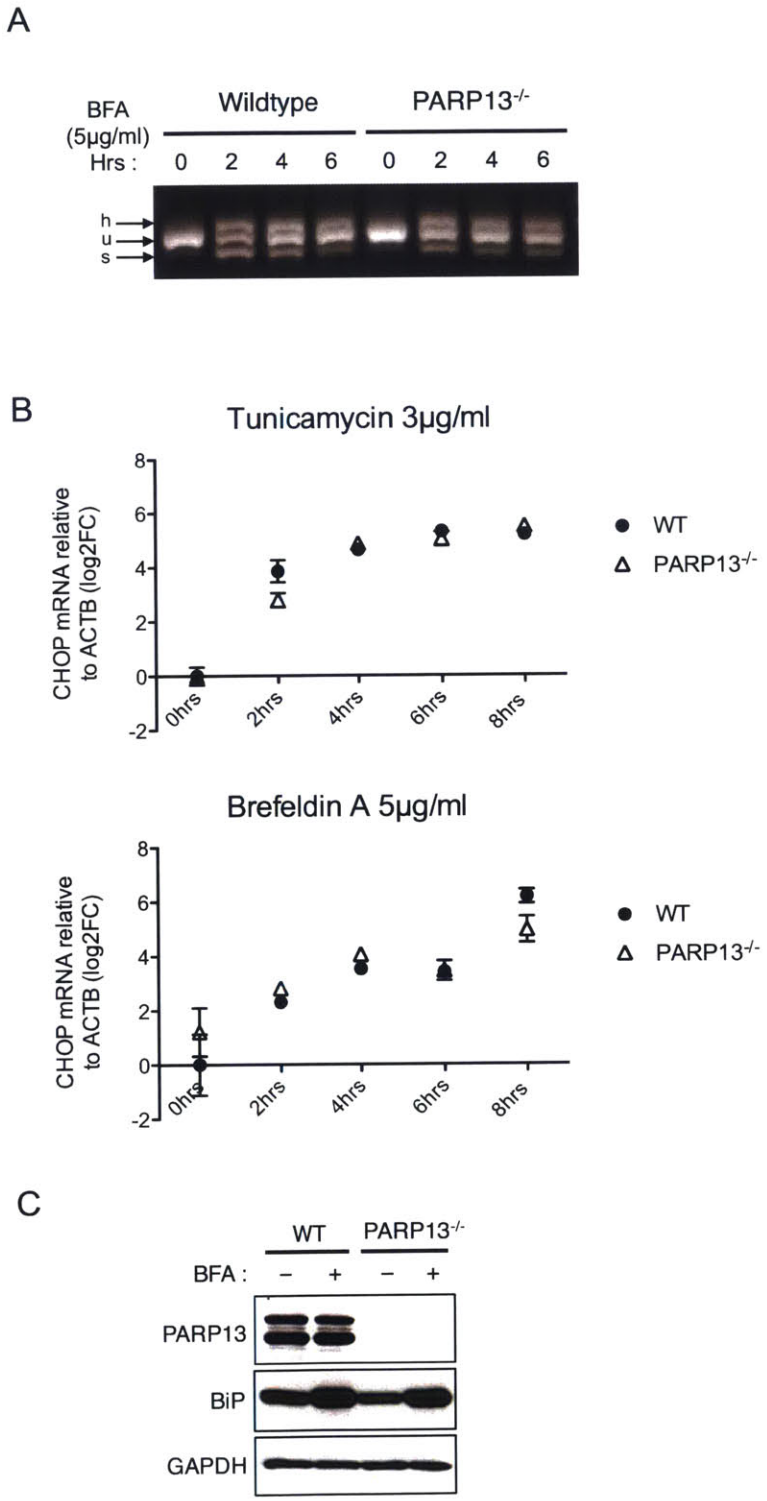
A
BFA (5µg/ml)
Hrs :
Wildtype
PARP13-/-
0 2 4 6 0 2 4 6
h
u
s
B
Tunicamycin 3µg/ml
CHOP mRNA relative to ACTB (log2FC)
WT
PARP13-/-
0hrs
2hrs
4hrs
6hrs
8hrs
Brefeldin A 5µg/ml
C
WT
PARP13-/-
BFA :
PARP13
BiP
GAPDH

Figure 5. PARP13 does not affect *XBP1* splicing, BiP or CHOP upregulation during adaptive ER stress response. (A) Wildtype or PARP13$^{-/-}$ cells were treated with 5µg/ml BFA for 0, 2, 4, or 6 hours and splicing of *XBP1* mRNA was examined by PCR of spliced (s) product on 2.5% agarose gel. (u) denotes unspliced product and (h) denotes a hybrid band between unspliced and spliced ssDNA (Weinchert et al., 2011). **(B)** Wildtype or PARP13$^{-/-}$ cells were treated with 3µg/ml Tm (top) or 5µg/ml BFA (bottom) for 0, 2, 4, 6 or 8 hours and *TRAIL-R2* mRNA was measured by RT-qPCR and compared to mRNA levels at 0 hours (two-sided t-test, n=2, error bars represent S.D.) **(C)** Immunoblots of PARP13 and BiP in wildtype and PARP13$^{-/-}$ cells either treated with 5µg/ml BFA or mock treated for 8 hours using GAPDH immunoblot as loading control.

Similar to *TRAIL-R4* mRNA regulation under physiological conditions, we hypothesize that the PARP13 downregulation of *TRAIL-R4* during early ER stress response is also dependent on its RNA-binding activity. In order to confirm this we perform RT-qPCR to measure *TRAIL-R4* mRNA in BFA treated and untreated wildtype HeLa cells and PARP13$^{-/-}$ cells transfected with either full length SBP-PARP13.1, RNA-binding mutant SBP-PARP13.1^{VYFHR} or mock transfected. Figure 6 shows that, as expected, cells expressing endogenous PARP13 (wildtype) or exogenous PARP13.1 (SBP-PARP13.1) demonstrated downregulation of *TRAIL-R4* mRNA upon 6 hours of BFA treatment. On the contrary, cells lacking RNA-binding competent PARP13 or PARP13 altogether (PARP13$^{-/-}$, mock PARP13$^{-/-}$, PARP13$^{-/-}$ + SBP-PARP13.1^{VYFHR}) did not demonstrate any *TRAIL-R4* mRNA regulation as compared to untreated cells. This result confirms that PARP13 is responsible for the downregulation of *TRAIL-R4* mRNA seen upon early ER stress and suggests that RNA-binding activity is required for the regulation to occur.

PARP13-dependent *TRAIL-R4* downregulation does not affect ER-stress mediated apoptosis

Recently, Lu and colleagues showed that unmitigated ER stress promotes cell-autonomous apoptosis through the upregulation of death receptor TRAIL-R2 (Lu et al., 2014). This study further suggests that TRAIL-R2 accumulation and multimerization at the membrane nucleates the DISC complex which activates caspase activity that leads to apoptosis (Lu et al., 2014). Given that a previous study had demonstrated that TRAIL-R4 receptor is able to prevent TRAIL-mediated initiator

FIGURE 6

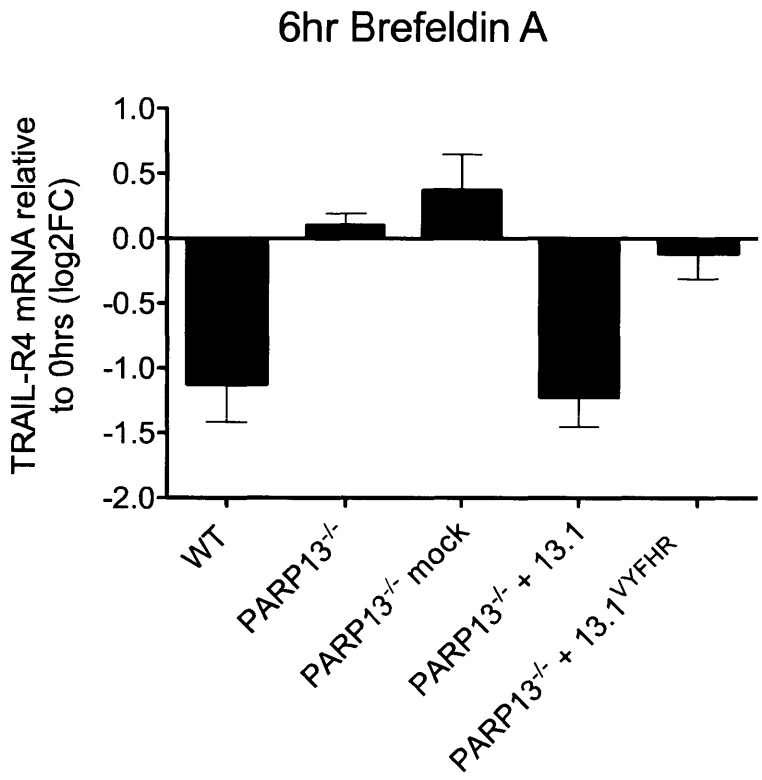

Figure 6. PARP13 RNA binding activity is required for *TRAIL-R4* downregulation upon ER stress. Wildtype, PARP13$^{-/-}$ cells, or PARP13$^{-/-}$ cells transfected with SBP-PARP13.1, SBP-PARP13^{VYFHR}, or mock transfected were treated with 5μg/ml BFA for 0 or 6 hours and the mRNA levels of *TRAIL-R4* were measured by RT-qPCR and compared to mRNA levels at 0 hours (two-sided t-test, n=3, ** p-value<0.01, error bars represent S.D.).

FIGURE 7

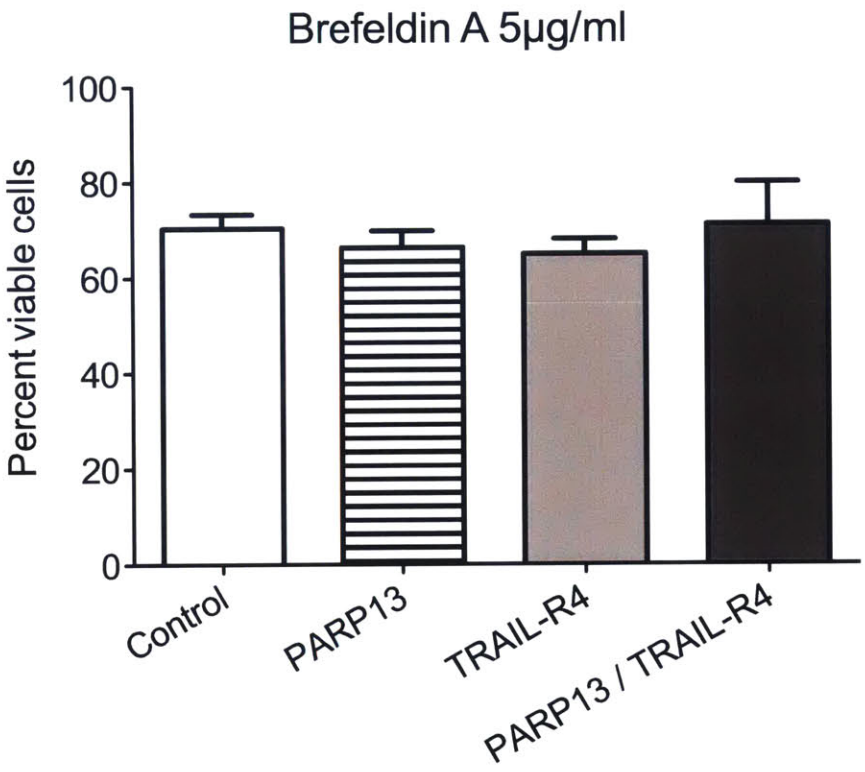

Figure 7. PARP13, TRAIL-R4 or PARP13-dependent regulation of *TRAIL-R4* does not affect ER stress-mediated apoptosis. HeLa cells were depleted for PARP13, TRAIL-R4 or simultaneously for PARP13 and TRAIL-R4 using siRNAs and treated with 5µg/ml BFA for 24 hours. Viable cells were measured by propidium iodine and Annexin V staining using fluorescence-activated cell sorting and the percentage of viable cells was plotted for each knockdown (two-sided t-test compared to control siRNA, n=3, error bars represent S.D.).

caspase activation by interacting with TRAIL-R2, we sought to determine if PARP13, TRAIL-R4 or the PARP13-dependent *TRAIL-R4* downregulation had an effect in ER-mediated cell death (Mérino et al., 2006). To test this we measured the viability of HeLa cells depleted of PARP13, TRAIL-R4 and of both PARP13 and TRAIL-R4 simultaneously, upon BFA treatment for 24 hours (Figure 7). Depletion of either PARP13, TRAIL-R4 or the combination of both, showed no difference in cell viability as compared to control knockdown cells suggesting that the protein levels of PARP13, TRAIL-R4 receptor o the regulation of *TRAIL-R4* mRNA by PARP13 during the early ER stress response does not ultimately affect ER-stress mediated apoptosis.

DISCUSSION

Cellular stress responses are generated due to environmental stressors and are required for the cell to initiate protective or destructive responses depending on the severity of the stress (Fulda et al., 2010). In this appendix we described that *TRAIL-R4* mRNA is downregulated during ER stress and not in other environmental stresses such as oxidative or heat stress, and that this ER stress regulation is dependent on PARP13's RNA binding activity. Treatment with three mechanistically different ER stress inducers confirms that the *TRAIL-R4* downregulation response is specific to ER stress, although other stresses like DNA damage should also be tested.

Why is PARP13 regulating *TRAIL-R4* mRNA under ER stress conditions? Given that PARP13 is a known host antiviral factor and viral infection triggers an ER

stress response, one possibility is that inducing ER stress in cells triggers an antiviral-like response that activates PARP13 to regulate its cellular target transcripts. Although possible, this is unlikely since PARP13's direct binding to the viral mRNA is what triggers PARP13's antiviral activity but in the case of *TRAIL-R4*, the mRNA is constitutively present in the cell and its levels do not increase upon ER stress, suggesting that only the ability to bind to *TRAIL-R4* is probably not sufficient to trigger its rapid ER stress-dependent downregulation.

Another possibility is that the downregulation of *TRAIL-R4* mRNA is not due to an antiviral-like response but part of the gene regulation required during the early ER stress response. This possibility is not implausible since it has been shown that gene expression regulation of TRAIL receptors, such as TRAIL-R2, is essential for the cellular response to ER stress (Lu et al., 2014). Although we show that PARP13-dependent *TRAIL-R4* mRNA regulation has no effect in the ER stress-mediated apoptotic response, it is possible that the regulation is important for the adaptive/survival pathway which, as *TRAIL-R4* regulation, also takes place during the initial phase of the ER stress response. In this context, we have preliminary results that showed that PARP13 activity is not required for ER stress induced BiP upregulation, *CHOP* transcriptional activation or *XBP1* mRNA splicing, thus suggesting that, if in fact *TRAIL-R4* mRNA regulation is part of the ER stress response, it most likely affects a process downstream of these events.

Alternatively, under ER stress conditions, PARP13 could be regulating the same set of transcripts it regulates during basal/physiological conditions, independent of a role the gene product of that transcript might play during ER-stress

response. Given that during the adaptive phase of the unfolded protein response the cell tries to restore ER homeostasis by a number of ways, including the degradation of ER-localized transcripts, this idea would define PARP13 as an important contributor to ER homeostasis under basal and stress conditions.

METHODS

Reagents

Brefeldin A, tunicamycin, thapsigargin and propidium iodide were from Sigma. Annexin V (640912) conjugated to Alexa 647 was from Biolegend. Dithiothreitol was from IBI scientific. Sodium arsenite was from Fluka. All qPCR primers were pre-designed from Sigma (KiCqStart SYBR Green Primers). Antibodies used: PARP13 (In house HM928 or Genetex, GTX120134), GAPDH (Genetex, GTX282445), BiP (Cell Signaling, C50B12).

Cell lines and transfection conditions

Experiments were performed using HeLa Kyoto cells or HeLa Kyoto PARP13 knockout cell line ($PARP13^{-/-\ A}$) described previously (Todorova et al., 2014). Both cell lines were cultured in Dulbecco's Modified Eagle's Medium (DMEM) containing 10% Fetal Bovine Serum in 5% CO_2 at 37°C. Transfections were performed using Lipofectamine 2000 (Life technologies) as per manufacturer's instructions for 24 hours prior to assay. Knockdowns by RNAi were performed by double 48 hour transfections using Lipofectamine 2000 and 5nM of Silencer Select siRNAs (Life technologies).

RT-qPCR

cDNA was prepared using Prime Script RT reagent (Takara), 500ng of total RNA and random primers. RT-qPCR reactions were carried out with 100ng of cDNA using SYBR Select master mix reagent (Life Technologies) following manufacturer instructions. RT-qPCR was performed on a Roche 480 Light Cycler. Data analysis was performed using the $\Delta\Delta C_T$ method (Livak and Schmittgen, 2001). Actin-β (ACTB) was used as normalizing control.

***XBP1* mRNA RT-PCR splicing assay**

XBP1 splicing assays were carried out as previously described (Stroescu et al., 2013). PCR using specific XBP1 primers to detect both spliced and unspliced mRNA was performed with the following program: 4min 94°C, (10s at 94°C, 30s at 65°C and 30s at 72°C) x 35 cycles, 10min at 72°C. PCR products were resolved in 2.5% agarose gel.

Cell viability assays

Cells were washed twice in 1X PBS and stained with Annexin V and propidium iodide in Annexin binding buffer (10 mM HEPES pH 7.4, 140 mM NaCl and 2.5 mM $CaCl_2$) for 15 min at room temperature. Fluorescence-activated cell sorting analysis was performed on a FACScan instrument (BD) and cells negative for both Annexin V and propidium iodide were considered alive.

CONCLUSION AND FUTURE DIRECTIONS

PARP13 regulates mRNAs during viral infections (viral mRNA), cytoplasmic stress (by regulation of Ago2) and under physiological conditions (downregulation of *TRAIL-R4* mRNA) (Gao et al., 2002; Leung et al., 2011; Todorova et al., 2014). In this brief study we have showed that PARP13 downregulates *TRAIL-R4* mRNA during the first hours of the ER stress response and that this regulation does not affect the apoptotic outcome of prolonged ER stress exposure.

As demonstrated by previous studies, gene expression regulation of TRAIL receptors upon ER stress can be cell-type dependent, thus it would be of interest to analyze PARP13's *TRAIL-R4* regulation and apoptotic fate in different human cells lines (Condamine et al., 2014; Huang et al., 2004). In order to better understand how PARP13 regulates *TRAIL-R4* transcript under ER stress conditions, it is important to determine what triggers PARP13 activity during ER stress response. One way to address this is to determine binding partners of PARP13 upon early ER stress as PARP13's activity could be triggered by interaction with another protein. This could be done by mass spectrometry analysis of PARP13 immunoprecipitates with or without ER stress. Alternatively, activation could be due to posttranslational modifications such as ADP-ribosylation or phosphorylation. The presence of ER stress-dependent modifications like these could be easily probed by immunoblots and phosphatase assays or in more detail by mass spectrometry analysis.

To explore the mechanism of how PARP13 downregulates *TRAIL-R4* mRNA upon ER stress, we could determine if, like under physiological conditions, *TRAIL-R4*

downregulation is dependent on exosome complex activity for transcript degradation. In this context, it would also be interesting to investigate if there is any overlap between PARP13 target downregulation and the regulated IRE1-dependent decay (RIDD) mechanism under ER stress.

Lastly, it would be of great importance to determine if other PARP13 cellular targets, such as the ones identified in Chapter 2 of this thesis, are also downregulated upon ER stress. This study would aid to unveil the specificity of PARP13 targets during ER stress and help understand why the regulation is required. For this purpose, known putative targets can be tested individually or could be identified using RNAseq or CLIPseq protocols in ER stressed or unstressed cells. Overall, these experimental strategies would help elucidate the importance of PARP13 in the regulation of cellular mRNAs during the ER stress response, which could potentially be yet another important function for this RNA-binding PARP.

REFERENCES

Braakman, I., and Hebert, D.N. (2013). Protein folding in the endoplasmic reticulum. Cold Spring Harb Perspect Biol *5*, a013201.

Chakrabarti, A., Chen, A.W., and Varner, J.D. (2011). A review of the mammalian unfolded protein response. Biotechnol Bioeng *108*, 2777-2793.

Condamine, T., Kumar, V., Ramachandran, I.R., Youn, J.I., Celis, E., Finnberg, N., El-Deiry, W.S., Winograd, R., Vonderheide, R.H., English, N.R., et al. (2014). ER stress regulates myeloid-derived suppressor cell fate through TRAIL-R-mediated apoptosis. J Clin Invest *124*, 2626-2639.

Danial, N.N., and Korsmeyer, S.J. (2004). Cell Death: Critical Control Points. Cell *116*, 205-219.

Fulda, S., Gorman, A.M., Hori, O., and Samali, A. (2010). Cellular stress responses: cell survival and cell death. Int J Cell Biol *2010*, 214074.

Gao, G., Guo, X., and Goff, S.P. (2002). Inhibition of retroviral RNA production by ZAP, a CCCH-type zinc finger protein. Science *297*, 1703-1706.

Hollien, J., Lin, J.H., Li, H., Stevens, N., Walter, P., and Weissman, J.S. (2009). Regulated Ire1-dependent decay of messenger RNAs in mammalian cells. J Cell Biol *186*, 323-331.

Hollien, J., and Weissman, J.S. (2006). Decay of endoplasmic reticulum-localized mRNAs during the unfolded protein response. Science *313*, 104-107.

Huang, L., Xu, J., Li, K., Zheng, M.H., and Kumta, S.M. (2004). Thapsigargin potentiates TRAIL-induced apoptosis in giant cell tumor of bone. Bone *34*, 971-981.

Kischkel, F.C., Hellbardt, S., Behrmann, I., Germer, M., Pawlita, M., Krammer, P.H., and Peter, M.E. (1995). Cytotoxicity-dependent APO-1 (Fas/CD95)-associated proteins form a death-inducing signaling complex (DISC) with the receptor. EMBO J *14*, 5579-5588.

Kischkel, F.C., Lawrence, D.A., Chuntharapai, A., Schow, P., Kim, K.J., and Ashkenazi, A. (2000). Apo2L/TRAIL-dependent recruitment of endogenous FADD and caspase-8 to death receptors 4 and 5. Immunity *12*, 611-620.

Kroemer, G., Marino, G., and Levine, B. (2010). Autophagy and the integrated stress response. Mol Cell *40*, 280-293.

Leung, A.K., Vyas, S., Rood, J.E., Bhutkar, A., Sharp, P.A., and Chang, P. (2011). Poly(ADP-ribose) regulates stress responses and microRNA activity in the cytoplasm. Mol Cell *42*, 489-499.

Li, G., Mongillo, M., Chin, K.T., Harding, H., Ron, D., Marks, A.R., and Tabas, I. (2009). Role of ERO1-alpha-mediated stimulation of inositol 1,4,5-triphosphate receptor activity in endoplasmic reticulum stress-induced apoptosis. J Cell Biol *186*, 783-792.

Lu, M., Lawrence, D.A., Marsters, S., Acosta-Alvear, D., Kimmig, P., Mendez, A.S., Paton, A.W., Paton, J.C., Walter, P., and Ashkenazi, A. (2014). Cell death. Opposing unfolded-protein-response signals converge on death receptor 5 to control apoptosis.

Livak, K.J., and Schmittgen, T.D. (2001). Analysis of relative gene expression data using real-time quantitative PCR and the 2(-Delta Delta C(T)) Method. Methods *25*, 402-408.

Merino, D., Lalaoui, N., Morizot, A., Schneider, P., Solary, E., and Micheau, O. (2006). Differential inhibition of TRAIL-mediated DR5-DISC formation by decoy receptors 1 and 2. Mol Cell Biol *26*, 7046-7055.

Oslowski, C.M., and Urano, F. (2011). Measuring ER stress and the unfolded protein response using mammalian tissue culture system. Methods Enzymol *490*, 71-92.

Oyadomari, S., and Mori, M. (2004). Roles of CHOP/GADD153 in endoplasmic reticulum stress. Cell Death Differ *11*, 381-389.

Pitti, R.M., Marsters, S.A., Ruppert, S., Donahue, C.J., Moore, A., and Ashkenazi, A. (1996). Induction of apoptosis by Apo-2 ligand, a new member of the tumor necrosis factor cytokine family. J Biol Chem *271*, 12687-12690.

Samali, A., Fitzgerald, U., Deegan, S., and Gupta, S. (2010). Methods for monitoring endoplasmic reticulum stress and the unfolded protein response. Int J Cell Biol *2010*, 830307.

Sano, R., and Reed, J.C. (2013). ER stress-induced cell death mechanisms. Biochim Biophys Acta *1833*, 3460-3470.

Sprick, M.R., Weigand, M.A., Rieser, E., Rauch, C.T., Juo, P., Blenis, J., Krammer, P.H., and Walczak, H. (2000). FADD/MORT1 and caspase-8 are recruited to TRAIL receptors 1 and 2 and are essential for apoptosis mediated by TRAIL receptor 2. Immunity *12*, 599-609.

Stroescu, A., Sima, L., Pena, F. (2013). Current methods for investigation of unfolded

protein response. Rom Biotech Lett *8*, 8539-50.

Thorburn, A. (2004). Death receptor-induced cell killing. Cell Signal *16*, 139-144.
Wang, S., and Kaufman, R.J. (2012). The impact of the unfolded protein response on human disease. J Cell Biol *197*, 857-867.

Todorova, T., Bock, F.J., and Chang, P. (2014). PARP13 regulates cellular mRNA post-transcriptionally and functions as a pro-apoptotic factor by destabilizing TRAILR4 transcript. Nat Commun *5*.

van Schadewijk, A., van't Wout, E.F., Stolk, J., and Hiemstra, P.S. (2012). A quantitative method for detection of spliced X-box binding protein-1 (XBP1) mRNA as a measure of endoplasmic reticulum (ER) stress. Cell Stress Chaperones *17*, 275-279.

Wiley, S.R., Schooley, K., Smolak, P.J., Din, W.S., Huang, C.P., Nicholl, J.K., Sutherland, G.R., Smith, T.D., Rauch, C., Smith, C.A., et al. (1995). Identification and characterization of a new member of the TNF family that induces apoptosis. Immunity *3*, 673-682.